Experiments to resolve structure and structural dynamics

Structural methods:

(1) NMR spectroscopy (μs, native environment, atomic resolution)

(2) X-ray diffraction (fs, crystals, atomic resolution, destructive)

(3) Vibrational spectroscopy (fs, native environment, atomic resolution)

(4) Nonlinear vibrational Spectroscopy:

information about couplings

(5) Visible (electronic) spectroscopy

(6) EPR spectroscopy

(7) Microscopy

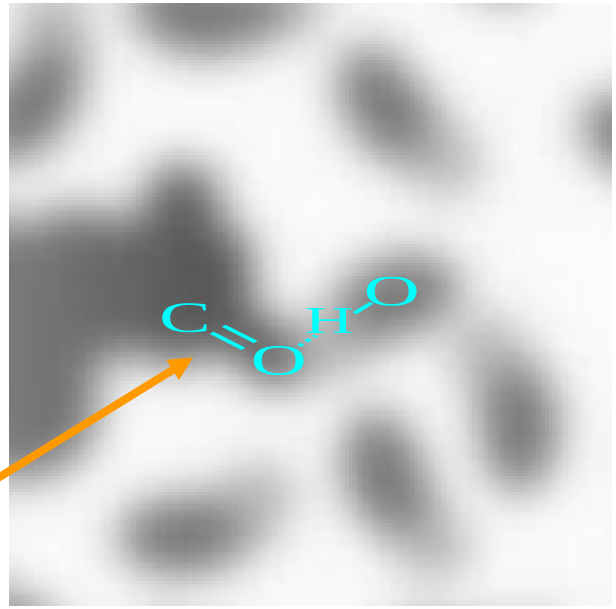

Local vibrational modes are
local probes of chemical bonds

The Electromagnetic spectrum

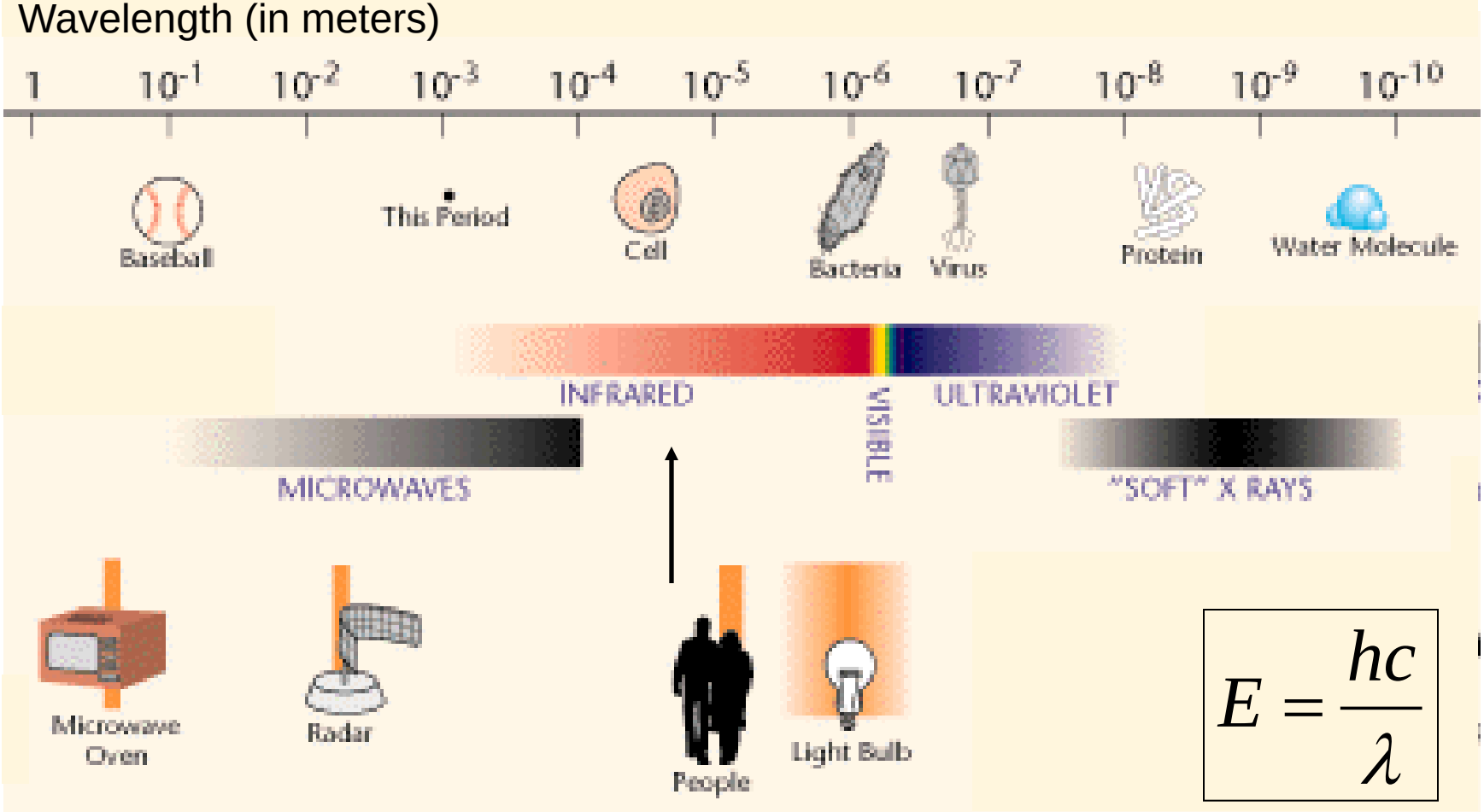

$$E = \frac{hc}{\lambda}$$

Spin transitions

Electronic transitions

Vibrational transitions

nuclear transitions

Vibrational spectroscopy

- Nuclear motion (vibration) , structural information

Vibrational degrees of freedom

Linear molecule : 3N - 5

General : 3N - 6

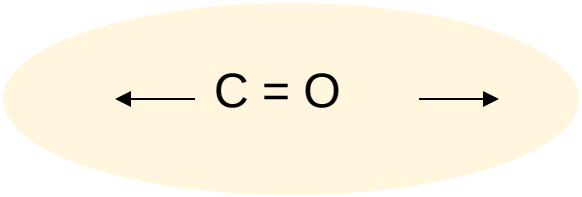

Energy : $E = h\nu = hc\,\bar{\nu} = hc$ 2134 cm^{-1} ; $6.4 \times 10^{13}\ s^{-1}$

gas phase : $$E = \frac{h}{8\pi^2 cI} J(J+1) \qquad I = \frac{m_1 m_2}{m_1 + m_2} r^2 = \mu r^2$$

Schrödinger equation for a diatomic molecule:

$$\left[\frac{\hbar^2}{2\mu}\nabla^2 + V(R)\right] \mathrm{X}(R) = E\mathrm{X}(R)$$

V(R) : Potential energy surface

Vibrational spectroscopy

Rotational-Vibrational transitions:

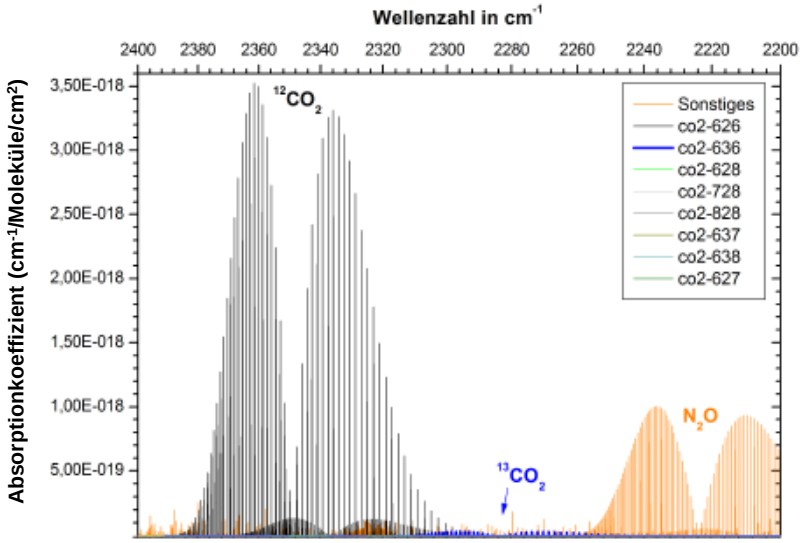

characteristic absorption lines per molecule

frequency position is often known very precisely ~ 0,01 cm^{-1}

narrow linewidths ~ 0.1 cm^{-1}

variety of different absorption lines per molecule

line shapes and intensities are strongly temperature dependent

Vibrational spectroscopy

Rotational-Vibrational transitions:

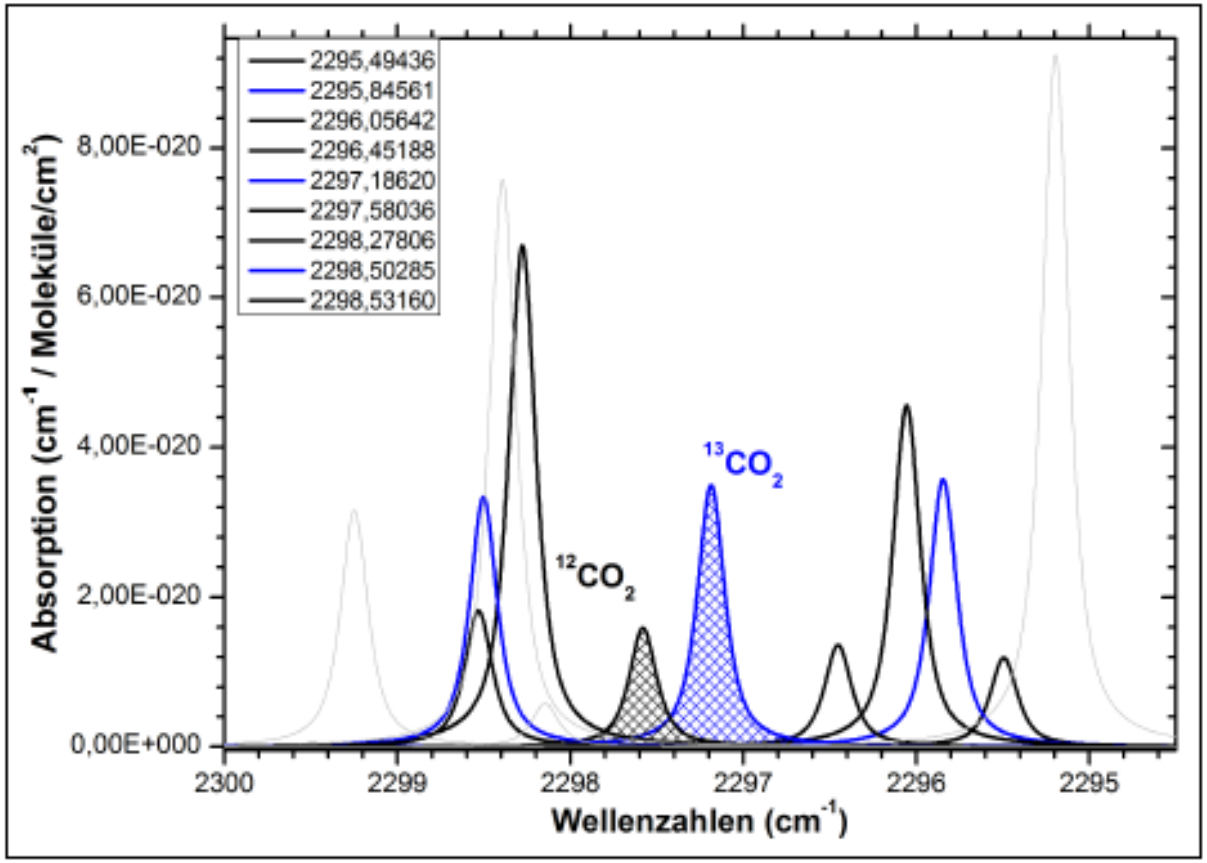

Potential energy surface V(R) of a diatomic molecule

Morse potential

$$V(R) = D_e\left[1 - e^{a(R-R_e)}\right]^2$$

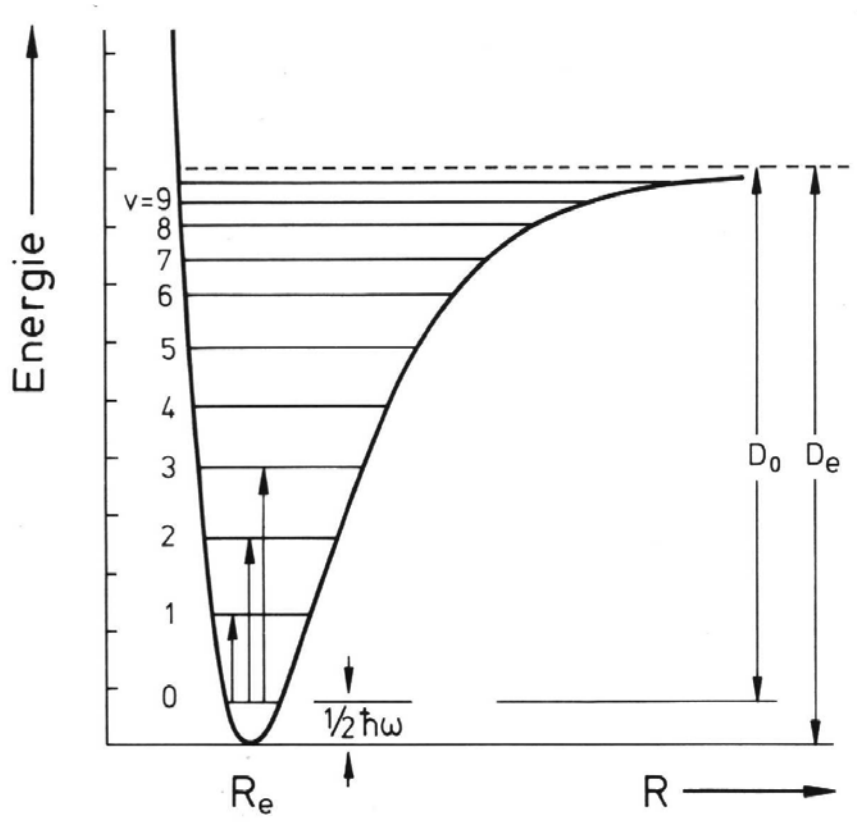

$$a = \sqrt{\frac{\mu}{2D_e}}\omega_e \qquad \omega = 2\pi\nu$$

D_e : Dissociation energy

R_e : Equilibrium distance

Approximation of the Potential energy surface V(R)

Taylor expansion of V(R) around R_e:

$$V(R) = V(R_e) + \left.\frac{dV}{dR}\right|_{R_e} (R - R_e) + \frac{1}{2}\left.\frac{d^2V}{dR^2}\right|_{R_e} (R - R_e)^2 + \cdots$$

zero

Harmonic oscillator:

$$V(R) = \frac{1}{2} k (R - R_e)^2$$

$$\omega = \sqrt{\frac{k}{\mu}}$$

$$E_n = (n + \frac{1}{2}) hc\bar{\nu}$$

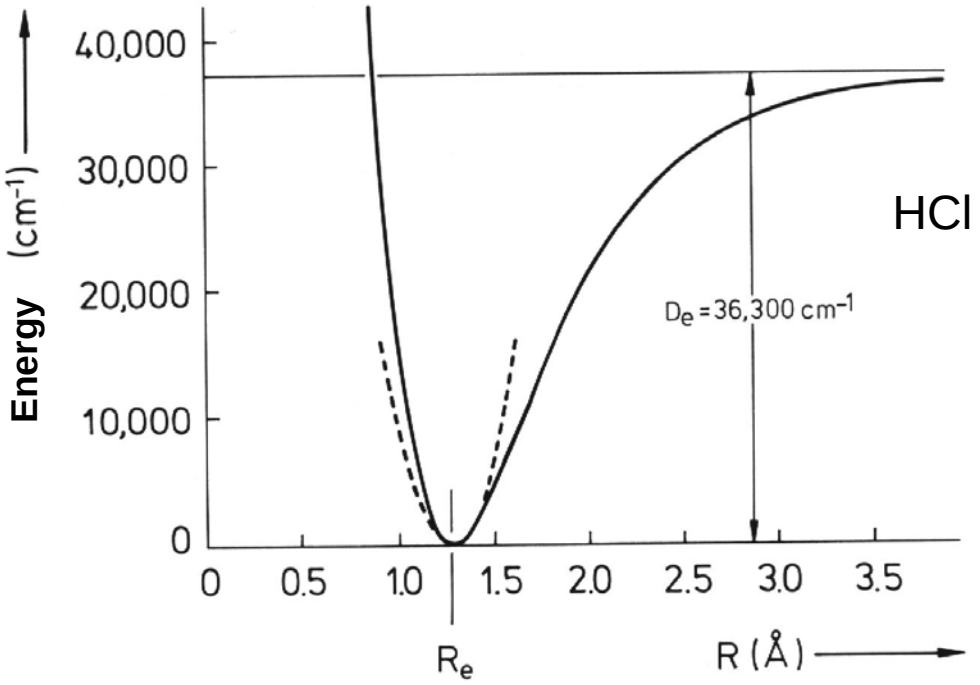

Polyatomic molecules

- Transformation to 3N-6 normal mode coordinates Q_i

$$H = \sum_i H(Q_i) = \sum_i \left(\frac{1}{2}\mu_i \dot{Q}_i^2 + \frac{1}{2} k_i Q_i^2 \right)$$

H_2O vibrations (gas phase)

3657 cm^{-1}

not IR active

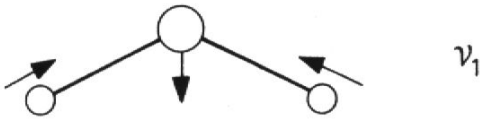

1595 cm^{-1}

IR active

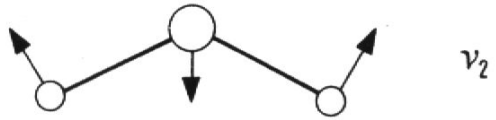

3756 cm^{-1}

IR active

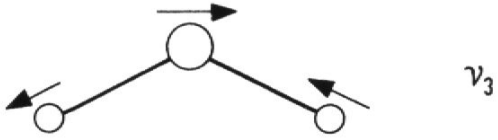

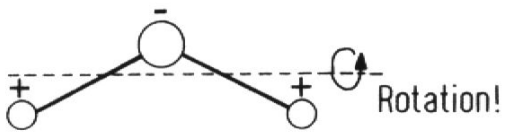

Fourier-Transform InfraRed Spectrometer

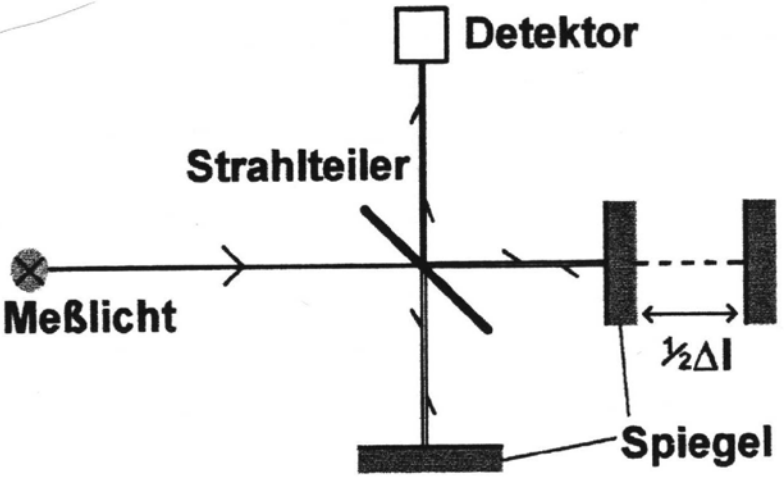

Monochromatic light source:

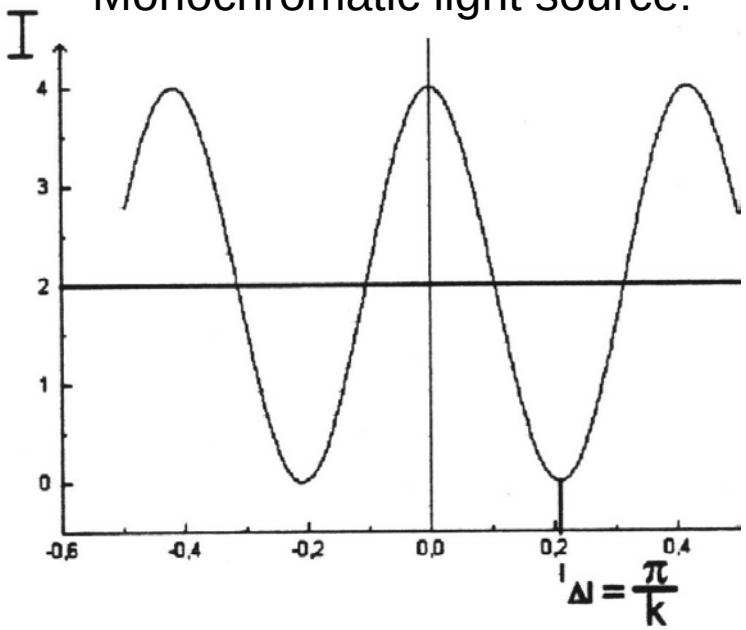

$$I(\Delta l) = \left| \frac{1}{2} E_0(k) + \frac{1}{2} E_0(k) e^{ik\Delta l} \right|^2 = \frac{1}{2} I_0 (1 + \cos(k\Delta l))$$

Fourier-**T**ransform **I**nfra**R**ed Spectrometer

Polychromatic light source:

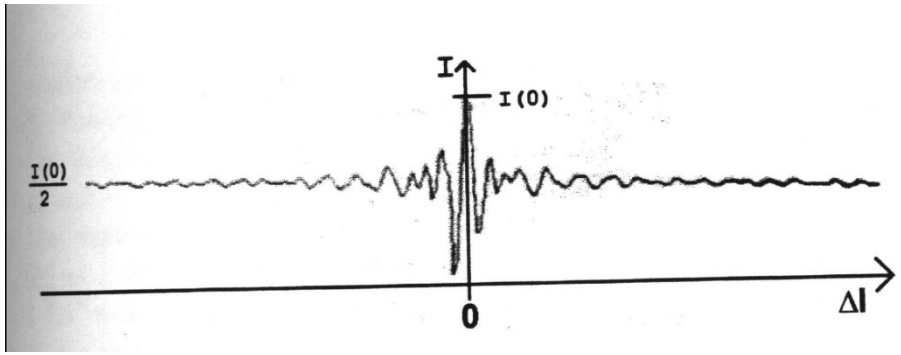

Removing the constant part of the Intensity trace:

$$I(\Delta l) \propto \int_{-\infty}^{\infty} B(\bar{\nu}) e^{-i2\pi\bar{\nu}\Delta l} d\bar{\nu}$$

Interferogram

$$B(\bar{\nu}) \propto \int_{-\infty}^{\infty} I(\Delta l) e^{i2\pi\bar{\nu}\Delta l} d(\Delta l)$$

Spectrum

Resolution: $$\Delta\bar{\nu} = \frac{3}{4\Delta l_{\max}}$$

Advantages: more light intensity

multiplexing

stray light suppression

Fourier-**T**ransform **I**nfra**R**ed Spectrometer

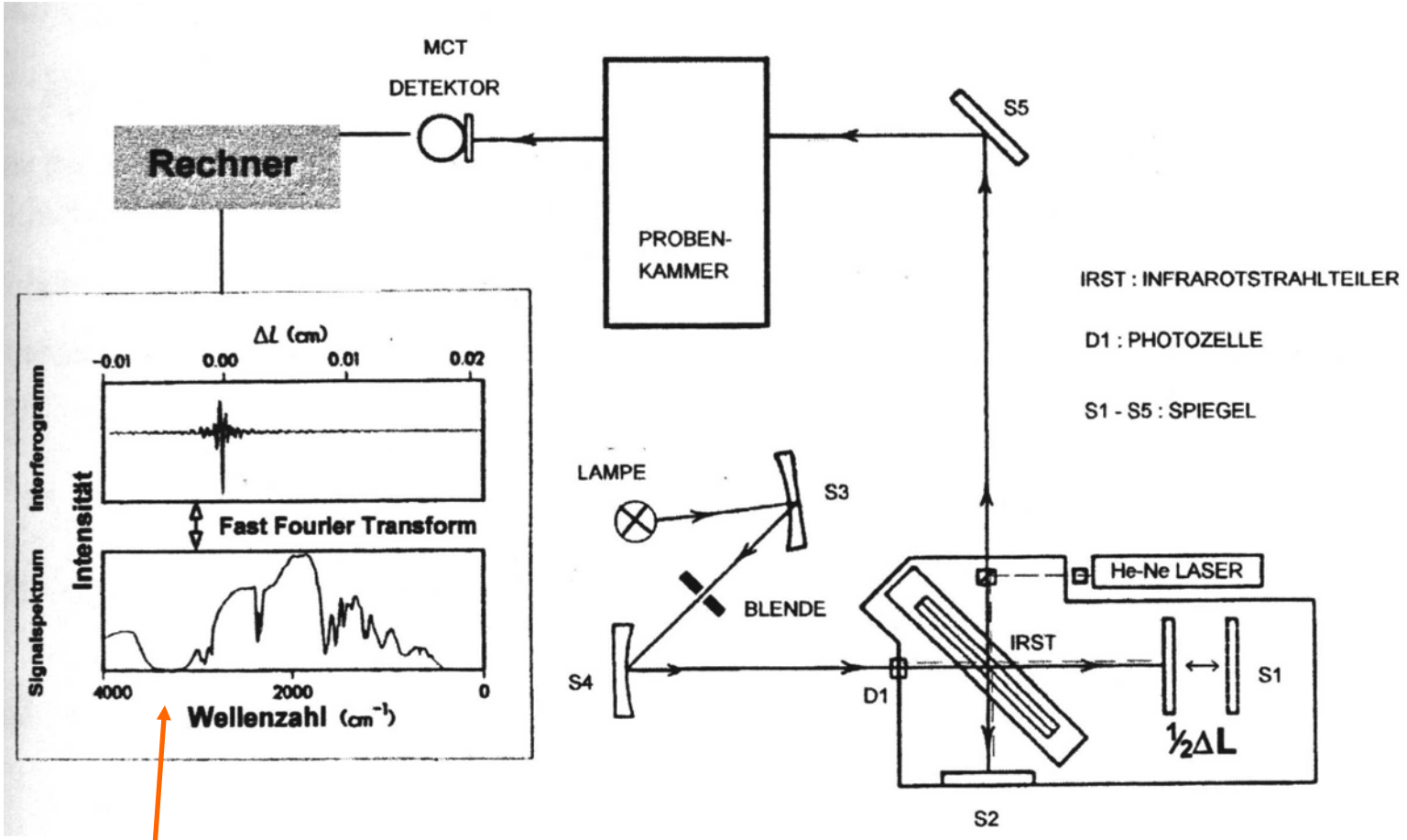

Ratio of this signal with and without sample gives the transmission spectrum T of the sample and -log(T) the absorption.

Lorentian line shape

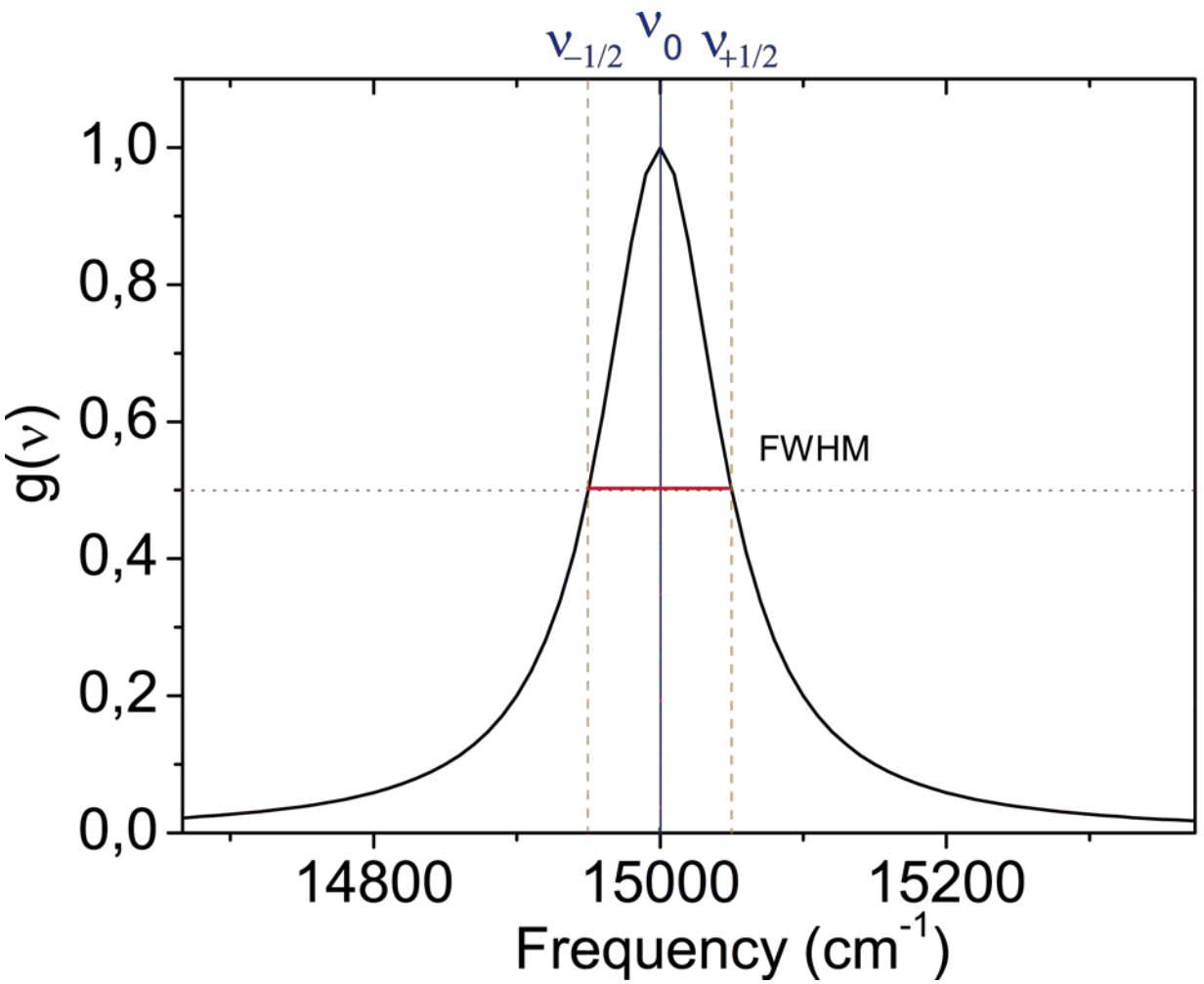

Polyatomic molecules

- Transformation to 3N-6 normal mode coordinates Q_i

$$H = \sum_i H(Q_i) = \sum_i \left(\frac{1}{2}\mu_i \dot{Q}_i^2 + \frac{1}{2} k_i Q_i^2 \right)$$

H_2O vibrations (gas phase)

3657 cm^{-1}

not IR active

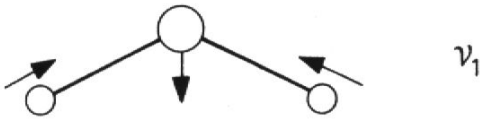

1595 cm^{-1}

IR active

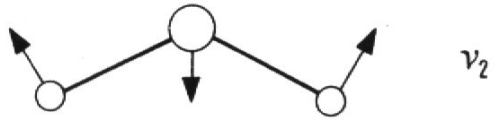

3756 cm^{-1}

IR active

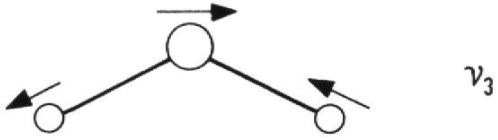

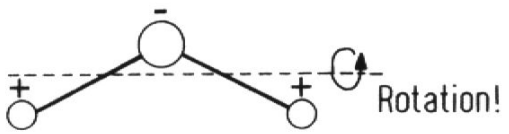

Spectra-Structure correlations

Table 2. Wavenumber ranges in which some functional groups and classes of compounds absorb in the mid- and far-infrared.

Range (cm^{-1}) and intensity[a]	Group and class	Assignment and remarks
3700–3600 (s)	–OH in alcohols and phenols	OH stretch; (dilute solution)
3520–3320 (m-s)	$–NH_2$ in aromatic amines, primary amines and amides	NH stretch; (dilute solution)
3420–3250 (s)	–OH in alcohols and phenols	OH stretch; (solids and liquids)
3400–3300 (vs)	–OO–H in hydroperoxides	Hydrogen bonded OO–H stretch
3360–3340 (m)	$–NH_2$ in primary amides	NH_2 antisymmetric stretch; (solids)
3320–3250 (m)	–OH in oximes	O–H stretch
3300–3250 (m-s)	≡CH in acetylenes	≡C–H stretch
3300–3280 (s)	–NH in secondary amides	NH stretch; (solids); also in polypeptides and proteins
3200–3180 (s)	$–NH_2$ in primary amides	NH_2 symmetric stretch; (solids)
3200–3000 (vs)	$–NH_3^+$ in amino acids	NH_3^+ antisymmetric stretching; very broad band
3100–2400 (vs)	–OH in carboxylic acids	H-bonded OH stretch ; very broad band
3100–3000 (m)	=CH in aromatic and unsaturated hydrocarbons	=C–H stretch
2990–2850 (m-s)	$–CH_3$ and $–CH_2–$ in aliphatic compounds	CH antisymmetric and symmetric stretching
2850–2700 (m)	$–CH_3$ attached to O or N	CH stretching modes
2750–2650 (w-m)	–CHO in aldehydes	Overtone of CH bending; (Fermi resonance)
2750–2350 (br)	$–NH_3^+$ in amine hydrohalides	NH stretching modes
2720–2560 (m)	–OH in phosphorus oxyacids	Associated OH stretching
2600–2540 (w)	–SH in alkyl mercaptans	S–H stretch

Infrared spectroscopy is a powerful tool

Polyatomic molecules - Examples

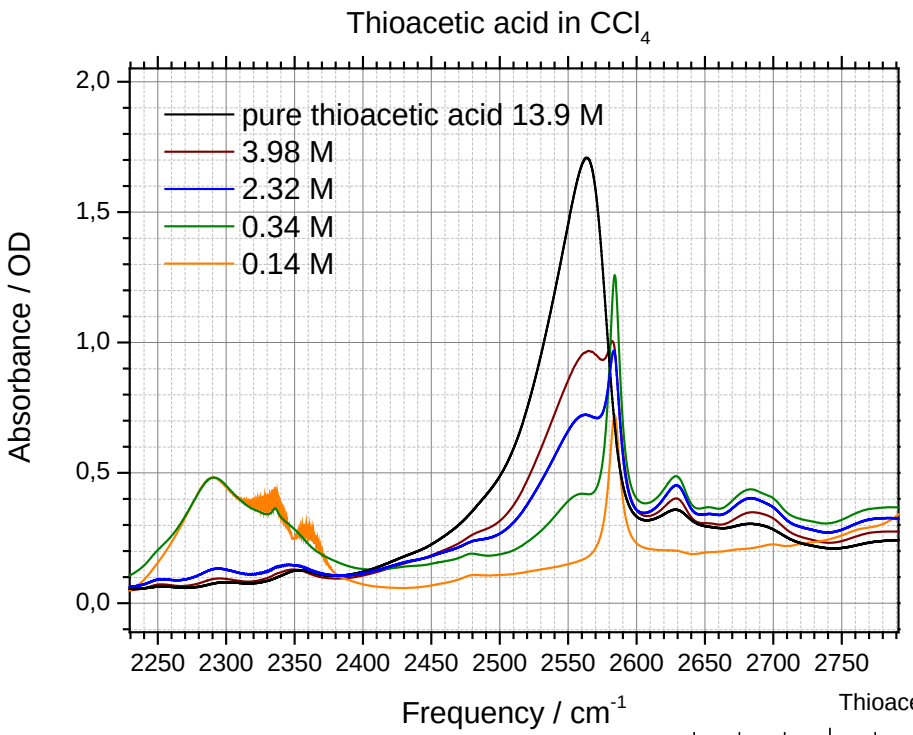

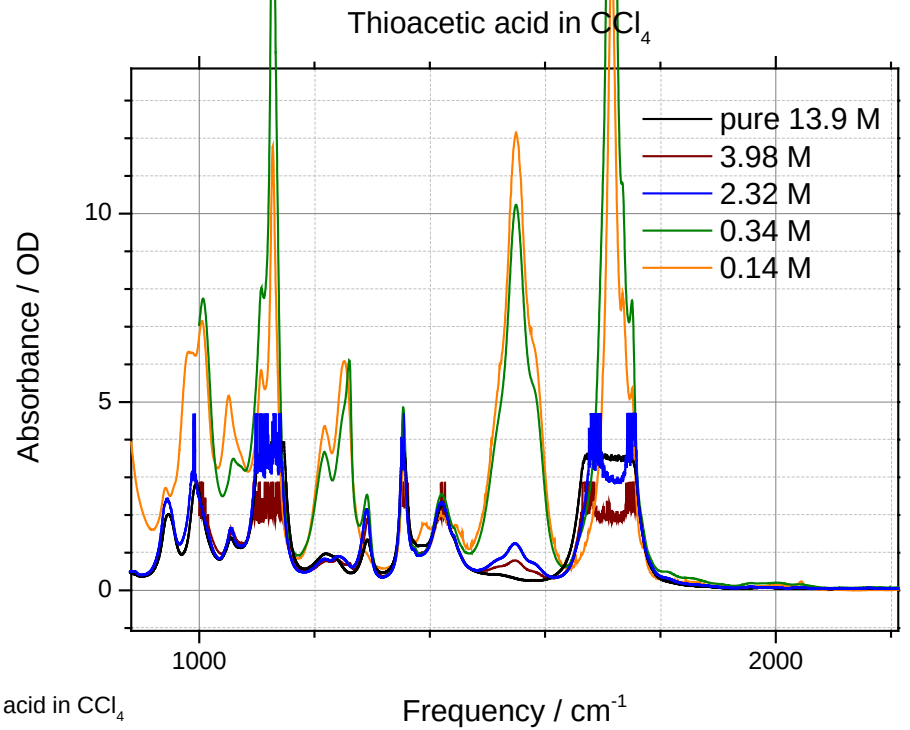

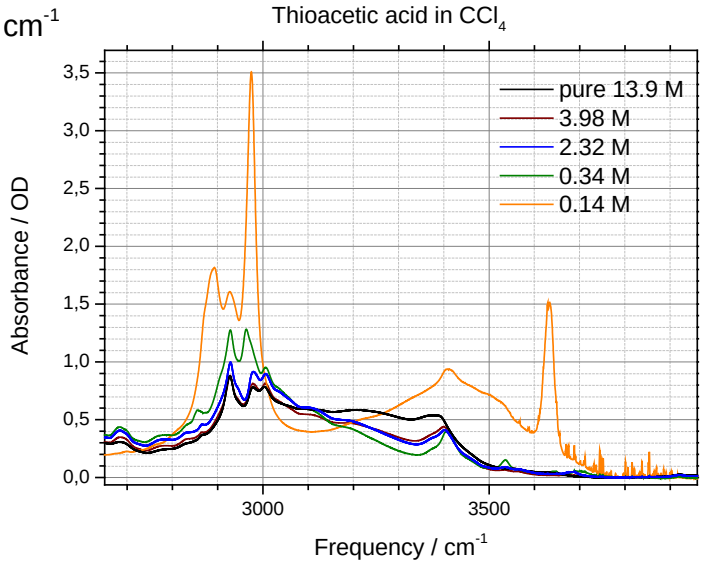

Infrared transitions

In the Born-Oppenheimer approximation the total initial wavefunction is given by:

$$\Psi_i(r,Q) = \Phi_k(r,Q)\mathrm{X}_n^k(Q)$$

k : quantum number of electronic state

n : Quantum number of nuclear state

Q : normal mode coordinates

Transition dipole moment M_{if} for a transition from state i to state f

$$M_{if} = \int \Psi_f^* \left[\sum_j eZ_j Q_j - \sum_l er_l \right] \Psi_i \, dr dQ$$

For a vibrational transition in the same electronic state, k does not change and the integration over dr leads to the permanent dipole moment $M_0(Q)$ in the electronic state k. The transition dipole moment vanishes if $M_0(Q)$ is constant zero.

$$M_{if} = \int \mathrm{X}_{n'}^{k*}(Q) M_0(Q) \mathrm{X}_n^k(Q) dQ$$

Infrared transitions

Vibrational transitions are infrared inactive if the permanent dipole moment $M_0(Q)$ does not depend on any change of Q, which can occur on symmetry reasons.

If we expand $M_0(Q)$ in a Taylor series around the equilibrium position:

$$M_{if} = \sum_i \left.\frac{\partial M}{\partial Q_i}\right|_{equ} \int \mathrm{X}_{n'}(Q) Q_i \mathrm{X}_n(Q) dQ$$

For harmomic oscillator wavefunction : $\Delta n = \pm 1$ for vibrational quanta

transition from v=0 (Boltzmann distribution); Overtones ($\Delta v = \pm 2$) are weak

Absorption coefficient $\alpha(\omega)$ is given by the ensemble average of the two-time dipole correlation function:

$$\alpha(\omega) = \frac{2\pi\omega}{3c\hbar nV}\left(1 - \exp\left(-\frac{\hbar\omega}{k_B T}\right)\right) \int_{-\infty}^{\infty} dt e^{-i\omega t} \left\langle M(0) M(t) \right\rangle$$

Polyatomic molecules

- Transformation to 3N-6 normal mode coordinates Q_i

$$H = \sum_i H(Q_i) = \sum_i \left(\frac{1}{2}\mu_i \dot{Q}_i^2 + \frac{1}{2} k_i Q_i^2 \right)$$

Isotope shift for a harmonic oscillator:

$$\frac{\omega}{\omega'} = \sqrt{\frac{\mu'}{\mu}} \approx \sqrt{\frac{m_H}{m_D}} = \sqrt{\frac{1}{2}}$$

same force constant

H_2O vibrations (gas phase)

3657 cm^{-1}

not IR active

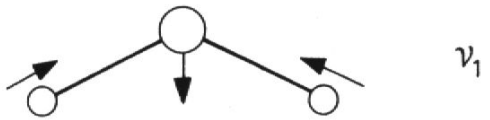

1595 cm^{-1}

IR active

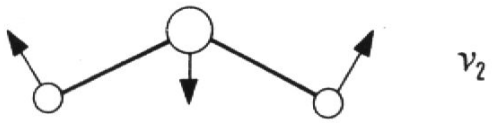

3756 cm^{-1}

IR active

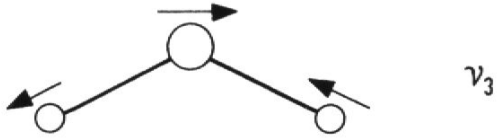

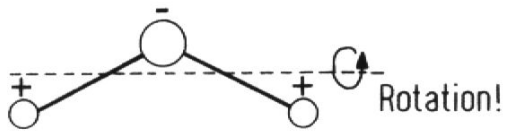

Fermi resonance

In special cases the strength of overtones or combination bands is enhanced if their energy matches a fundamental transition:

Theoretical unperturbed bands are shaded and observed bands are unshaded

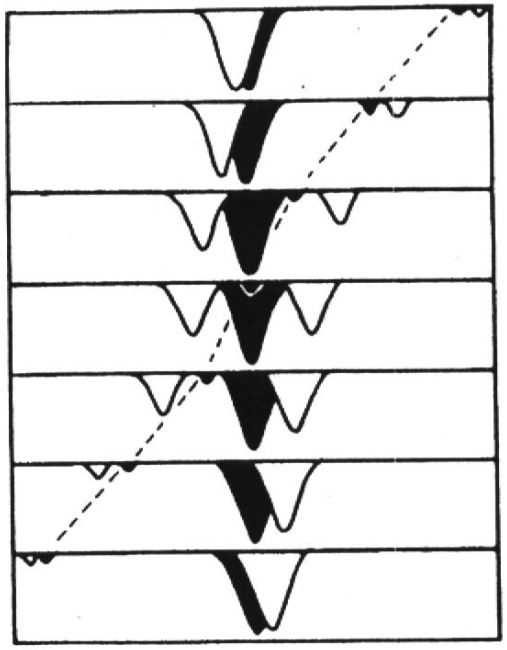

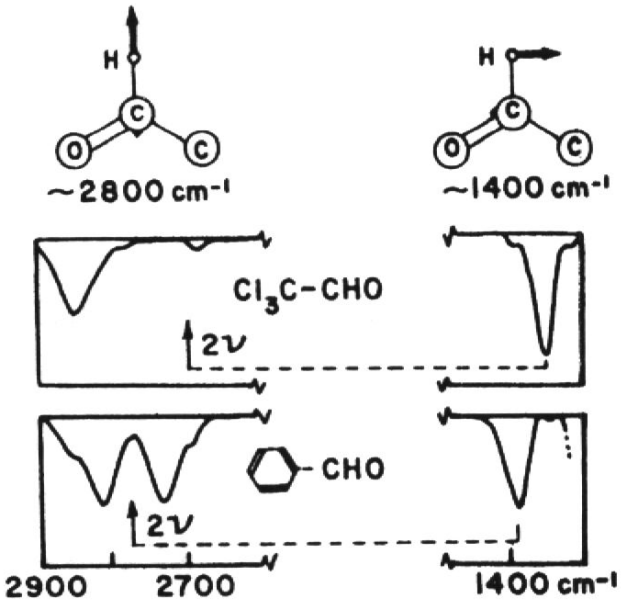

Estimation:

$$\overline{\nu}_{\pm} = \frac{1}{2}\left\{\overline{\nu}_a + 2\overline{\nu}_b \pm \sqrt{(\overline{\nu}_a - 2\overline{\nu}_b)^2 + \frac{4V^2{}_{ab}}{h^2}}\right\}$$

Infrared absorption spectra

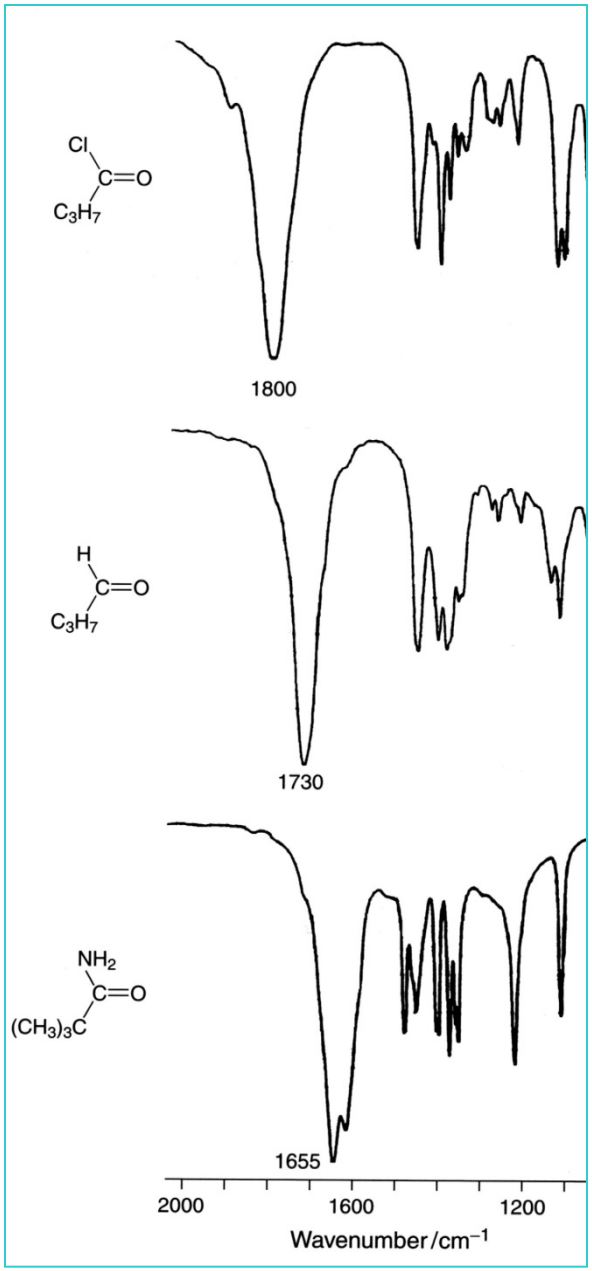

Contributions to IR band properties

- electronic effect: change in the distribution of electrons
- cis-trans isomers: higher symmetry in trans isomers -> smaller dipole moments
- steric effect: can change force constants e. g. ring strain
- solvent effect: shift frequencies
- temperature effect: higher T leads normally to lower frequencies and broader bands
- polar solvent-solute interaction: can cause dramatically shifts of group frequencies and alterations in band shapes for example: hydrogen bonds

Properties of hydrogen bonds: acceptor modes

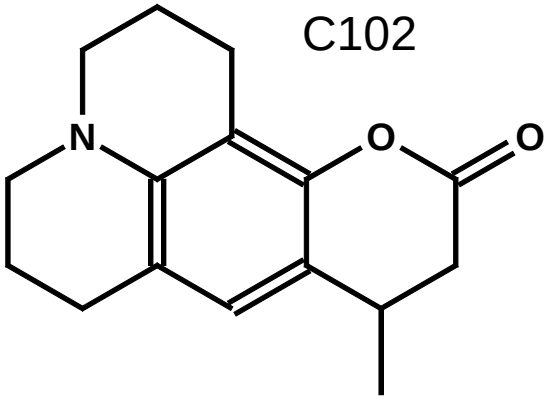

~ 30 cm^{-1} shift of the v(C=O) upon formation of a hydrogen bond to lower energies. Reduction of the C=O force constant due to the hydrogen bond.

Allows a detection of hydrogen bond acceptor modes

C102 in C_2Cl_4 with different phenol concentrations

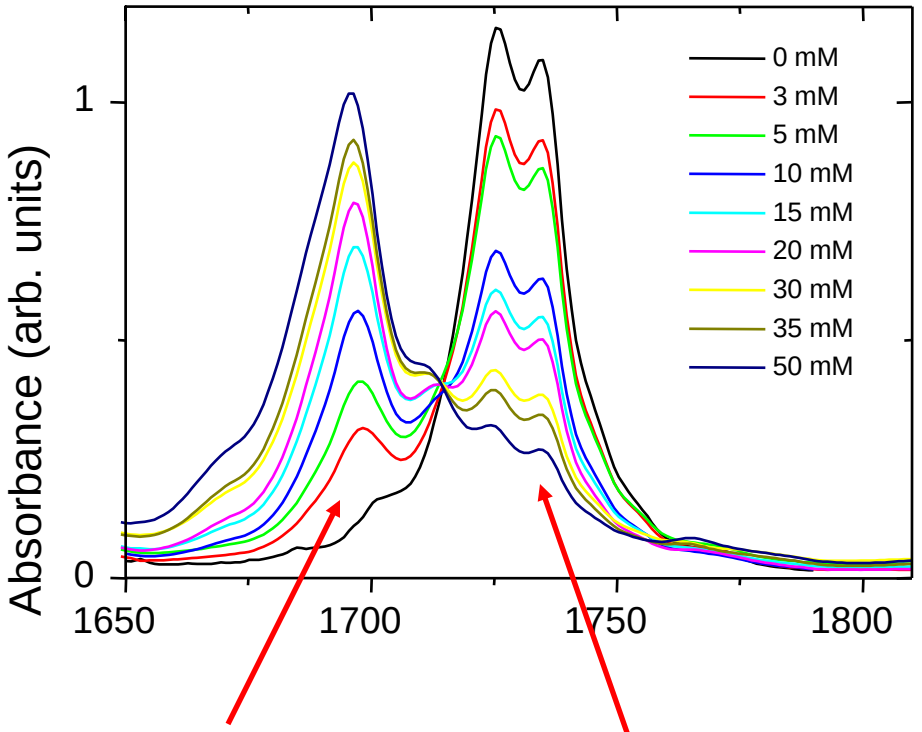

E. T. J. Nibbering et al., *Israel J. Chem*., 39, 1999, 333-346

Properties of hydrogen bonds: donor modes

The infrared band of the donor group (OH) is dramatically and entirely unusual changed upon formation of a hydrogen bond:

- Red-shift of ν(O-H)
  reduced force constant
- Very strong broadening
  - distribution of bond lengths
  - anharmonic coupling to low-frequency modes
  - Fermi resonances
  - homogeneous broadening

→ Peculiar bandshape

➢Halfwidth increases with temperature ~$T^{½}$.

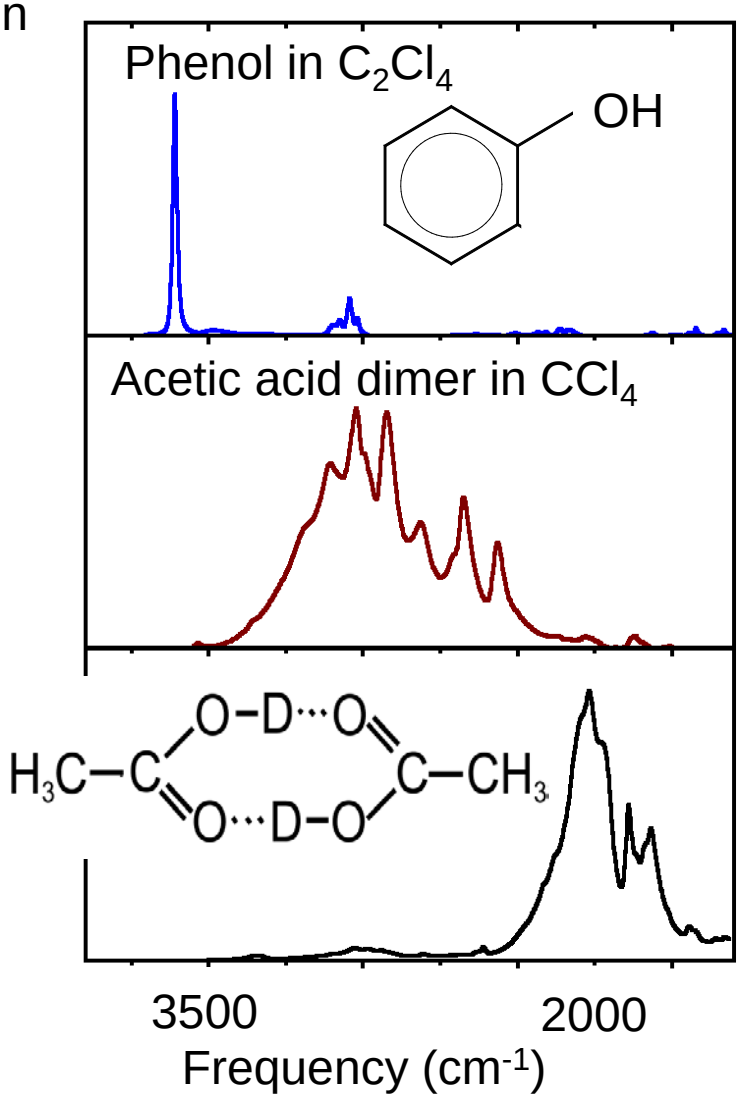

Anharmonicity of hydrogen bonds: donor modes

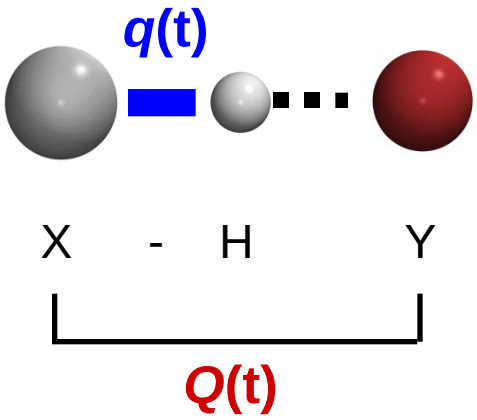

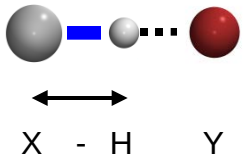

***q*(t) X-H stretching vibration**

high frequency ~ 3200 cm^{-1}

period ~10 fs

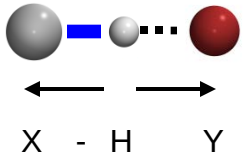

***Q*(t) X···Y H-bond vibration**

low frequency ~ 50-350 cm^{-1}

period ~ 100-500 fs

$$H(q,Q) = \frac{p^2}{2m} + \frac{1}{2} m\omega_{eff}^2(Q) q^2 + \frac{P^2}{2M} + \frac{1}{2} M\omega_{low}^2 Q^2, \quad \omega_{eff}(Q) = \omega_{high} + bQ + \ldots$$

$$= \frac{p^2}{2m} + \frac{1}{2} m\omega_{high}^2 q^2 + \frac{P^2}{2M} + \frac{1}{2} M\omega_{low}^2 Q^2 \pm bm\omega_{high} q^2 Q + \frac{1}{2} mb^2 q^2 Q^2$$

X—H X···Y anharm. coupl.

Bond length of hydrogen bonds

The spectral position of the hydrogen bonded v(OH) vibration indicates the hydrogen bond length and its strength

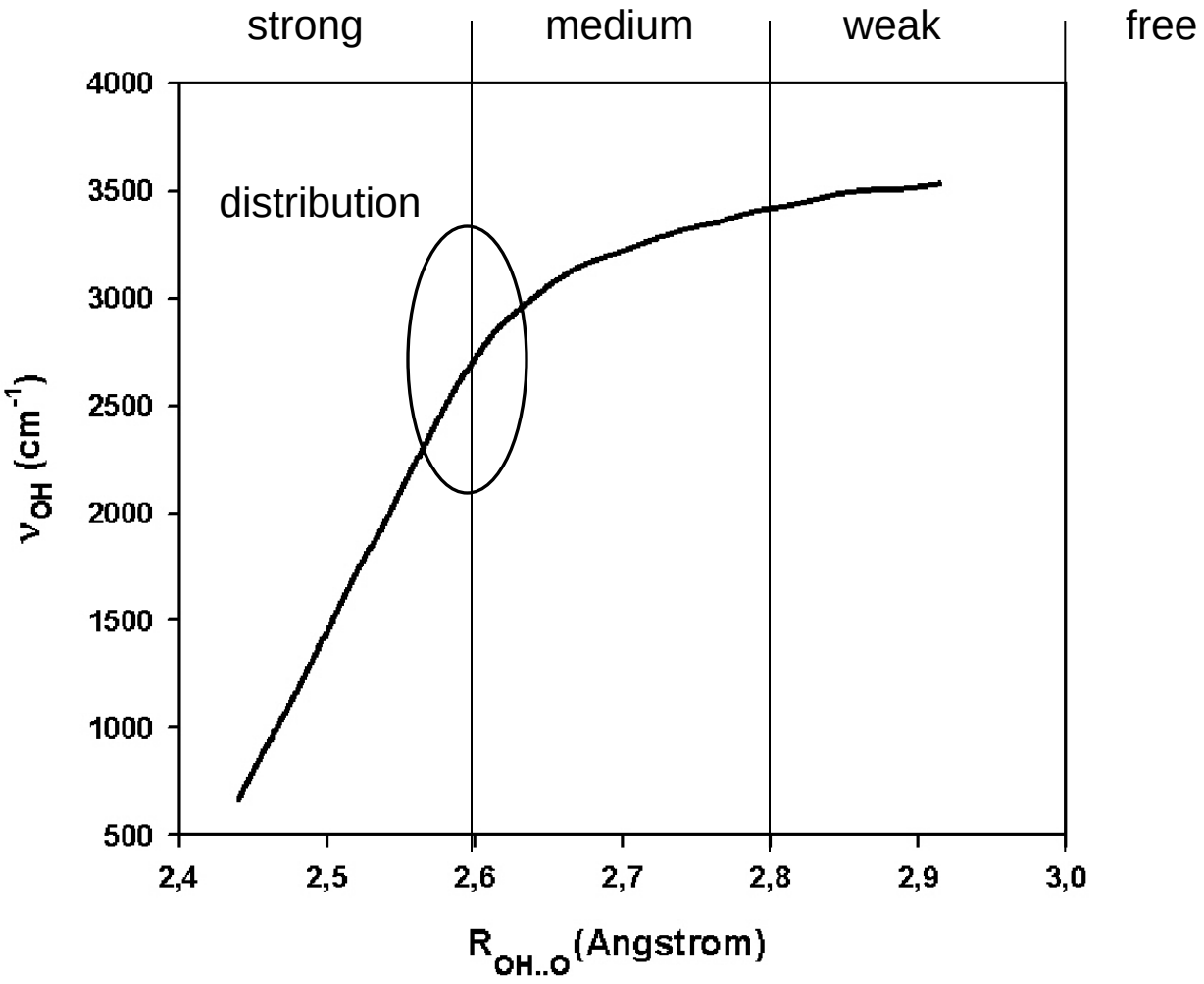

Types hydrogen bonds

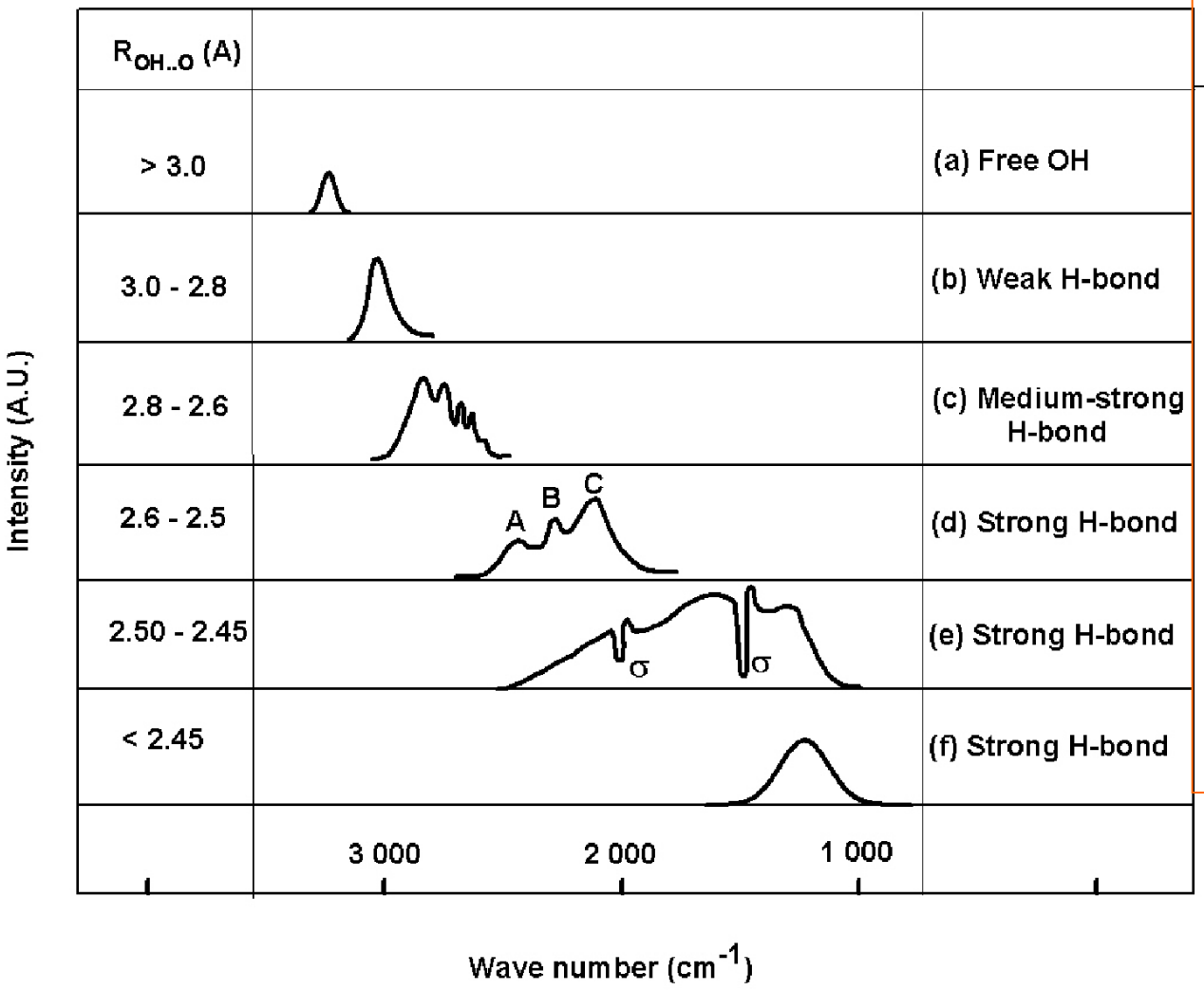

Δ-freq.	rel. Intensity	Width	Δ-isotop
0	1	10	1.41
100-300	5-10	100-300	1.4
300-1000	10-15	500	1.3
1000-1500	~ 30	1000-1500	1.1
1500-2000	> 30	2000	
2000-2500	> 3	200	

Ultrafast nonlinear infrared spectroscopy

How can we distinguish between Fermi resonances and low-frequency modes? How strong and relevant are the influences of each coupling?

Infrared Pump/Probe Setup:

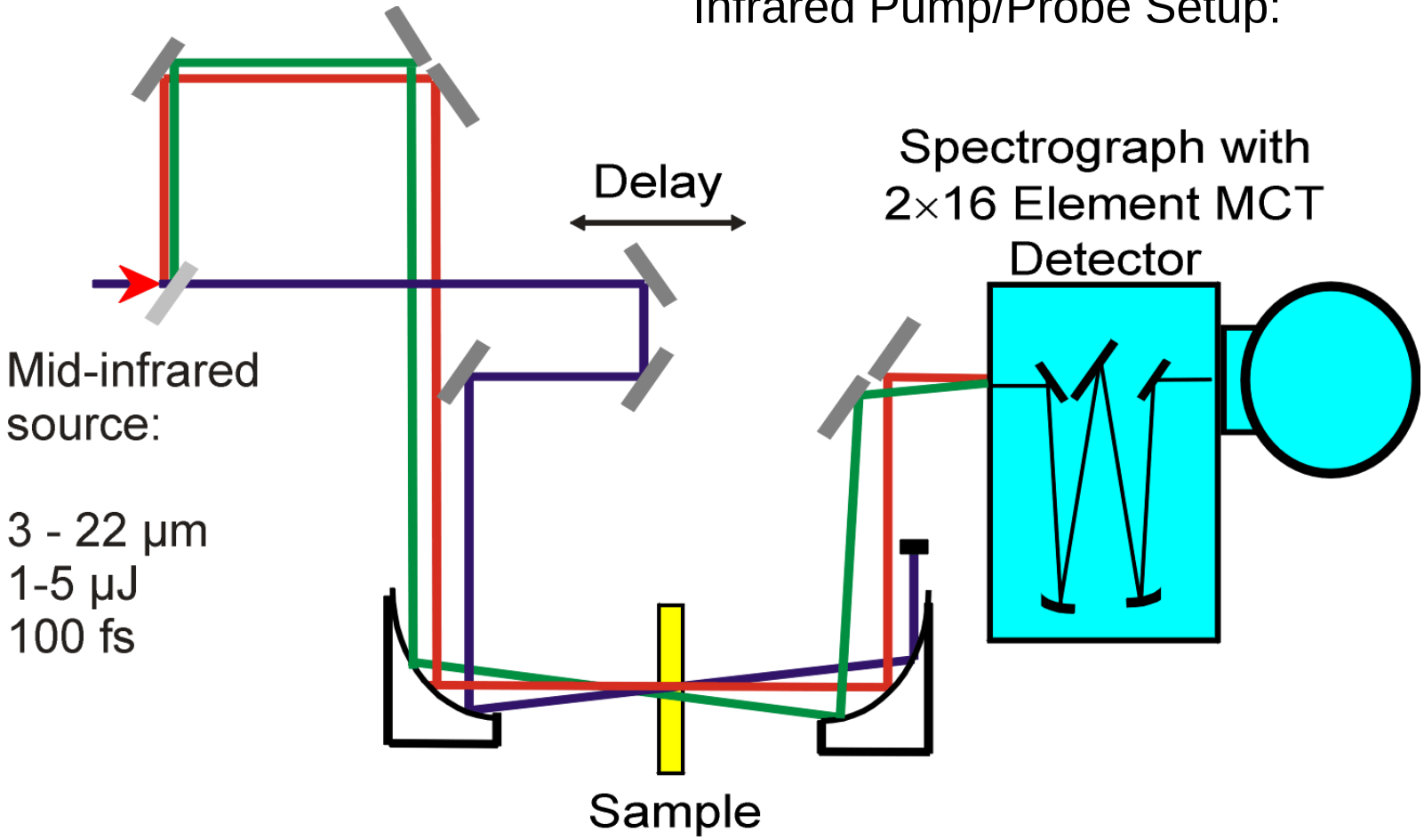

Folding of two functions

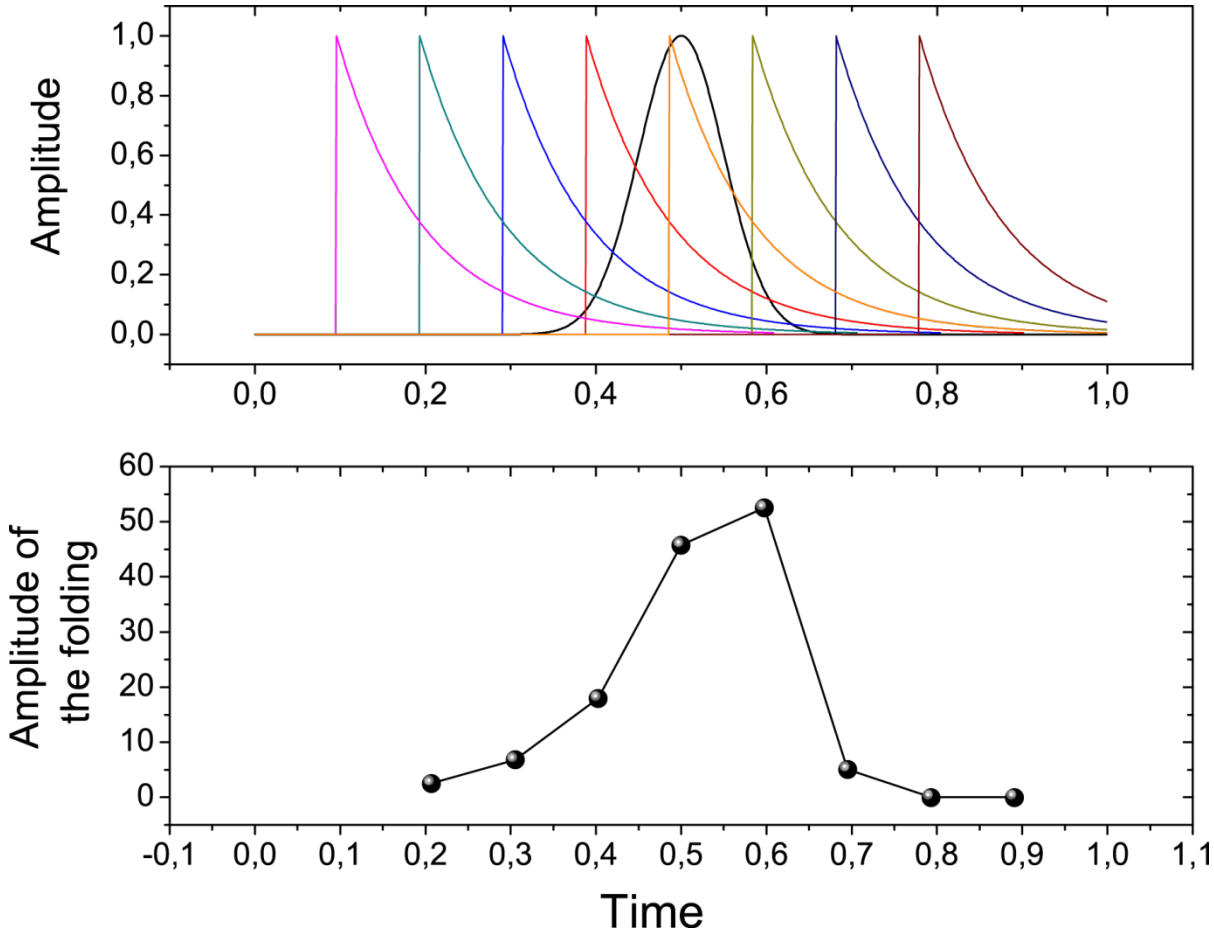

Ultrafast infrared pump-probe measurements

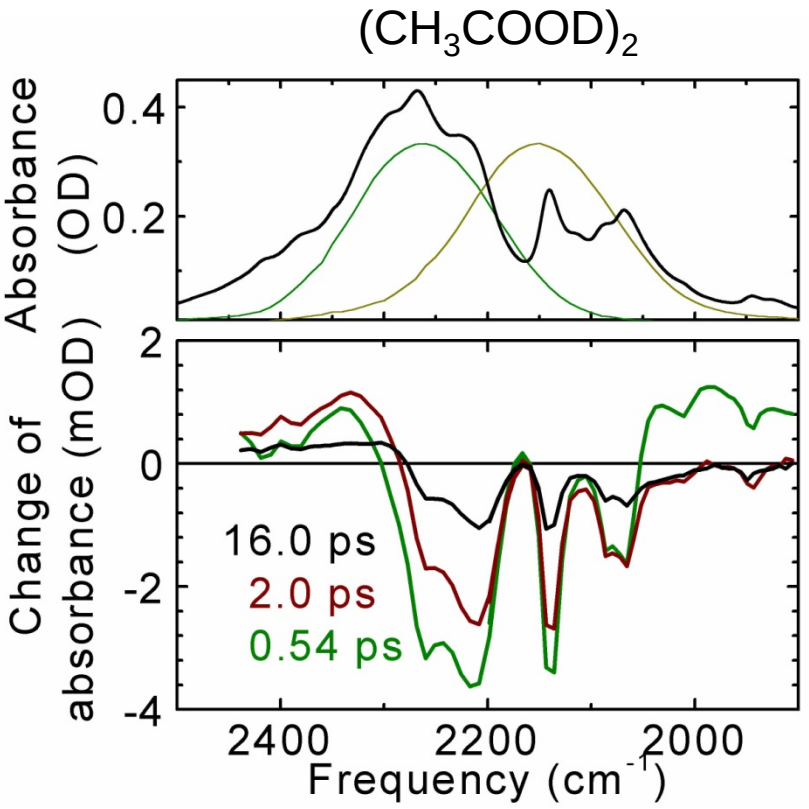

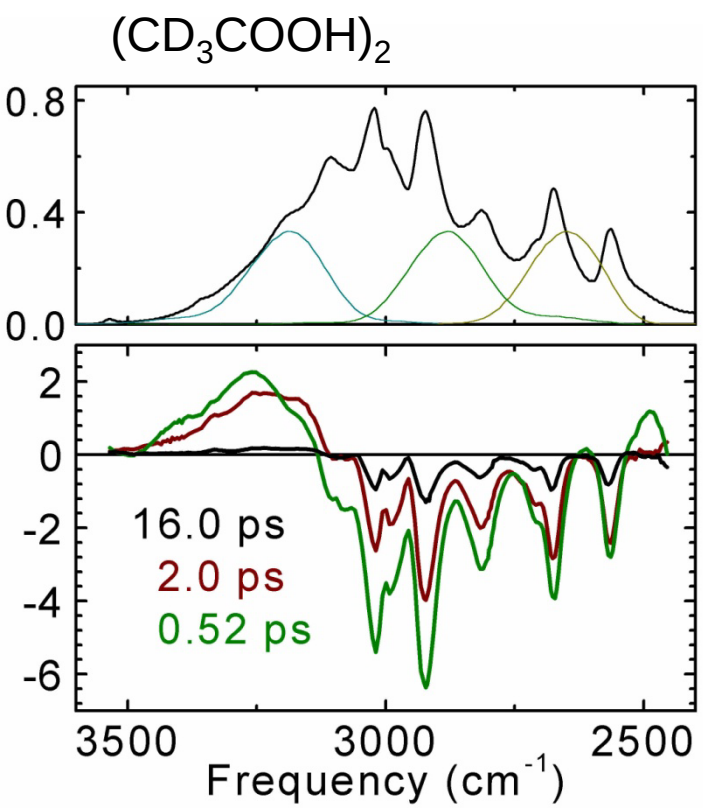

- No spectral diffusion
- Spectral width of holes: $T_2^{OH} \geq 180$ fs

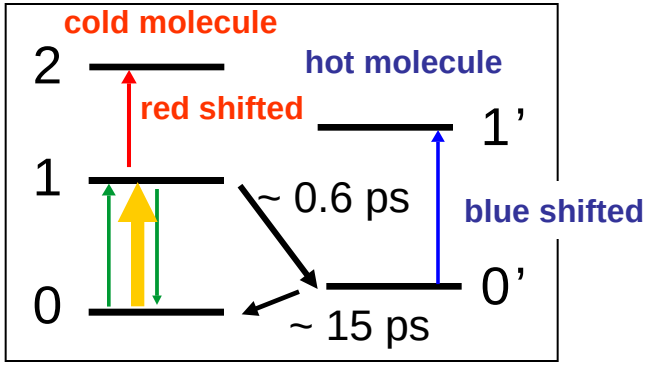

Excited state of the O-H stretching vibration

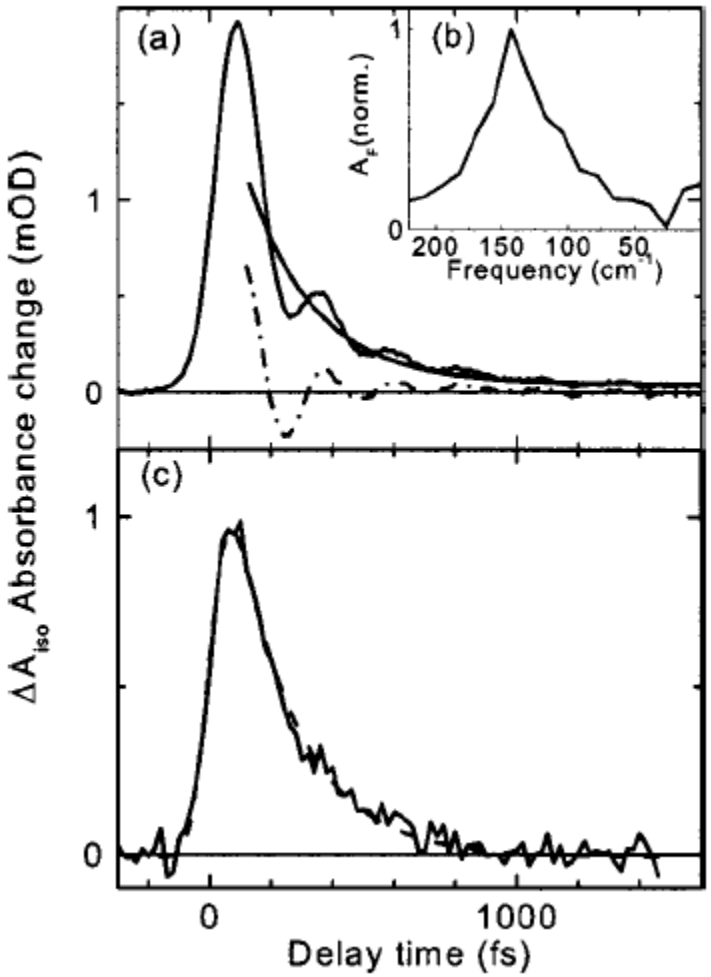

Excited state lifetime (ν=1): 200 fs
oscillation frequency ~ 160 cm^{-1}

Where does the energy go?

What is the relaxation channel?

Time - resolved pump-probe signals

$(CH_3COOD)_2$:

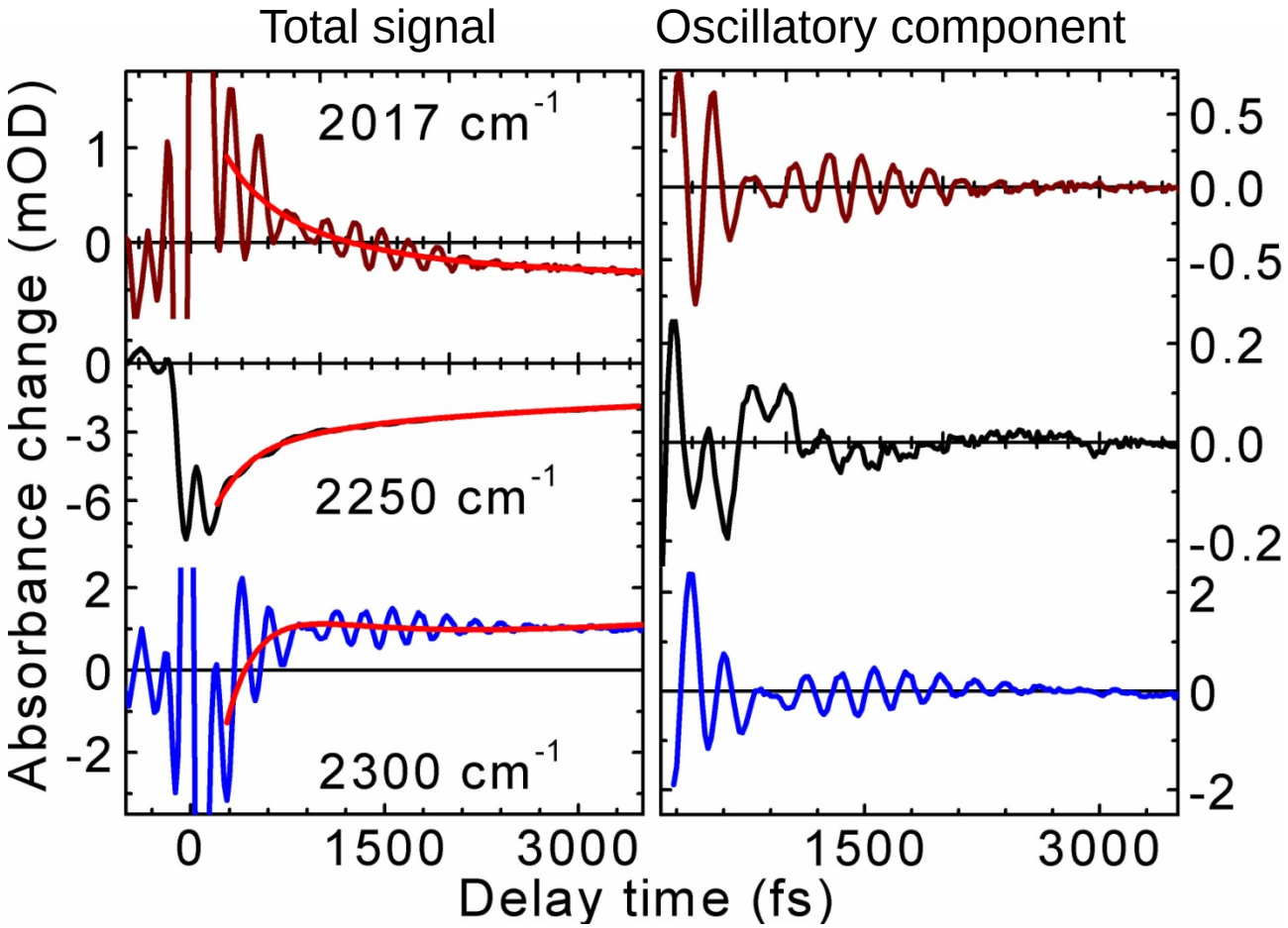

- Pronounced beating pattern indicate two different oscillation frequencies
- Damping of the oscillations: Dephasing times of about 1 ps

K. Heyne et al., Chem. Phys. Lett. 369 (2003) 591-596

Polarization interference; anharmonic and Davydov coupling

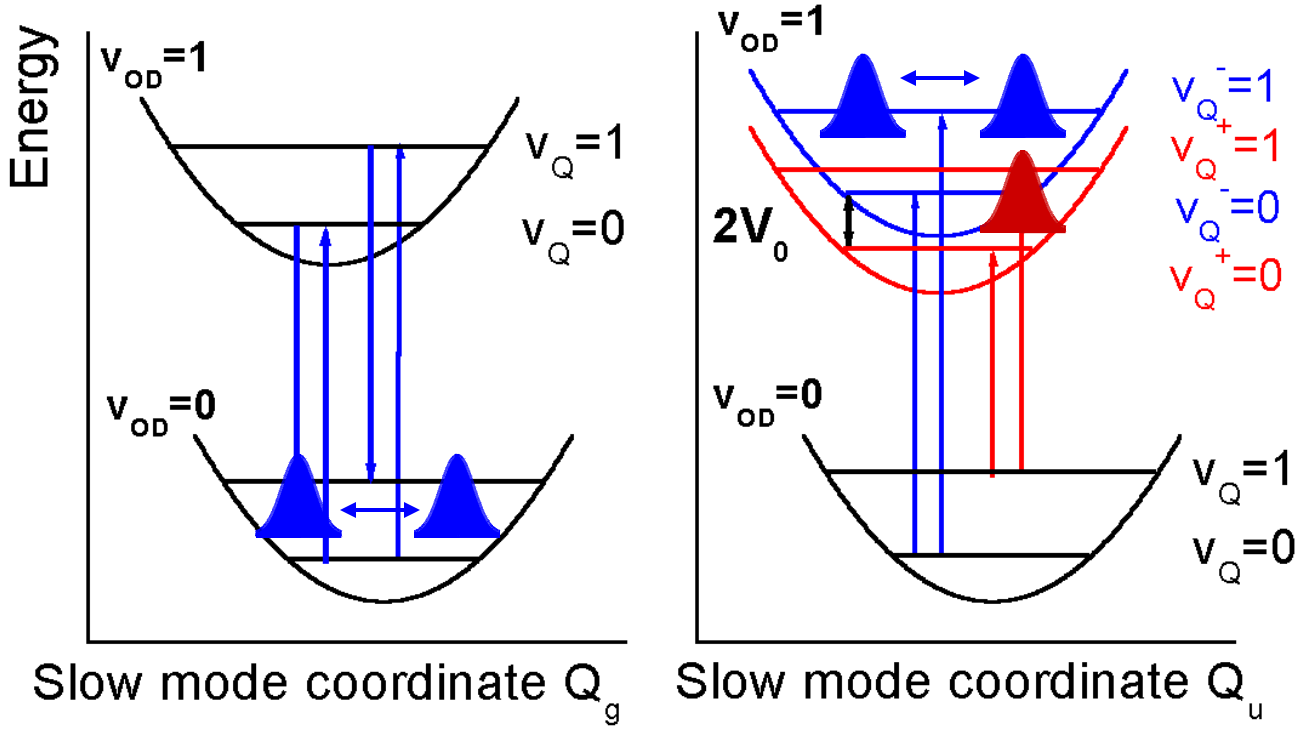

No oscillations due to excitonic coupling:

$$\Delta A(\omega) \propto -\omega \,\mathrm{Im}\left[\frac{P^{(3)}_{vQ=0}(\omega) + P^{(3)}_{vQ=1}(\omega)}{E_{pr}(\omega)}\right]$$

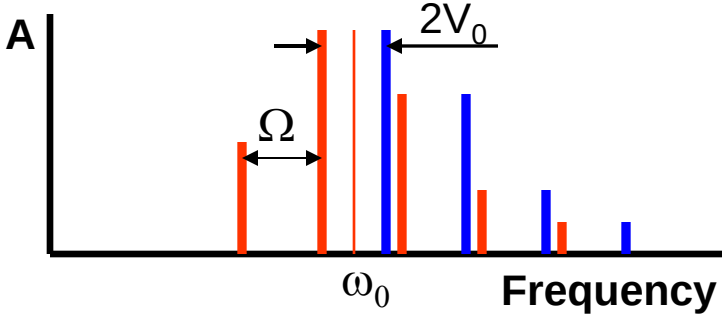

Oscillatory signals from mixed dimers

No excitonic coupling.

Single O-H

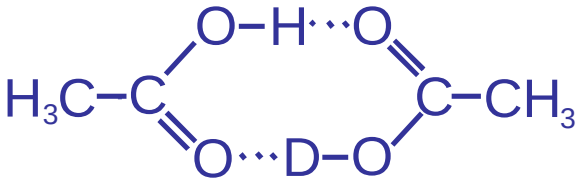

Single O-D

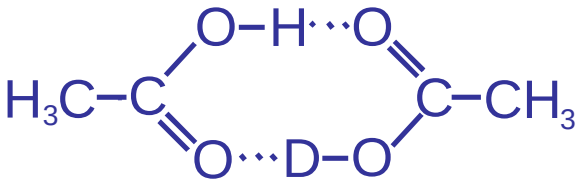

Identical oscillations.

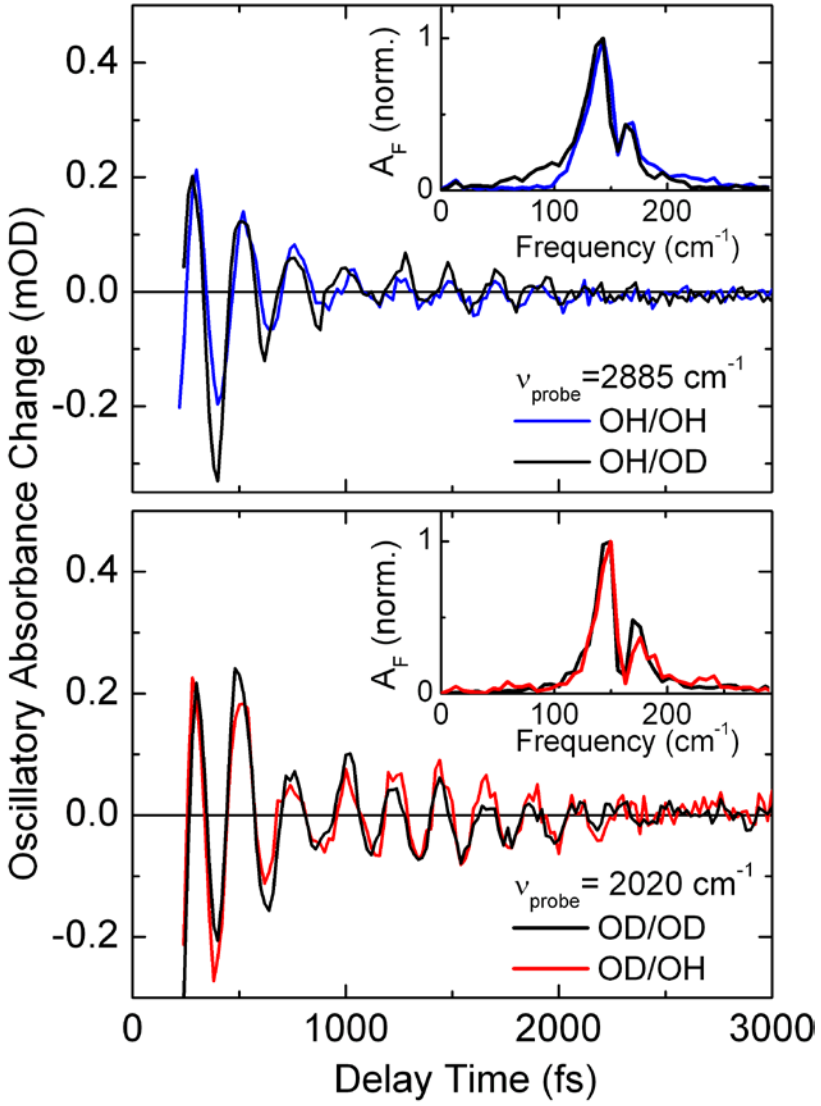

Dephasing of Coherent O-H Stretching Excitations

No excitonic coupling

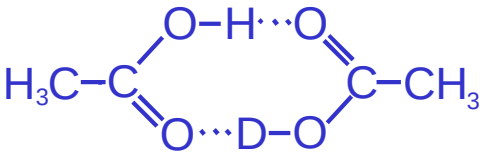

Excitonic coupling

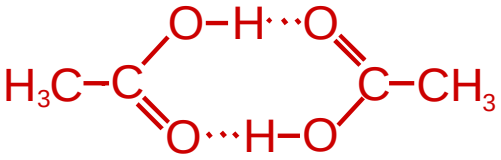

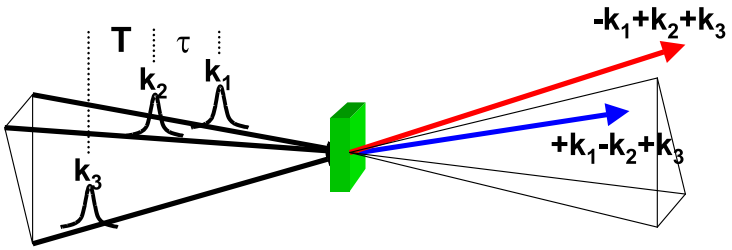

2-pulse photon echoes: T=0.

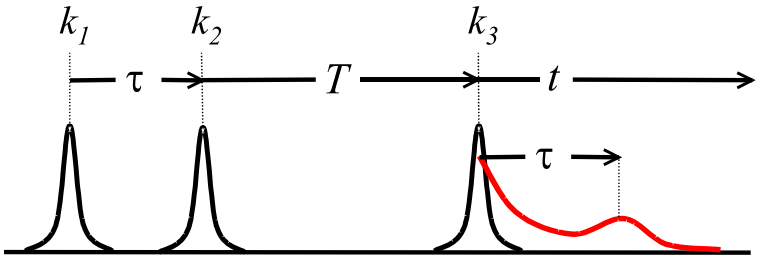

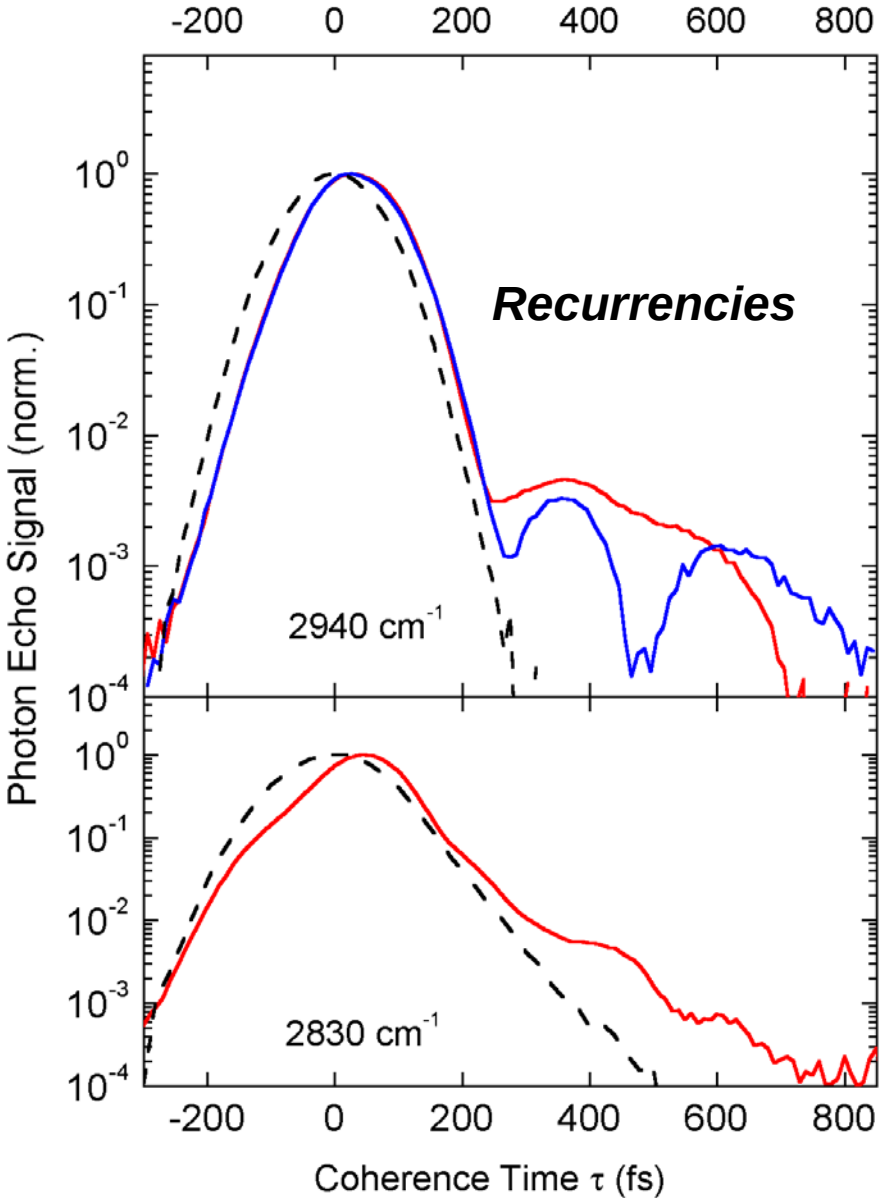

Dephasing of Coherent O-H Stretching Excitations

Simulations with one (dash-dotted line) and two (solid line) low-frequency modes and measured data (dots)

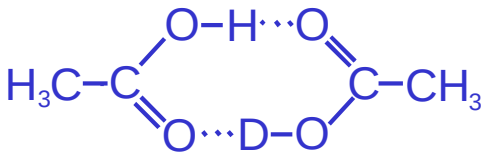

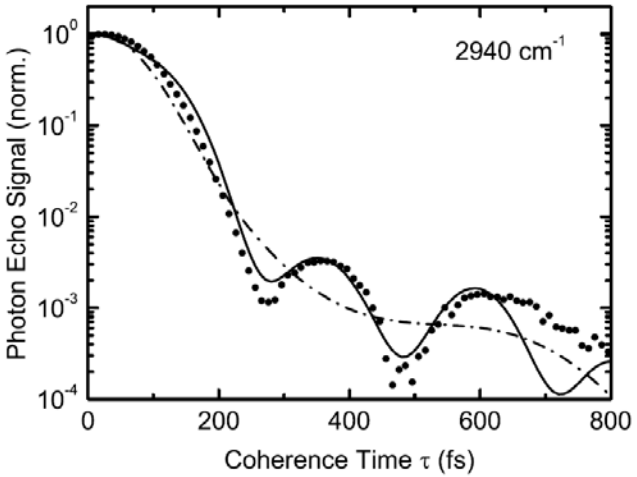

FIG. 3. Two-pulse photon-echo signals calculated as a function of coherence time for homodyne detection. In addition to the O-H stretching mode, the calculation includes two low frequency modes at 50 and 150 cm^{-1} (anharmonic coupling $\alpha_{50} = 0.2$, $\alpha_{150} = 0.7$, solid line) or a single 50 cm^{-1} mode ($\alpha_{50} = 0.2$, dash-dotted line, dephasing time $T_2^{OH} = 200$ fs). Symbols: Experimental result [cf. Figure 2(a)].

Dephasing of Coherent O-H Stretching Excitations

Multi-level character of O-H stretching excitation results in multi-level coherences:

- **Quantum beats due to anharmonic coupling to low-frequency modes**
- **Less relevant: Polarization interferences due to excitonic coupling.**

Simulations: density matrix approach (sum over states)

O-H stretching mode (T2=200 fs) + 2 low-frequency modes 50,150 cm^{-1} (T2=1 ps)

O-H stretching mode + 1 low-frequency mode at 50 cm^{-1}

O-H stretching mode

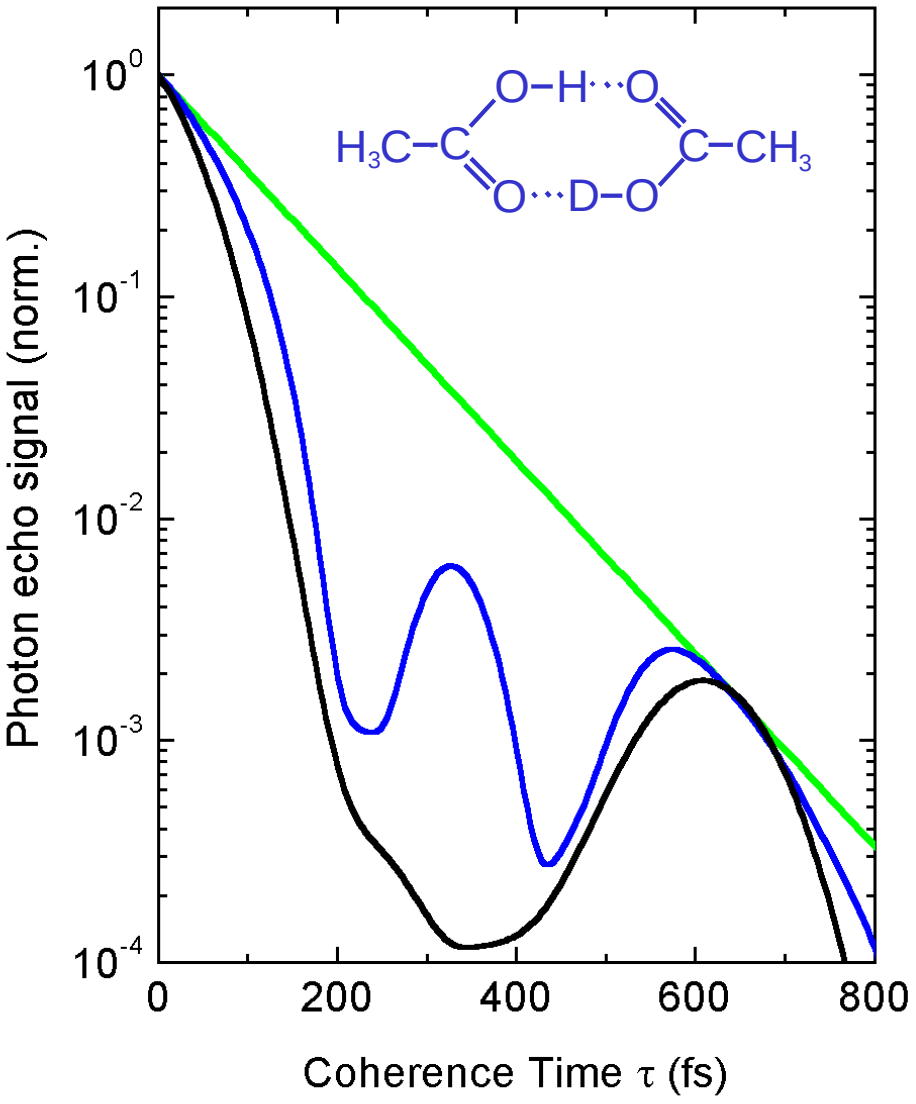

Time - resolved pump-probe signals

$(CH_3COOD)_2$:

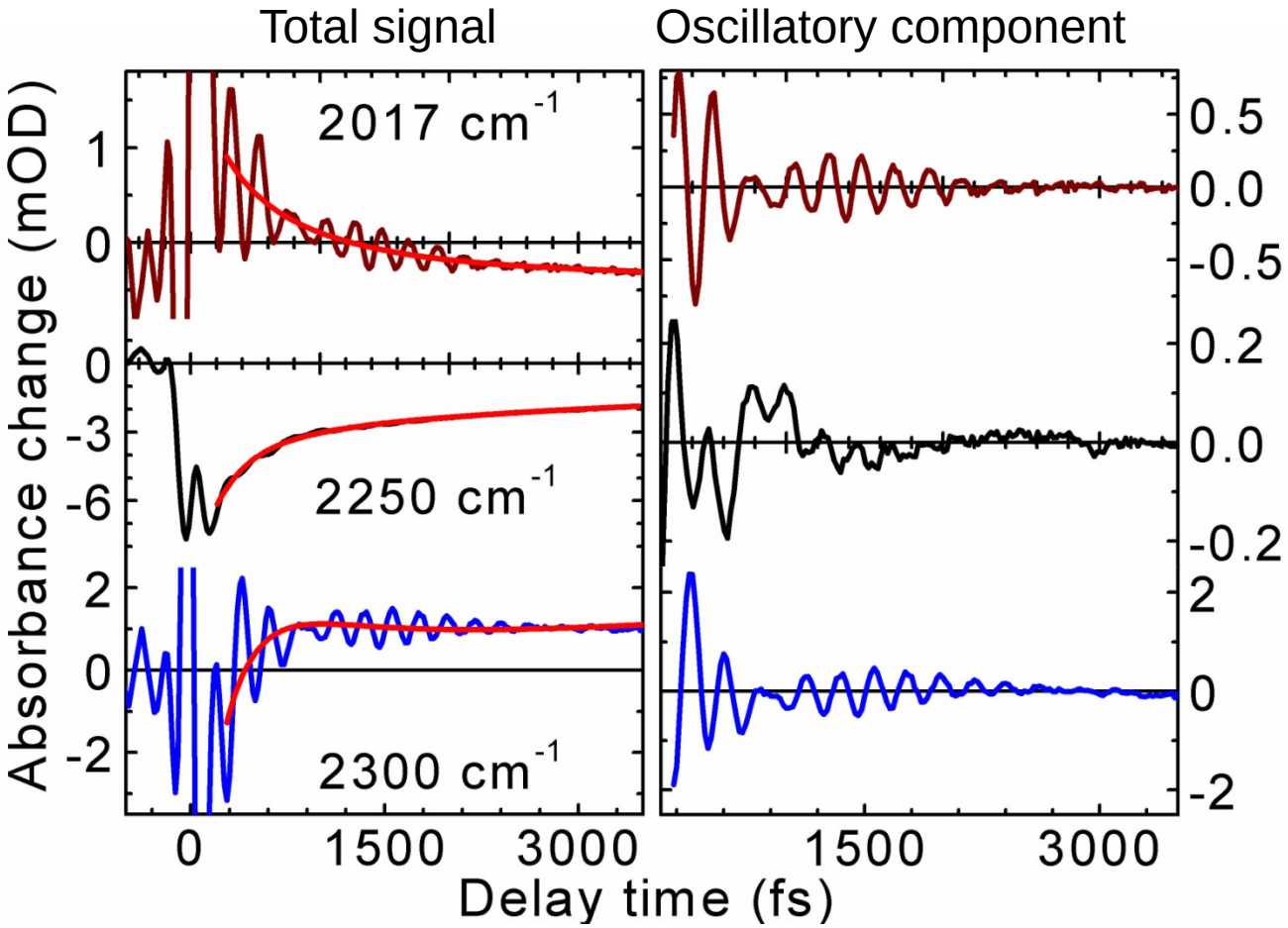

- Pronounced beating pattern indicate two different oscillation frequencies
- Damping of the oscillations: Dephasing times of about 1 ps

K. Heyne et al., Chem. Phys. Lett. 369 (2003) 591-596

Raman-active low-frequency modes

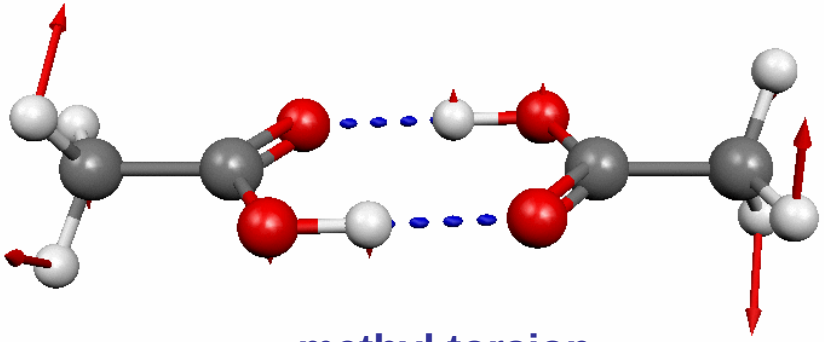

τ_{bg} **methyl torsion**

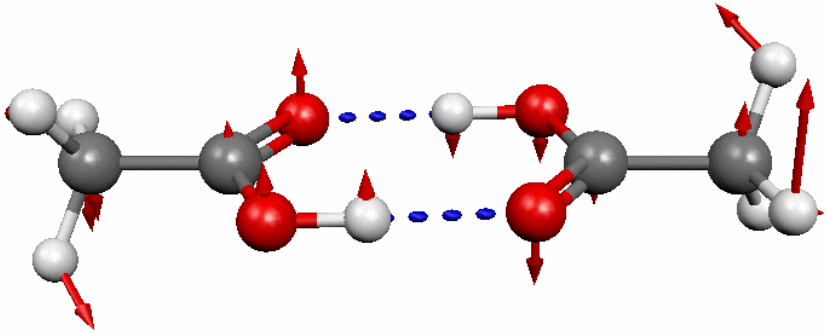

γ_{bg} **dimer oop wagging**

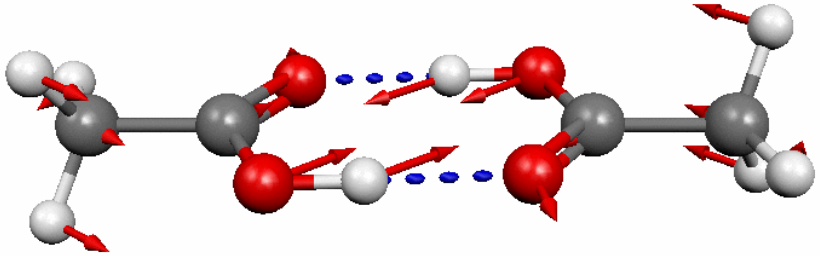

δ_{ag} **dimer ip bending**

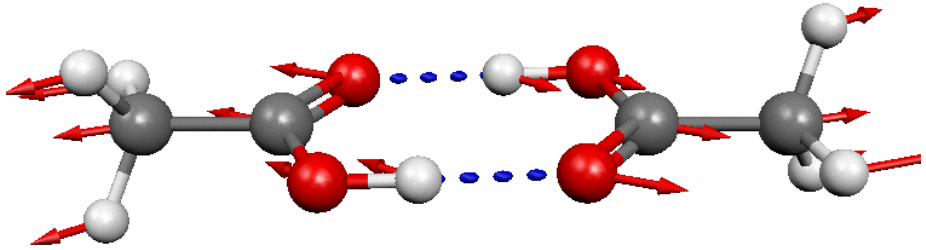

ν_{ag} **dimer ip stretching**

Origin of the coherent oscillations

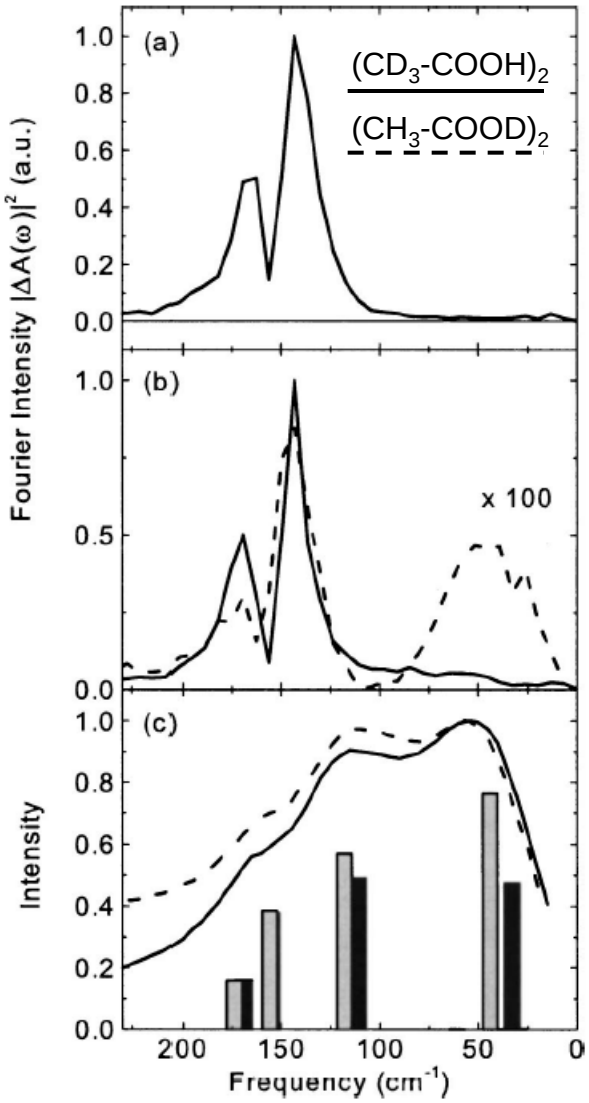

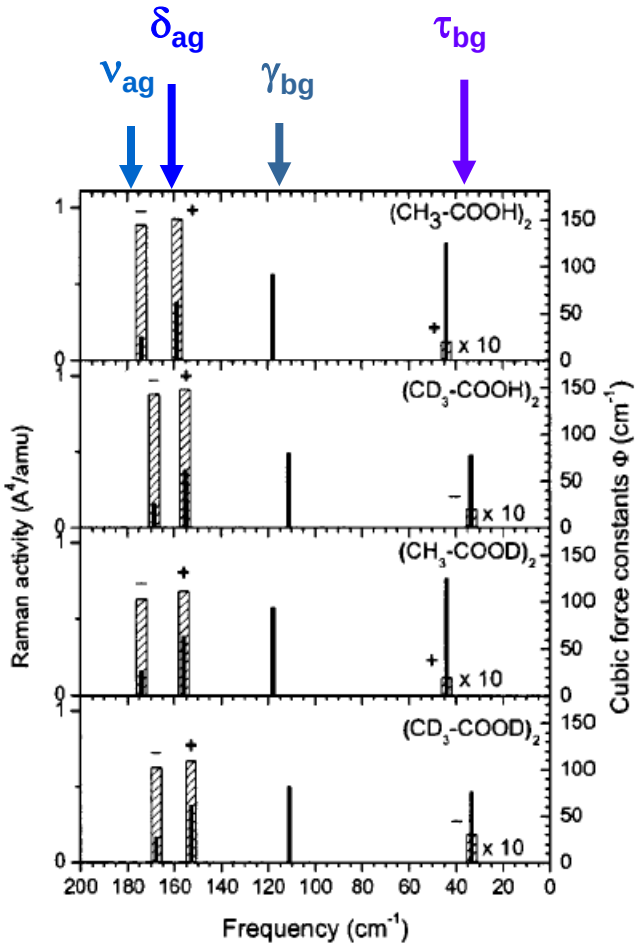

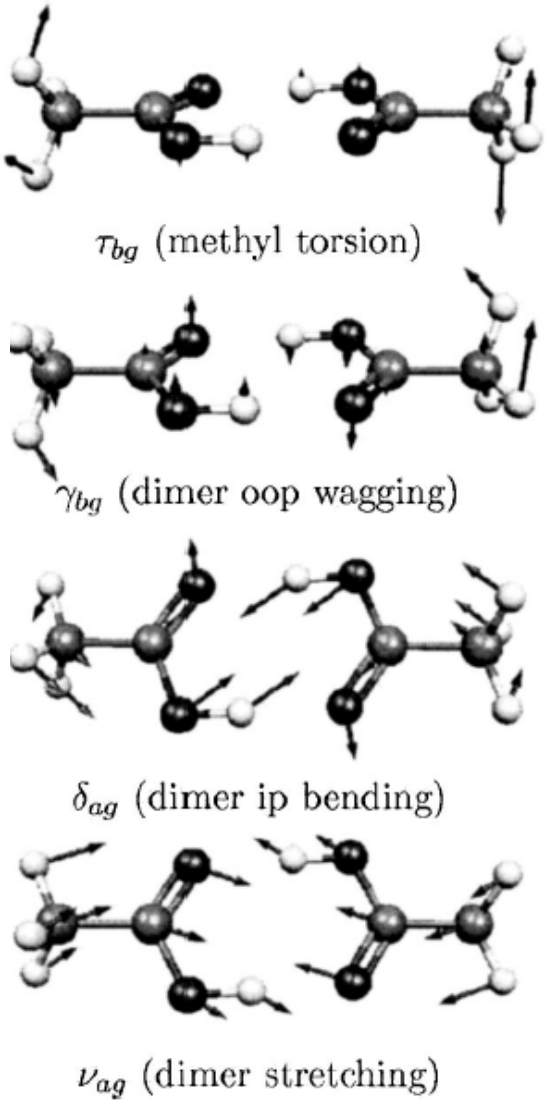

Fermi resonance

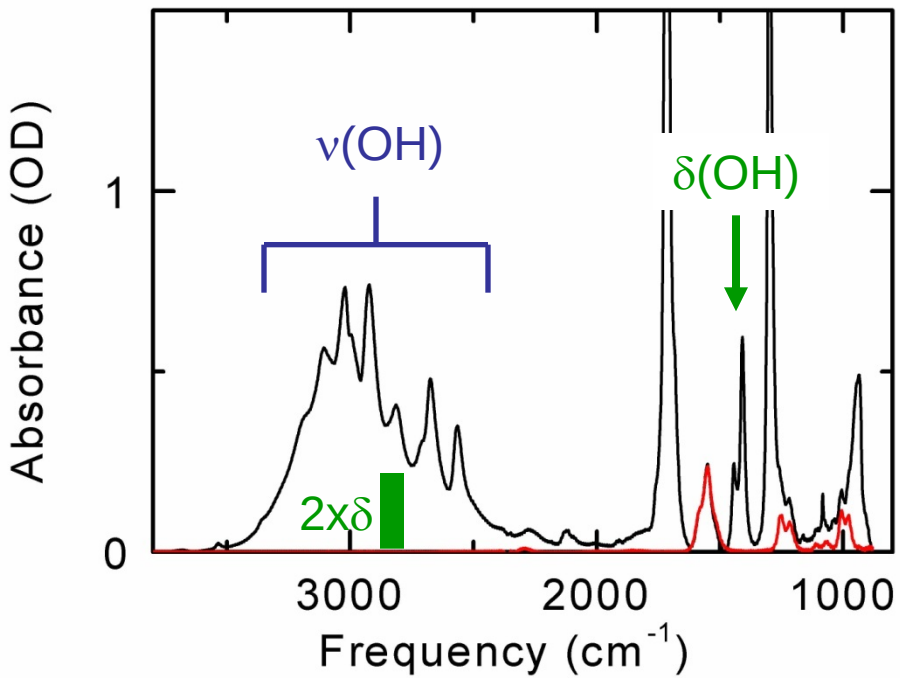

What is the role of the OH bending mode for intra- and intermolecular vibrational energy redistribution?

Is there an impact of Fermi resonances on the dynamics?

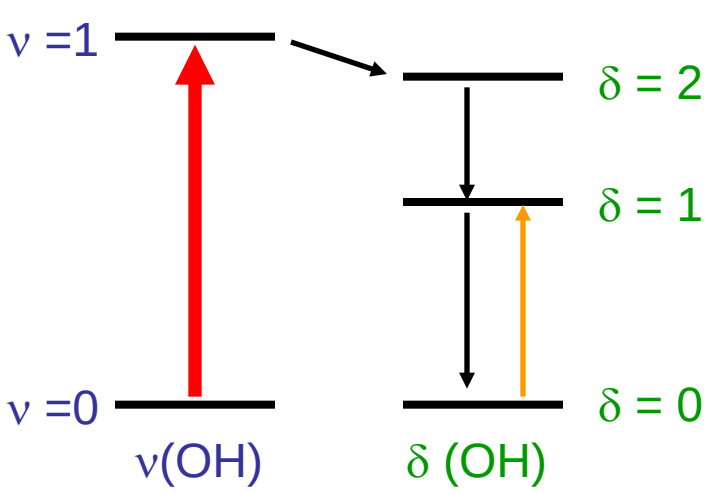

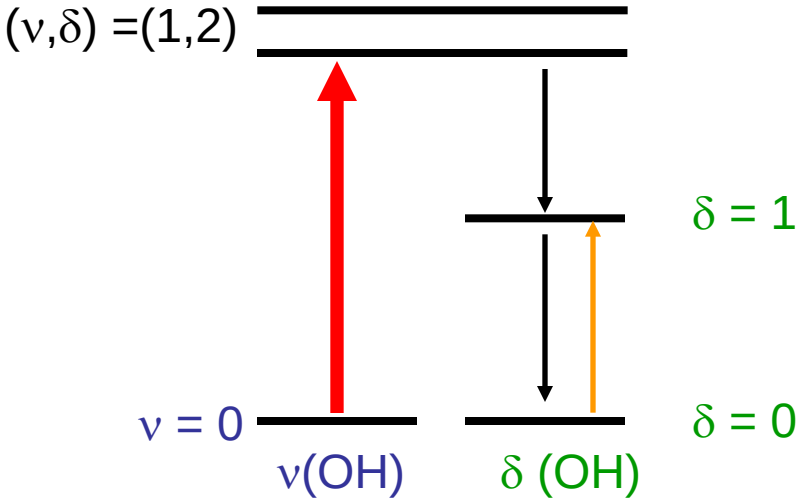

Coupling to O-H bending and C-O stretching modes

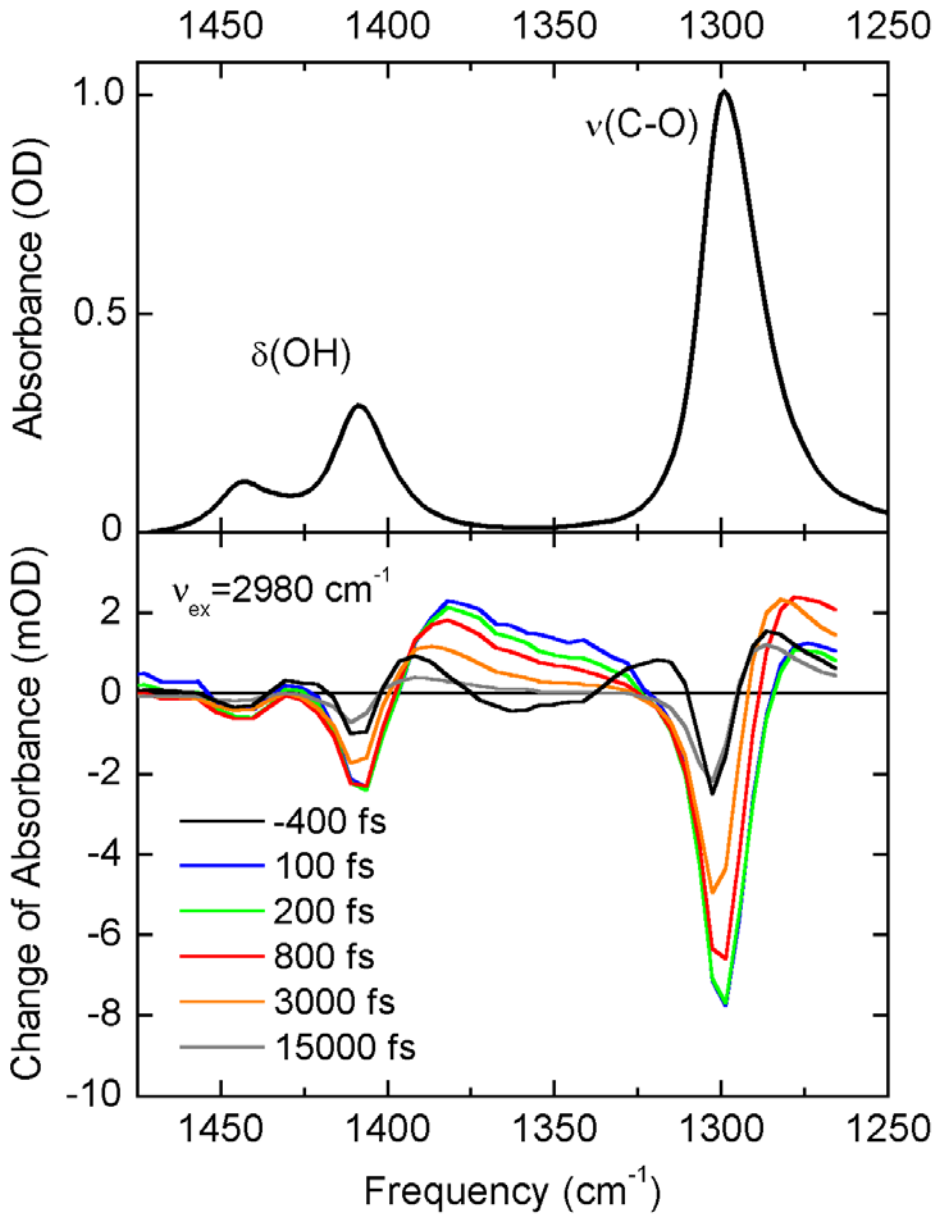

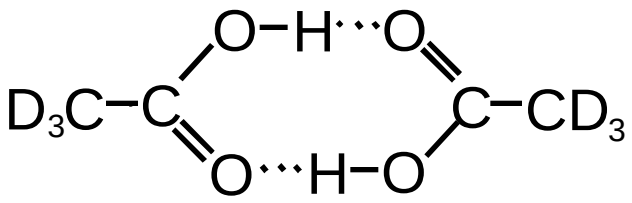

Excite O-H stretch (ν_{ex}=2980 cm^{-1})

Probe δ(OH) and ν(C-O).

- **Perturbed free induction decay on δ(OH) and ν(C-O) fundamentals.**
- **Similar rise of bleaching and enhanced absorption.**

Coupling to O-H stretching mode.

Direct O-H bending excitation

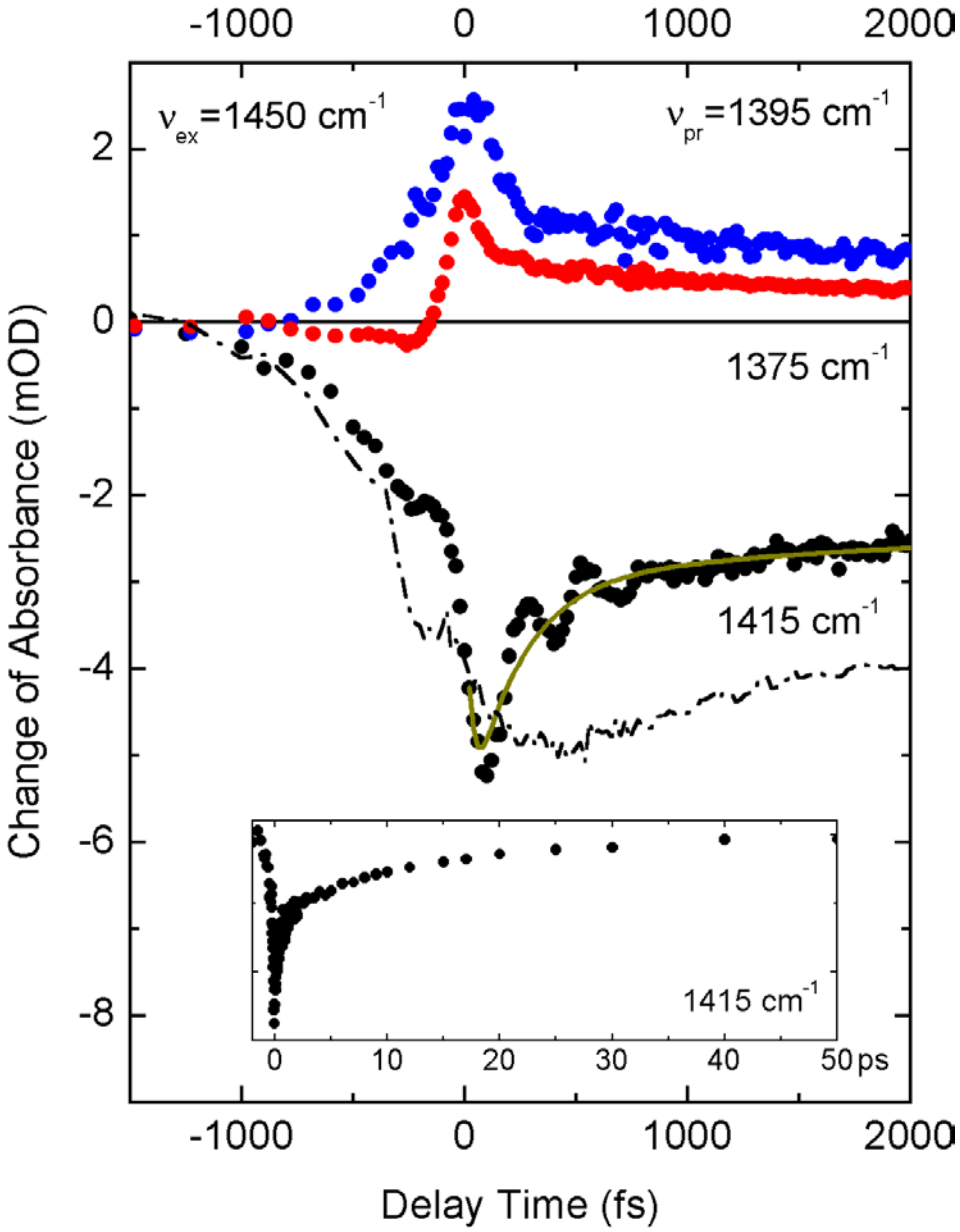

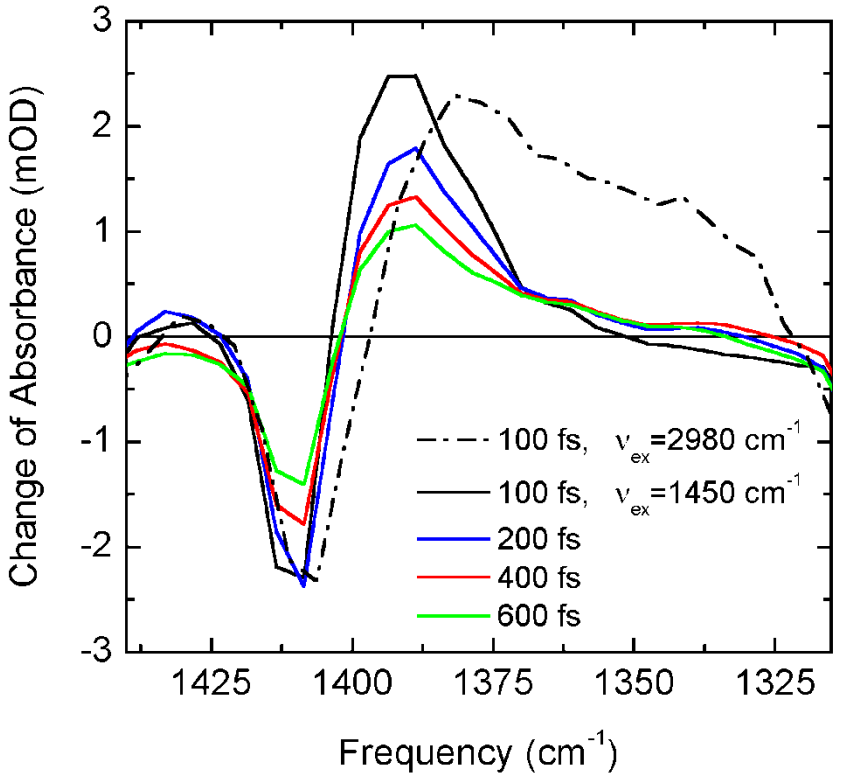

Perturbed free induct-ion decay: $T_2' \approx 500$ fs

Lifetime v=1 state $T_1 = 250$ fs

Vibrational cooling $T_r \approx 15$ ps

Coupling to O-H bending and C-O stretching modes

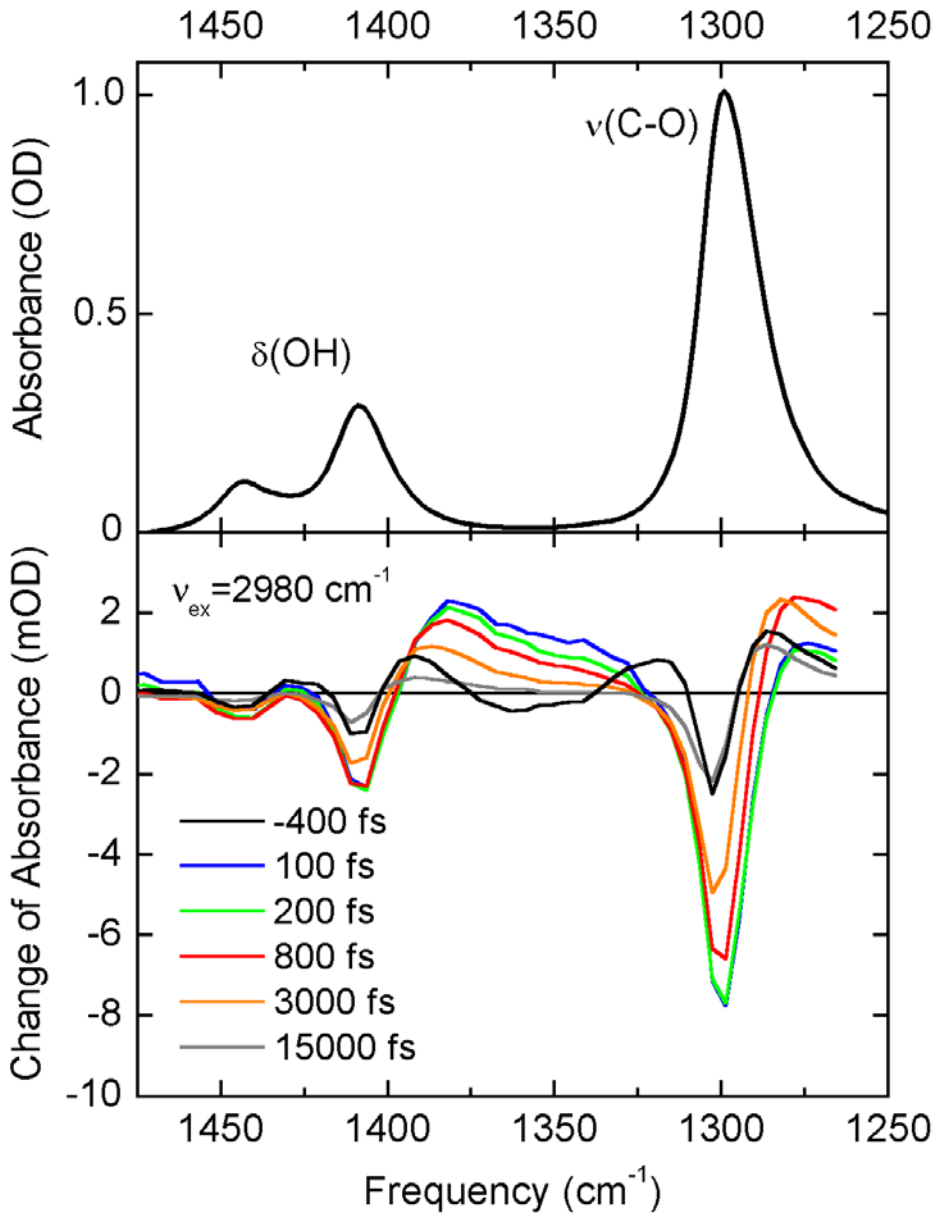

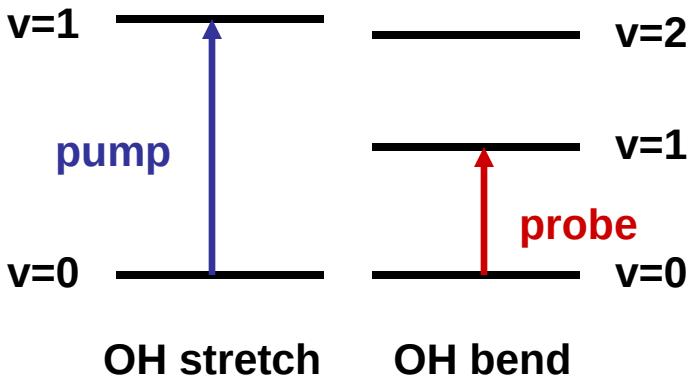

No indication of transient v≥1 populations of OH bending mode.

Our picture:

Red-shift of OH bend by excitation of other anharmonically coupled modes.
Early times: O-H stretch.
Late times: other (low-frequency) modes.

Fermi resonance coupling

IR

Raman

ν_{bu}C–O

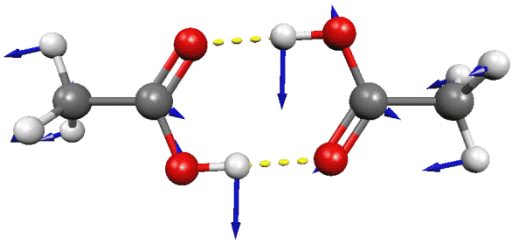

ν_{ag}C–O

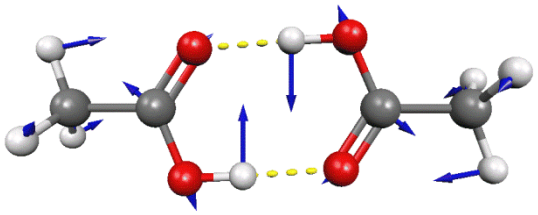

$\delta_{bu}CH_3$

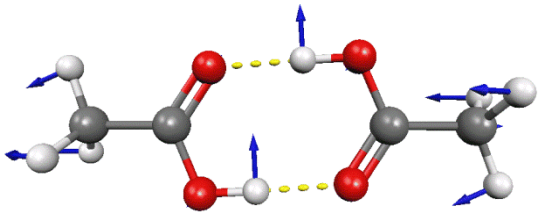

$\delta_{ag}CH_3$

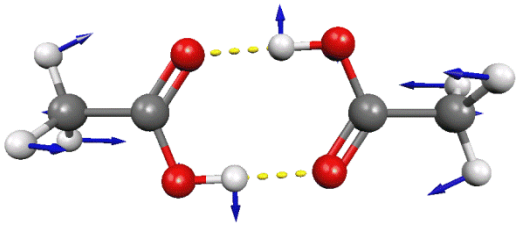

δ_{bu}O-H

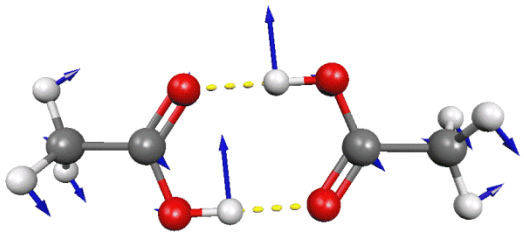

δ_{ag}O-H

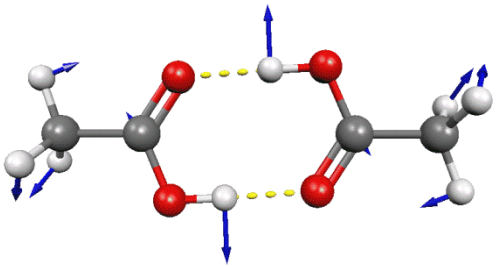

ν_{bu}C=O

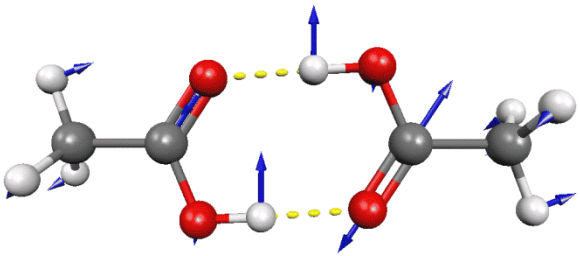

ν_{ag}C=O

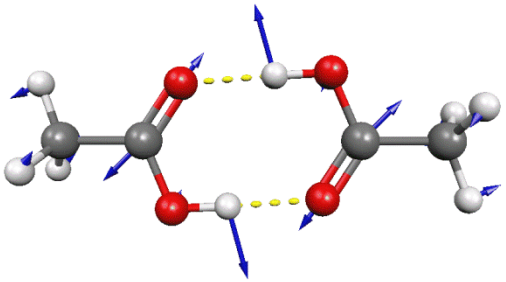

Intramolecular H-bond in PMME

PMME: Phthalic acid monomethyl ester

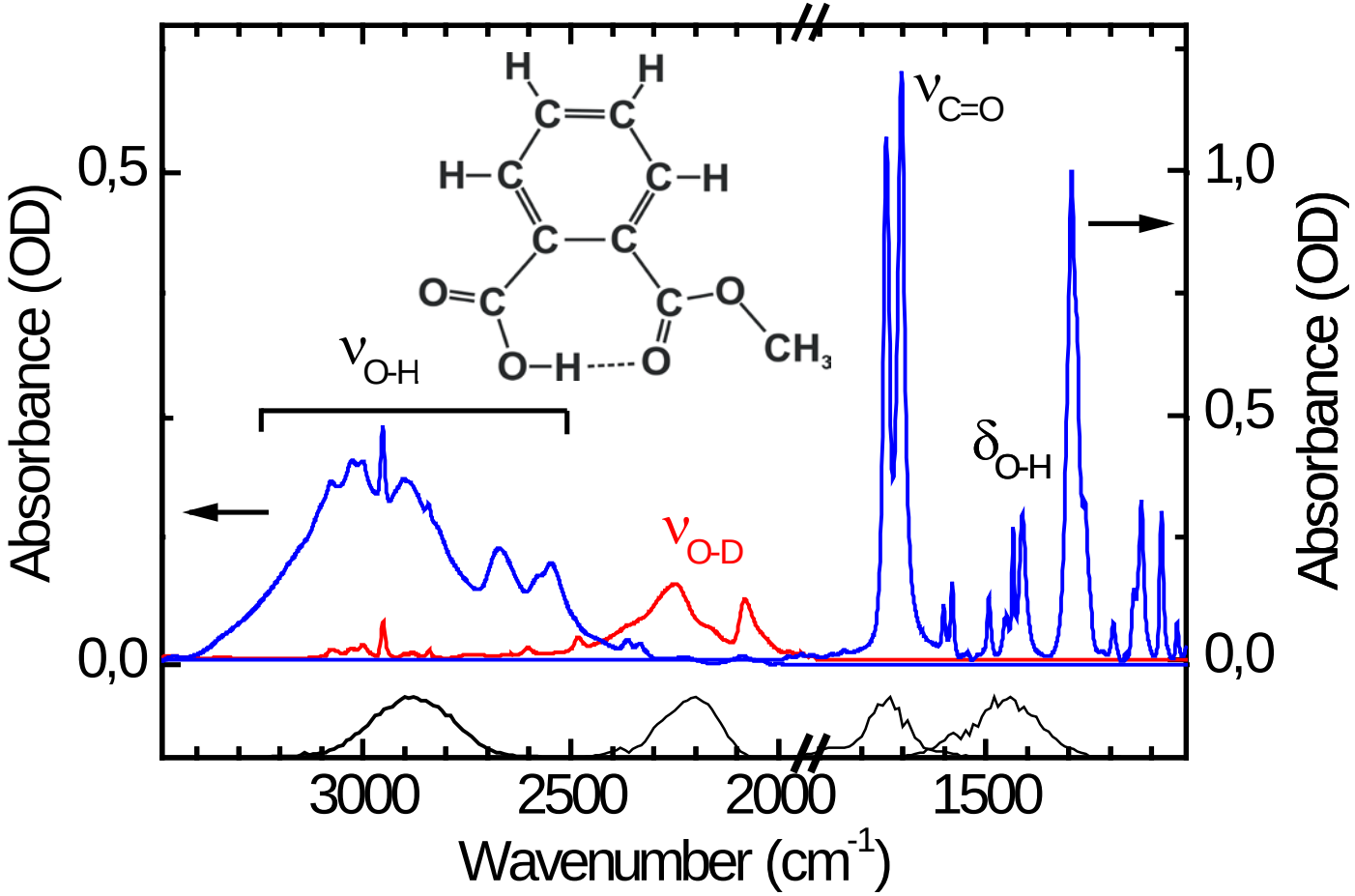

O-H stretch dynamics of a medium strong H-bond

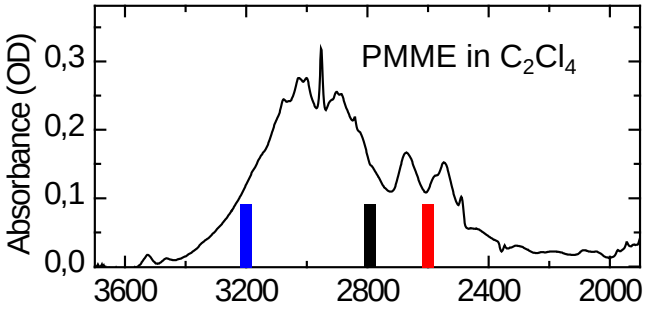

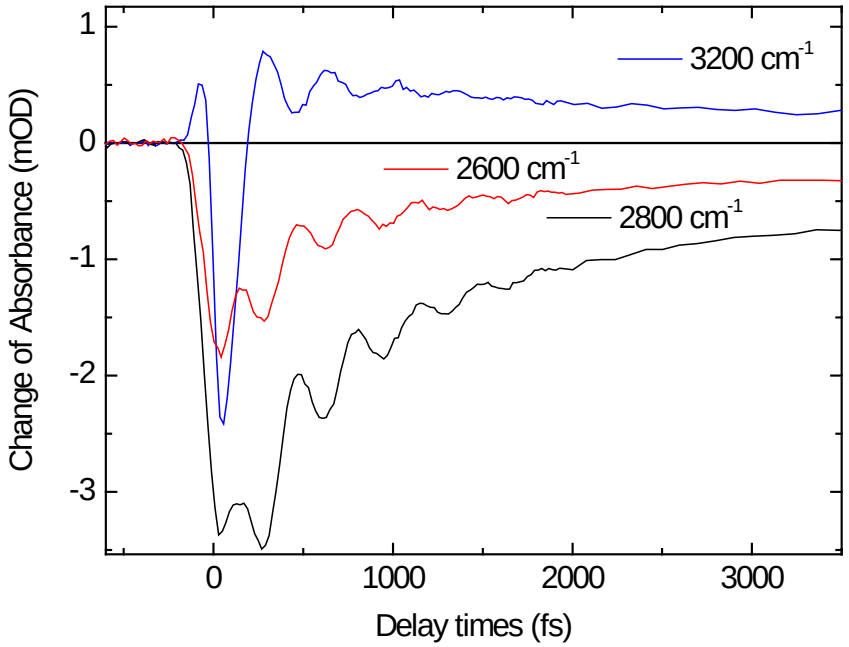

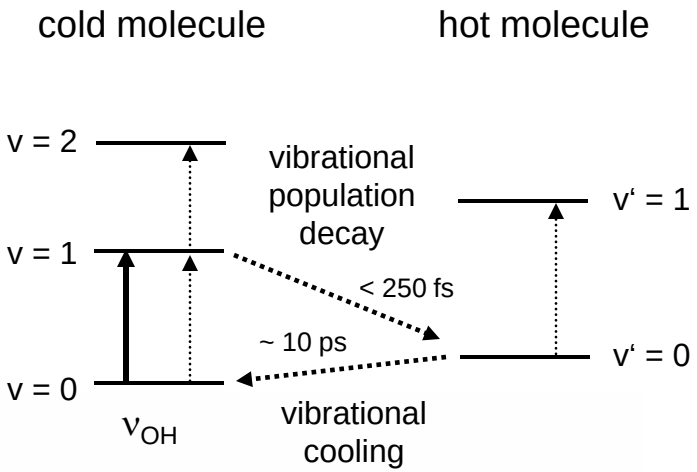

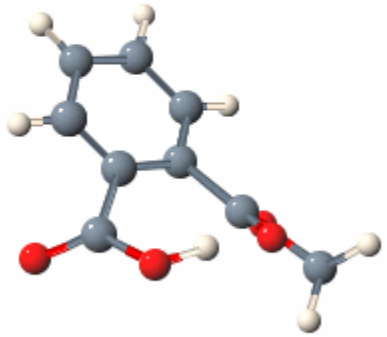

Low-frequency vibration

γ_{HB}

Madsen et al., Bull. Chem. Soc. Jpn., 75, 909 (2002)

Excited state O-H stretching vibration dynamics

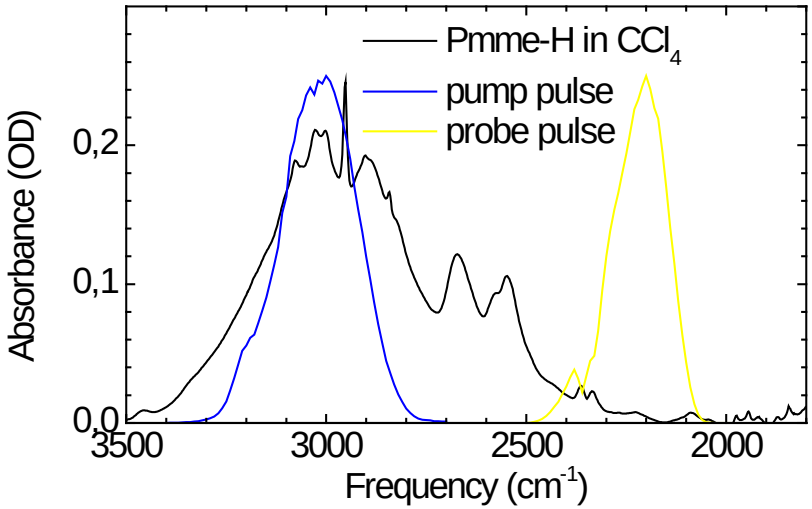

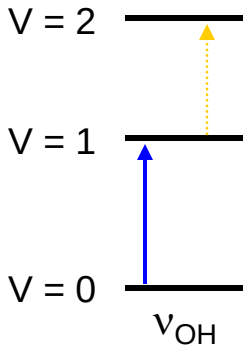

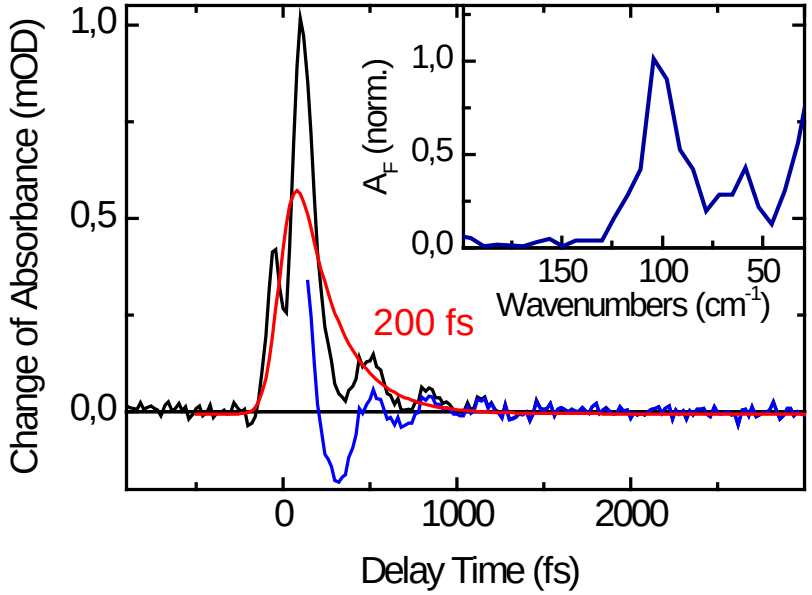

- v = 1 state of the ν_{OH} decays with 200 ± 80 fs
- coherent oscillations modulate the excited state dynamics with 100 cm^{-1}

Pump-probe experiments on PMME

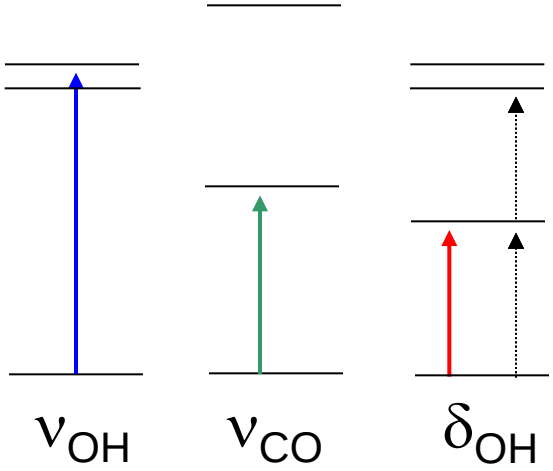

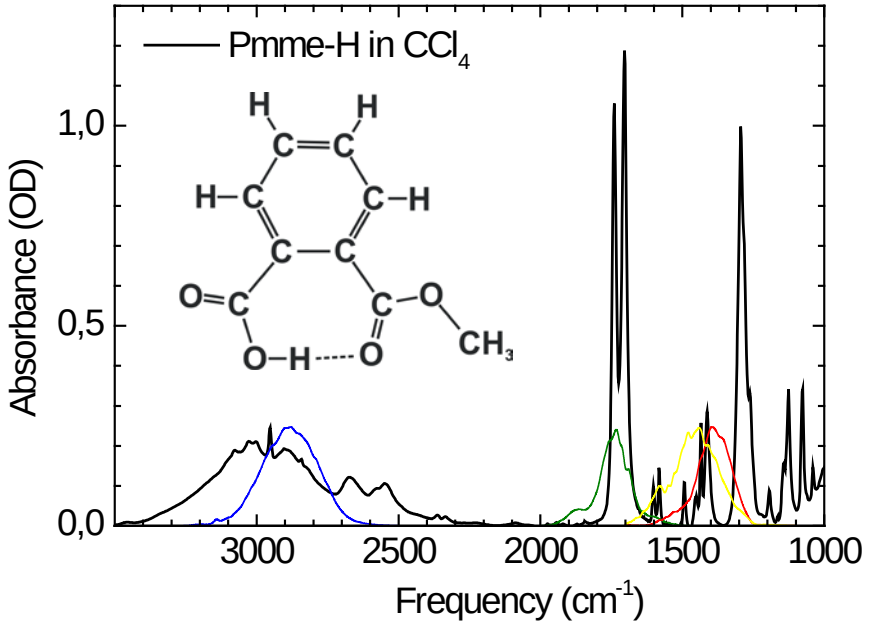

I. excite ν_{OH} ; probe δ_{OH}

II. excite δ_{OH} ; probe δ_{OH}

III. excite ν_{CO} ; probe δ_{OH}

Transient difference spectra

Spectral region of the δ_{OH} and δ_{CH3} absorption bands after excitation of the ν_{OH} (I), δ_{OH} (II) and $\nu_{C=O}$ (III) vibrations

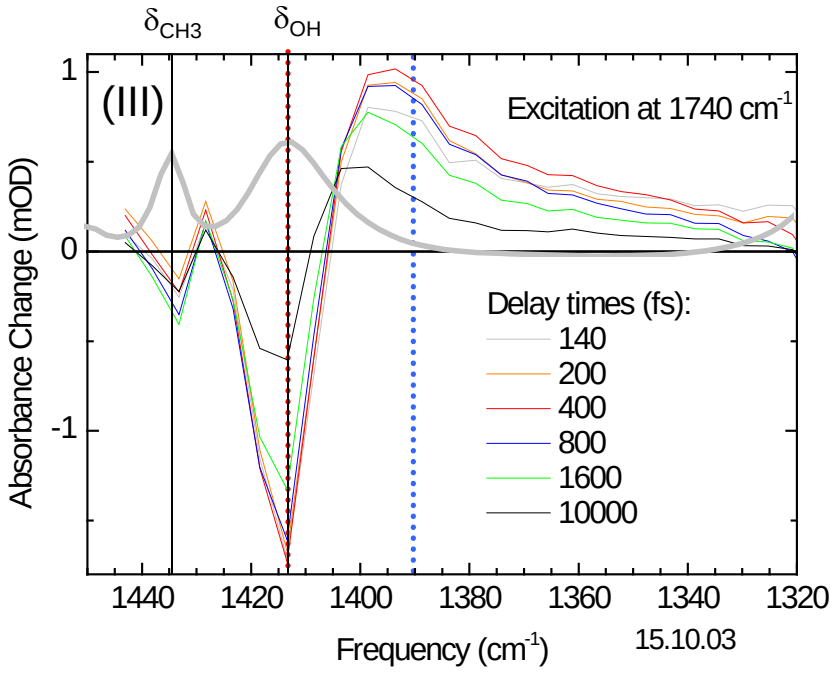

- Similar dynamics for excitation (I) and (II)
- Fast component around 1415 cm^{-1} and 1390 cm^{-1} in (III) is missing

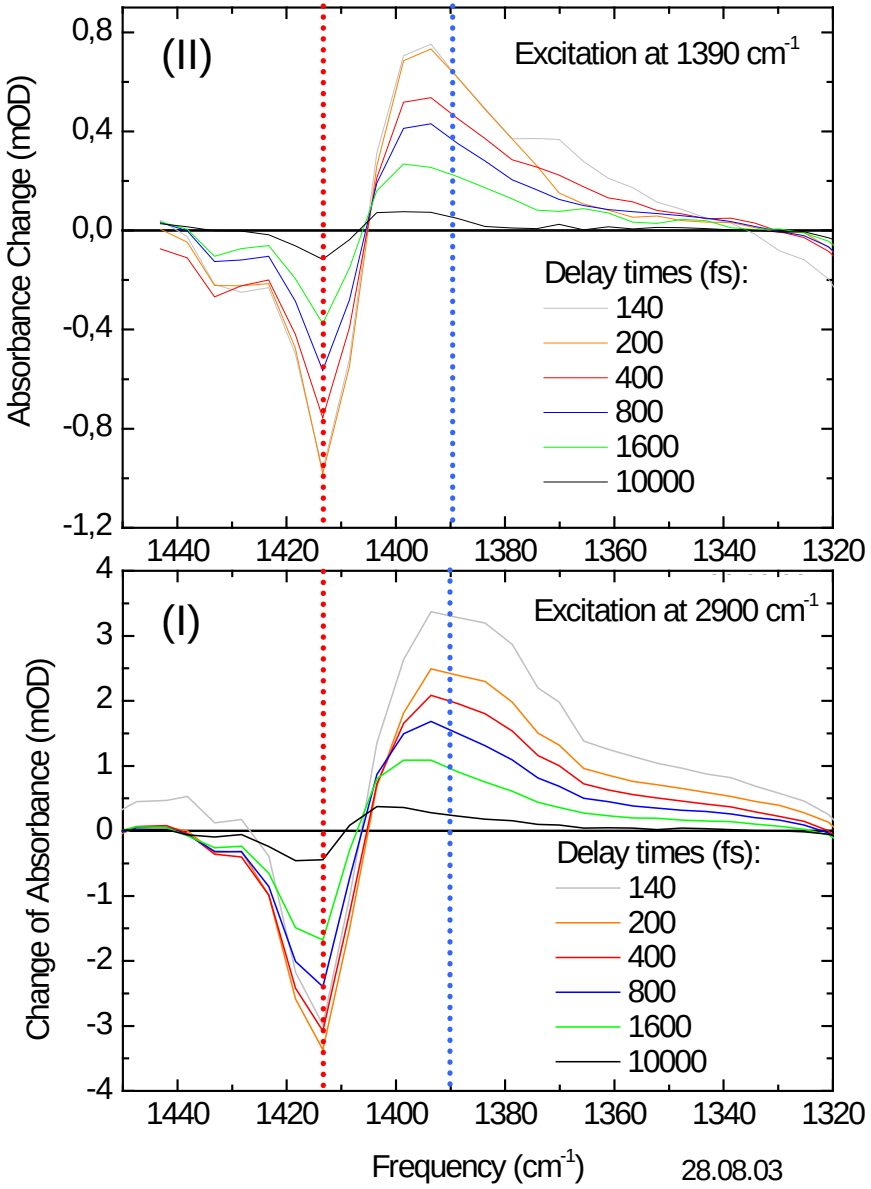

Dynamics at selected frequency positions

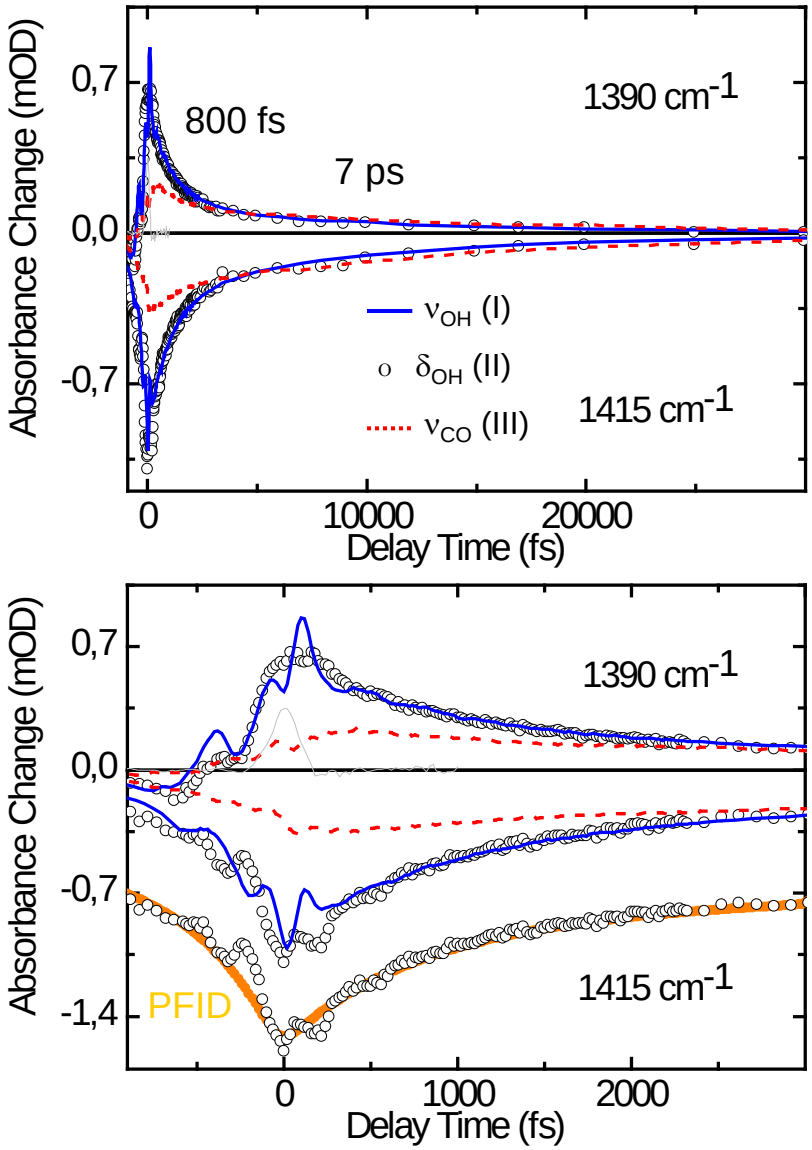

- negative and positive signals exhibit exhibit similar dynamics
- cooling of the δ_{OH} with about 7± 1 ps
- v = 1 decay of the δ_{OH} with 800 ± 100fs
- Perturbed free induction decay PFID with 550 fs ~ 19 cm^{-1} (18 cm^{-1} linewidth)
- upon ν_{CO} excitation only cooling
- after δ_{OH} and ν_{OH} excitation population of the v = 1 of the δ_{OH} vibration
- More than 30% of the δ_{OH} v = 1 level is populated after ν_{OH} excitation
- Efficient energy relaxation channel

Energy relaxation in PMME

Energy is redistributed from the OH stretching vibration over the OH bending vibration into lower energy modes

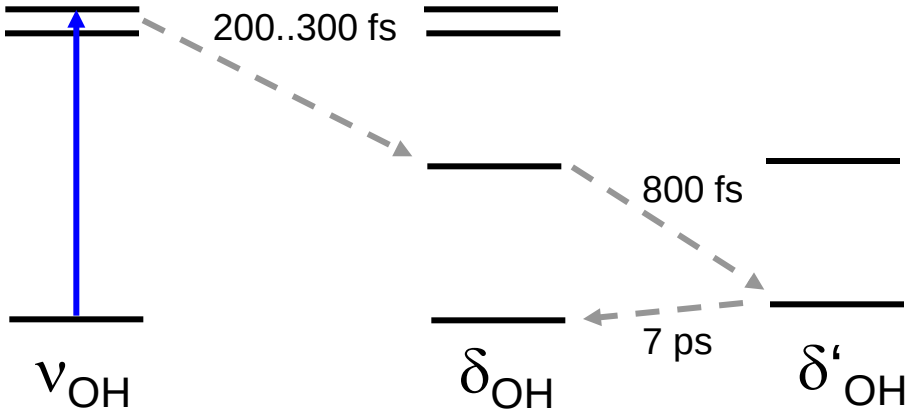

Energy relaxation channel from ν_{OH} involving the δ_{OH} v = 1 state is very efficient

Heyne et al. (2004)

Quantum chemistry calculations – model system

ν_{OH} = 3279 cm^{-1}

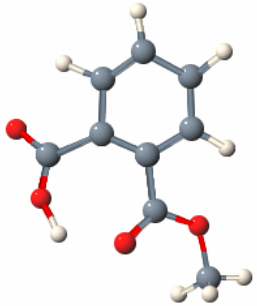

δ_{OH} = 1446 cm^{-1}

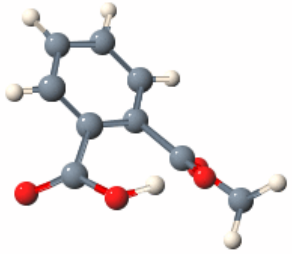

γ_{HB} = 39 cm^{-1}

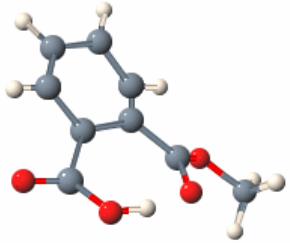

γ_{OH_1} = 785 cm^{-1}

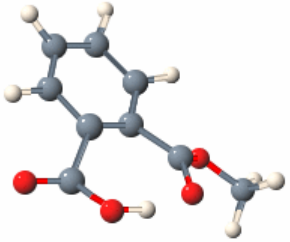

γ_{OH_2} = 682 cm^{-1}

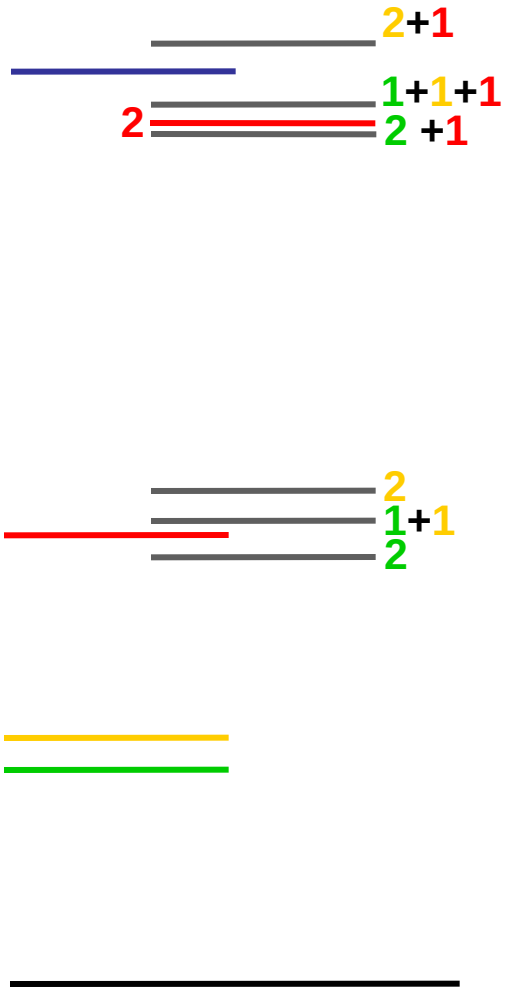

O-H stretching vibration

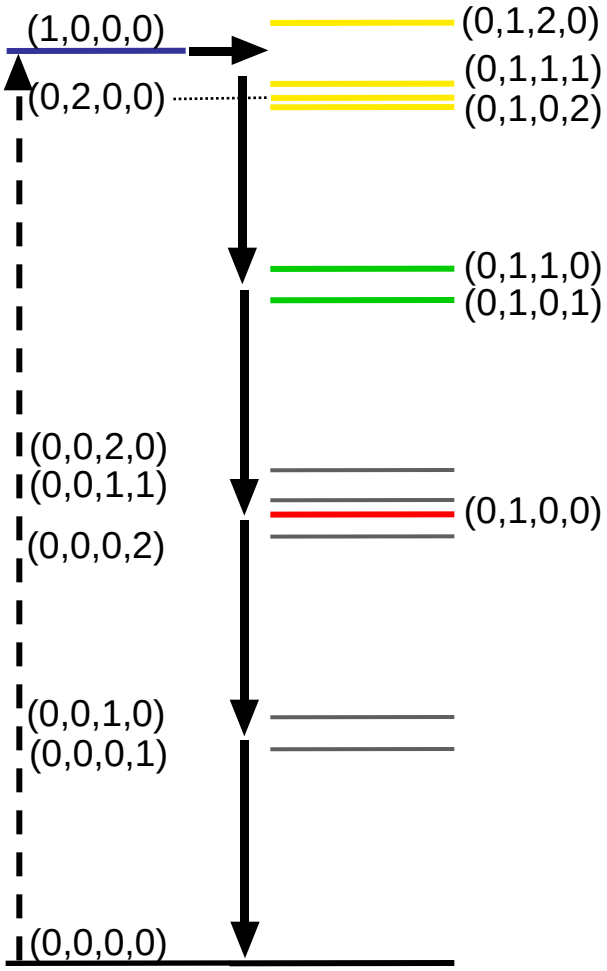

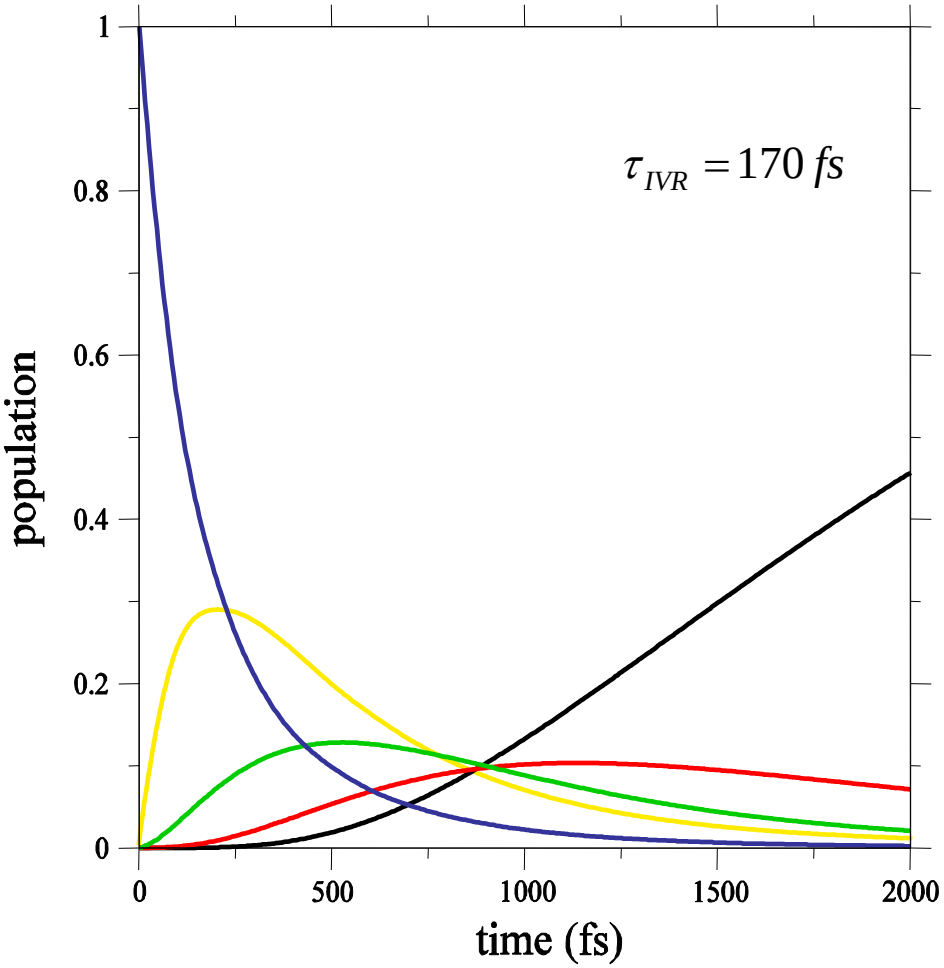

O-H bending vibration

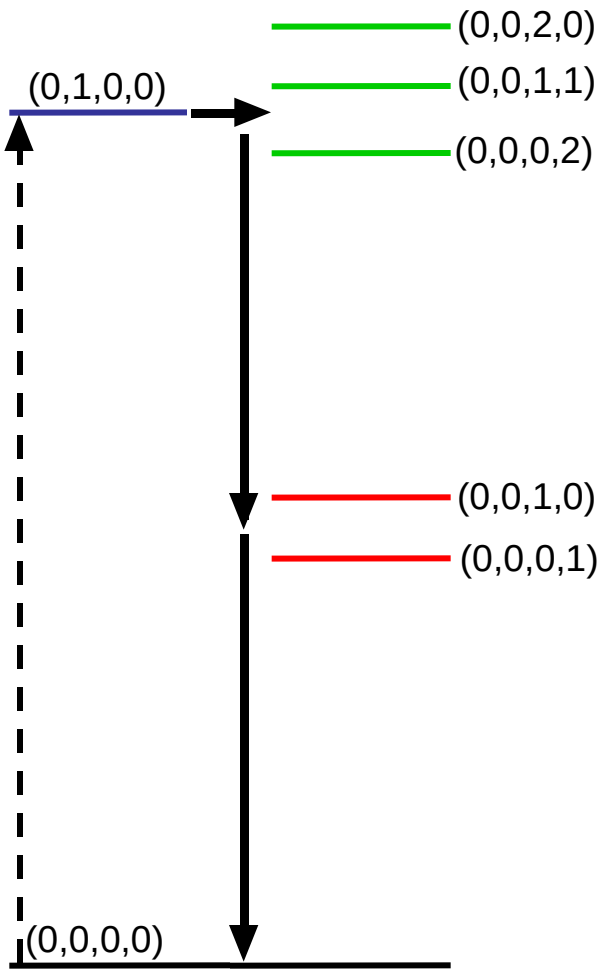

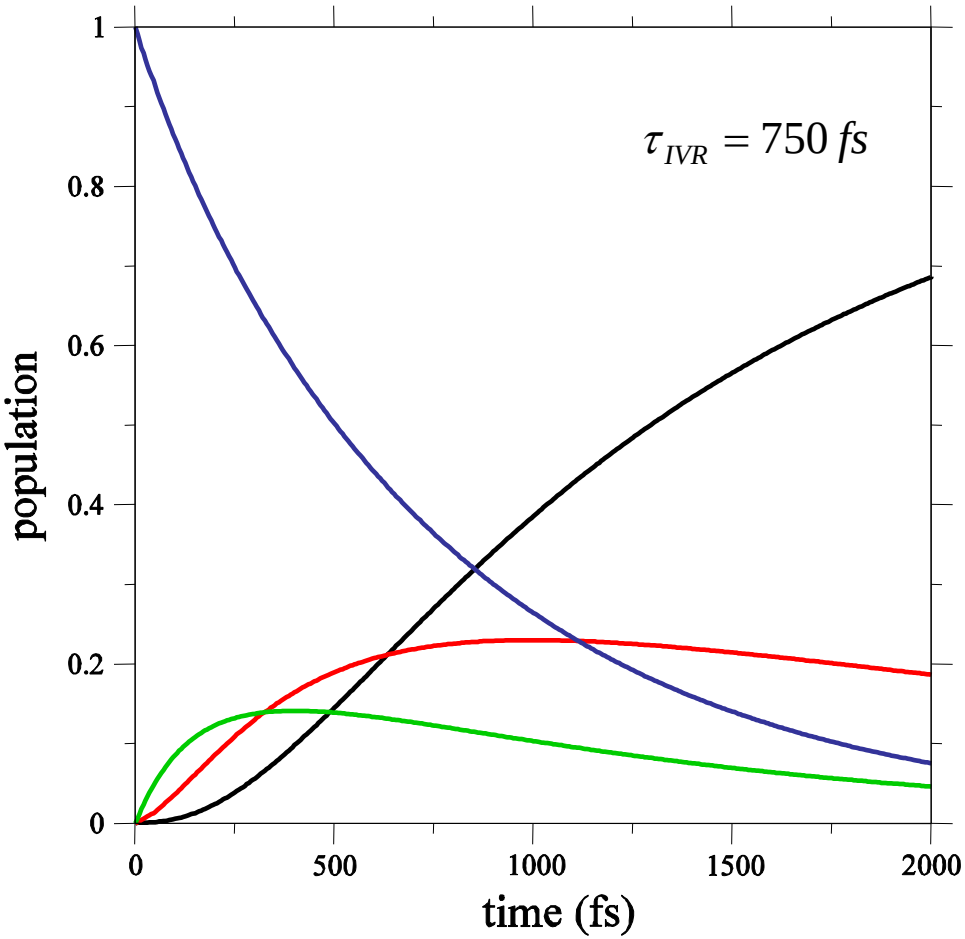

Part III

CARS and SRL microscopy

CARS: Coherent Anti-Stokes Raman Scattering
SRL: Stimulated Raman Loss; modulate ω_s, detect ω_p

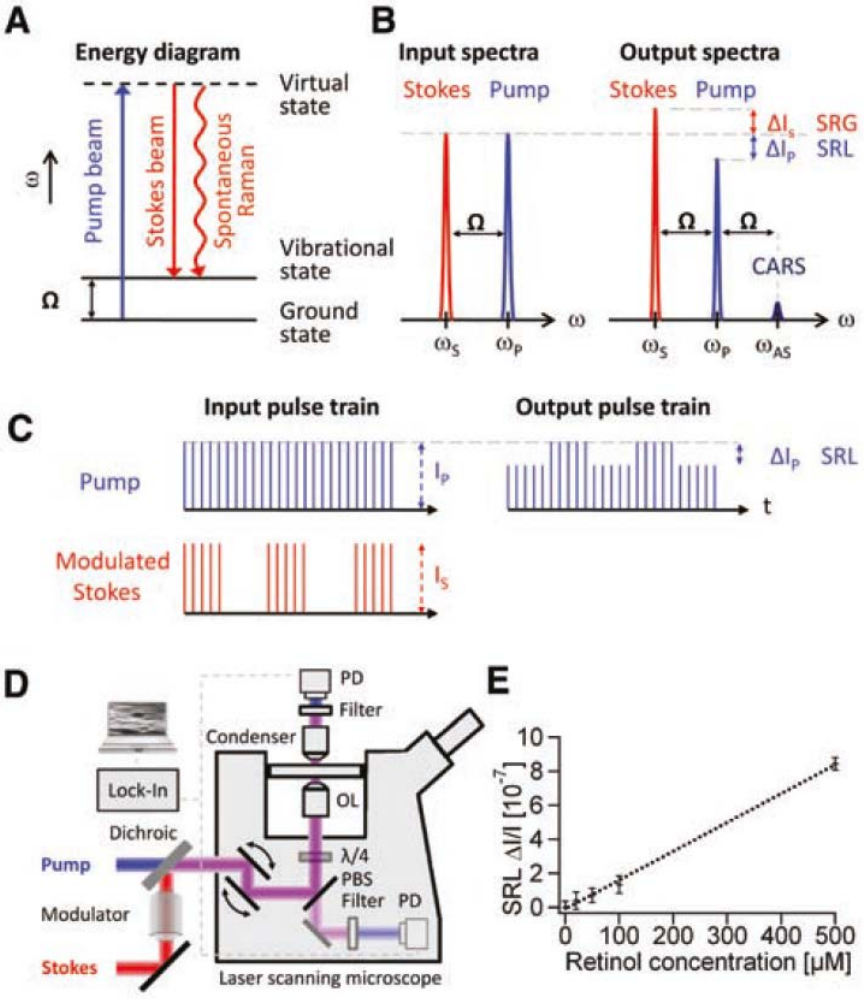

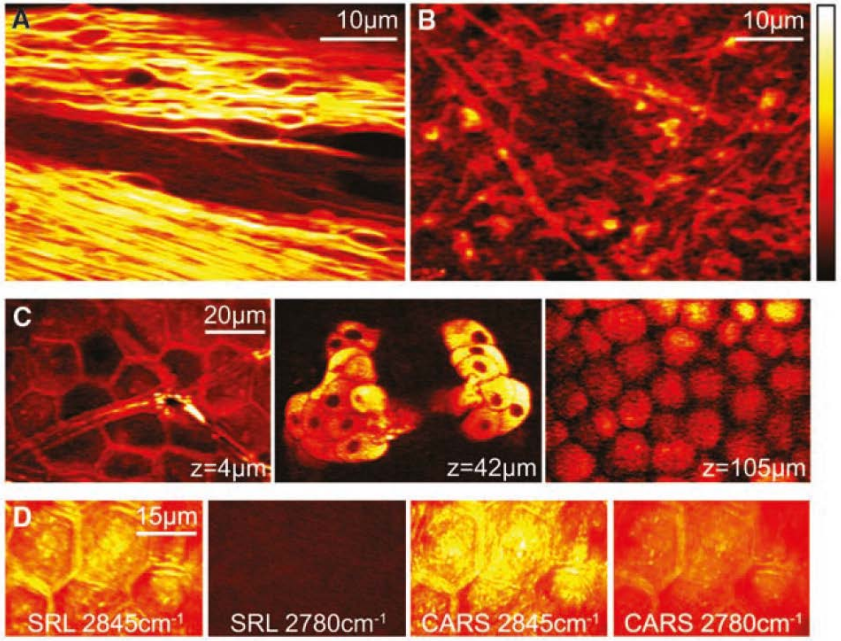

Fig. 3. SRL imaging of fresh mouse tissue. (**A**) Neuron bundles in corpus callosum of mouse brain imaged at 2845 cm^{-1} highlighting myelin sheaths rich in CH_2. See movie in (*18*). (**B**) Epi-detected SRL CH_2 image acquired from thick brain tissue. (**C**) SRL CH_2 images of mouse ear skin in the same area at the indicated depths. From left to right: stratum corneum (4 μm), sebaceous gland (42 μm), and subcutaneous fat layer (105 μm). See movie in (*18*). (**D**) Comparison of SRL and CARS images of stratum corneum on (2845 cm^{-1}) and off (2780 cm^{-1}) the CH_2 resonance. Unlike CARS, SRL has no nonresonant background.

Structural dynamics measured with time-resolved VIS/IR spectroscopy

Acetic acid dimer (HAc)

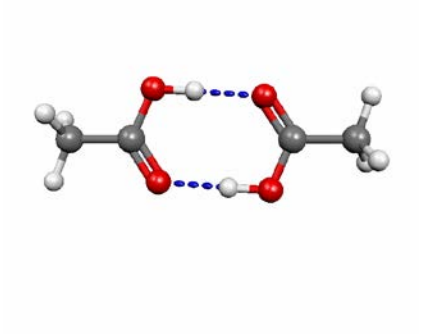

Electronic ground state

Photoactive Yellow Protein (PYP)

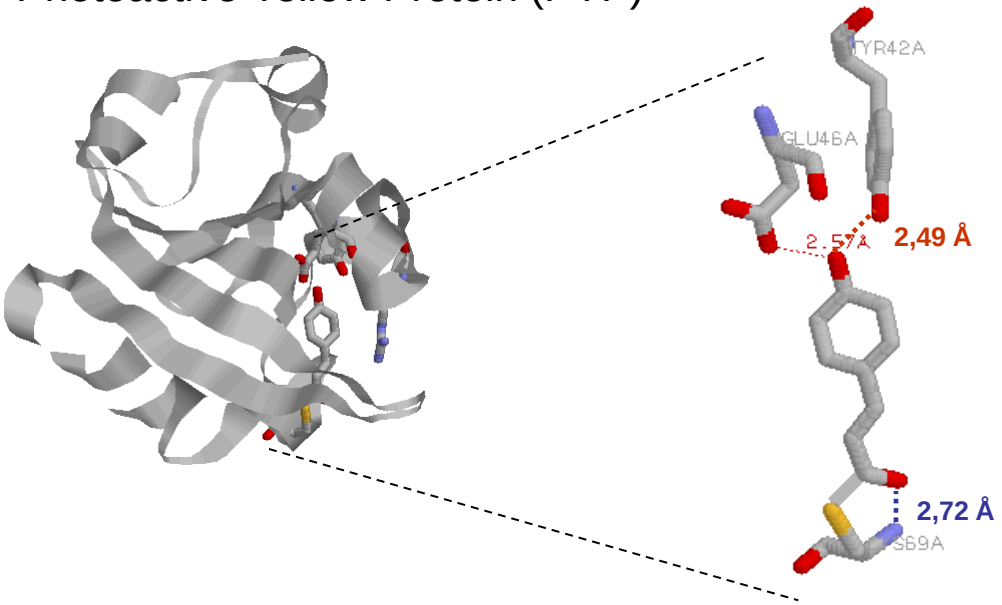

Electronic excited state

Ultrafast pump-probe spectroscopy

Ultrafast pump and probe pulses

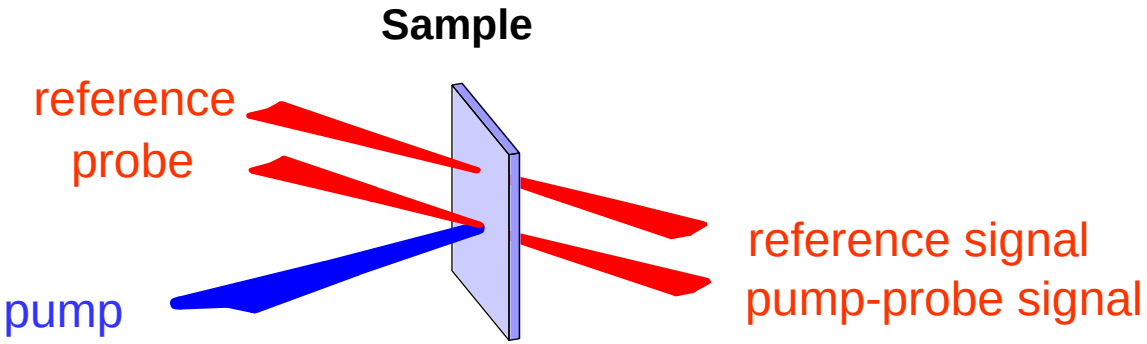

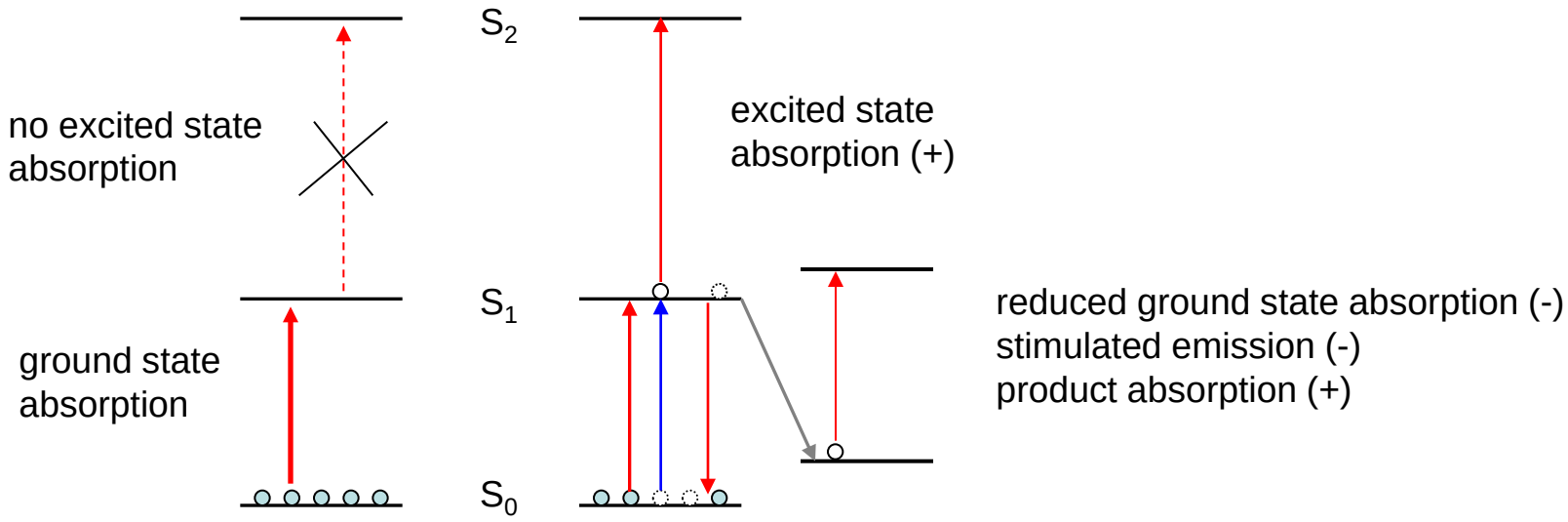

Ensemble of molecules in solution

VIS – pump VIS – probe experiments

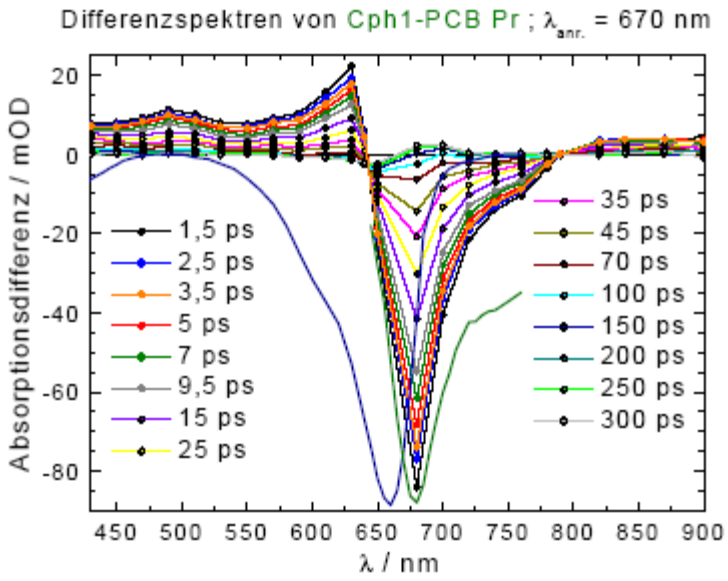

- dynamics of electronic transitions
- $S_0 \rightarrow S_1$; $S_1 \rightarrow S_2$ and $S_1 \rightarrow S_0$; $P_0 \rightarrow P_1$…
- strong overlapping of broad bands
- no direct structural information
- very sensitive to solvent dynamics (stokes shift)

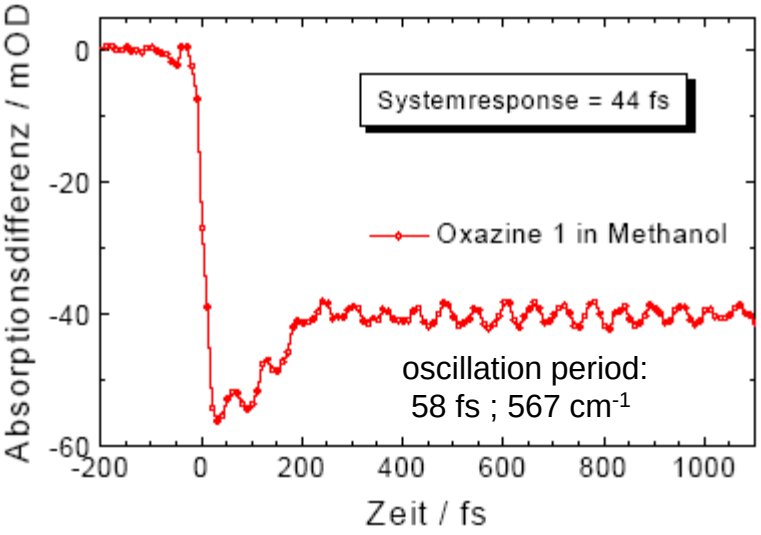

Wavepacket excitation due to spectral broad excitation pulses

coherent oscillations show Raman transitions coupled to the electronic transition

1000 cm^{-1} ≈ 15 fs or shorter

fingerprint vibrations 1000 .. 2000 cm^{-1}

Proteins are the workhorses of the cell

- Optimized by evolution
- Specific geometry of the light absorbing molecule and protein surrounding

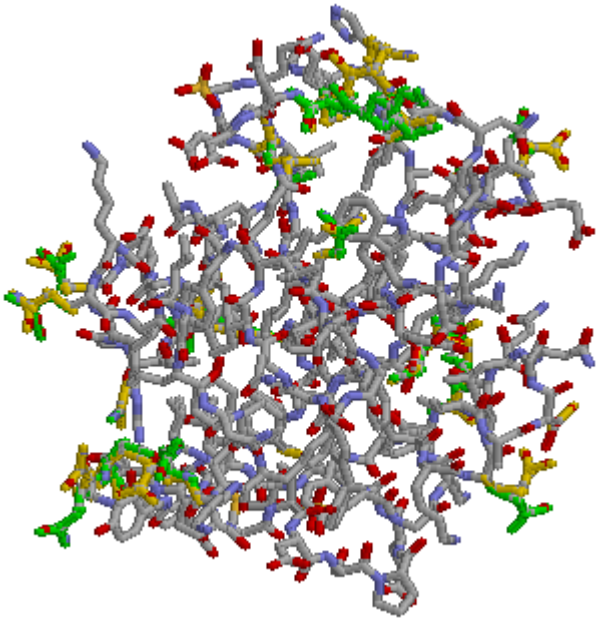

126 amino acids

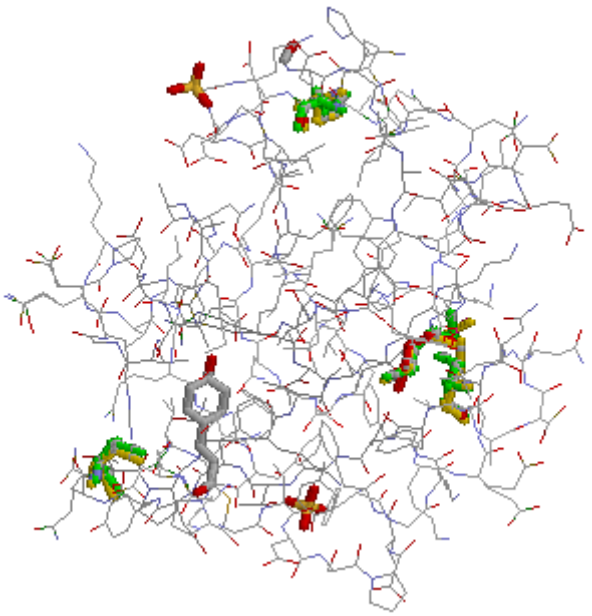

1 chromophore

Femtosecond experiments in proteins

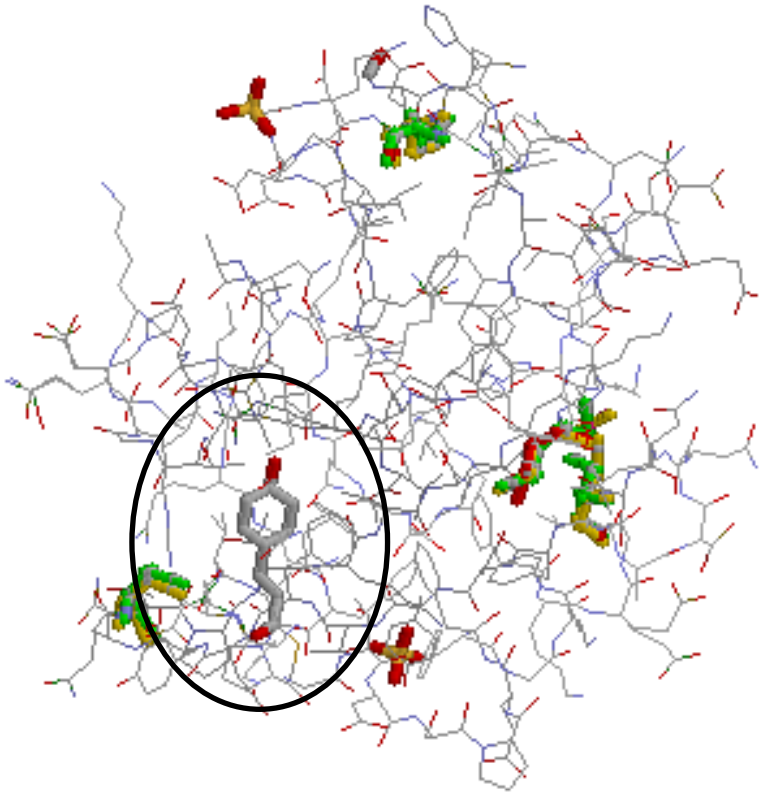

❖ Only local structure changes on a picosecond time scale

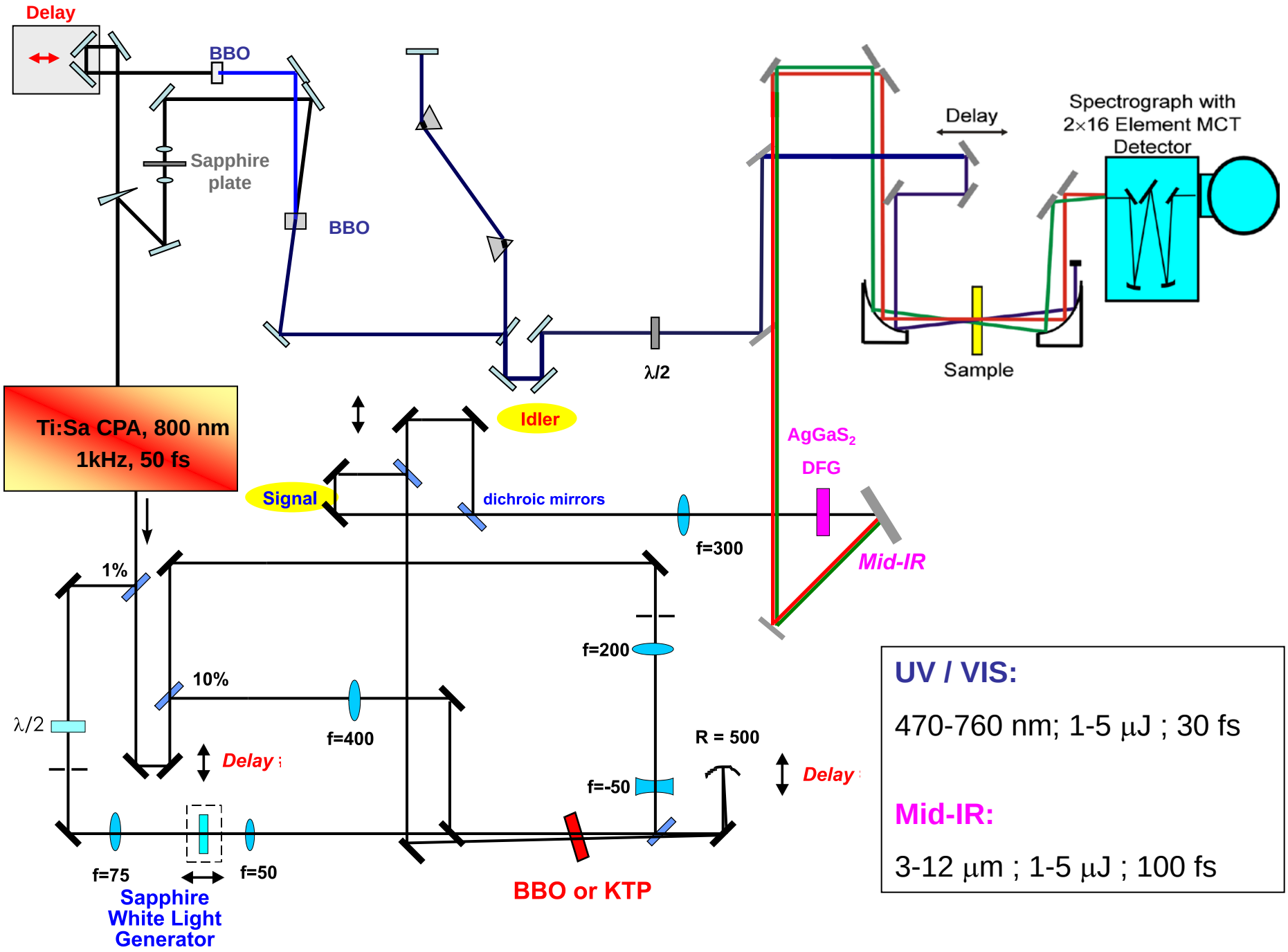

UV / VIS:

470-760 nm; 1-5 μJ ; 30 fs

Mid-IR:

3-12 μm ; 1-5 μJ ; 100 fs

Halobacterium salinarium

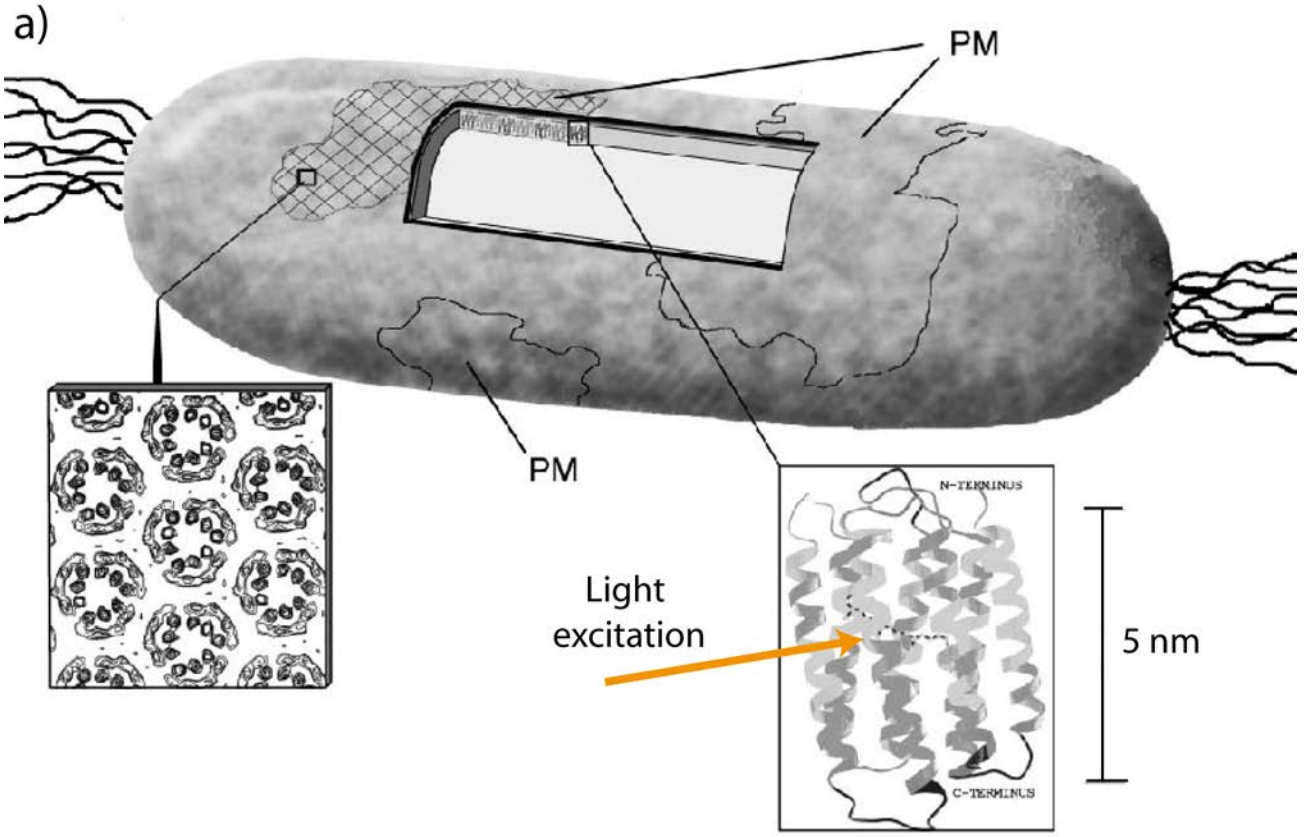

- Protein in the purple membrane is bacteriorhodopsin (bR)
- The chromophore in bR is Retinal

The light driven proton pump bR

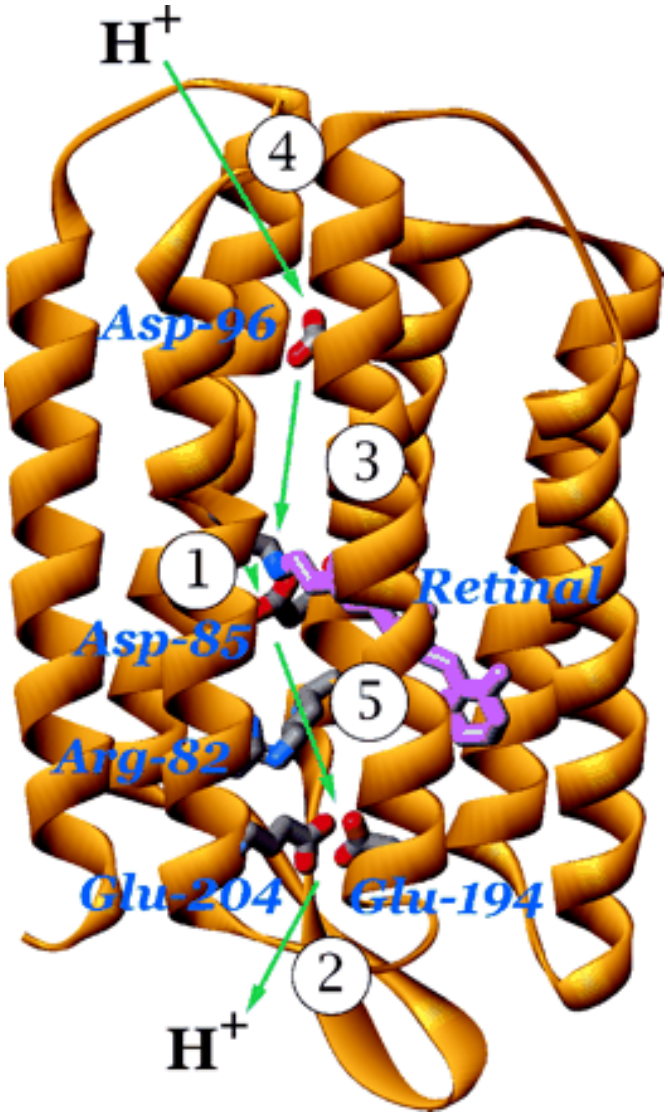

Luecke et al., *Science* 286, 1999

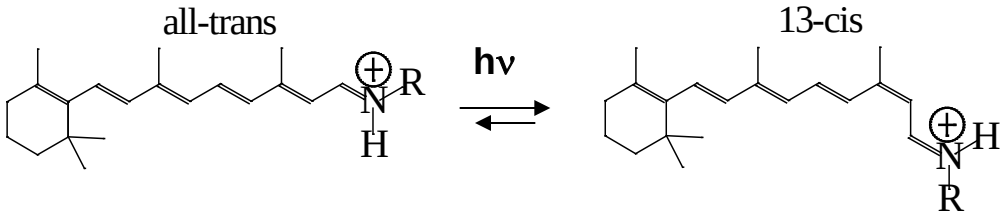

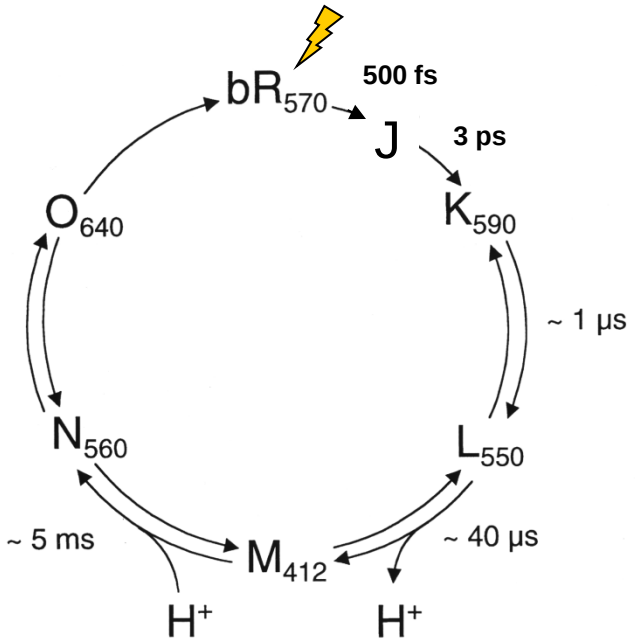

Chromophore binding pocket of bR

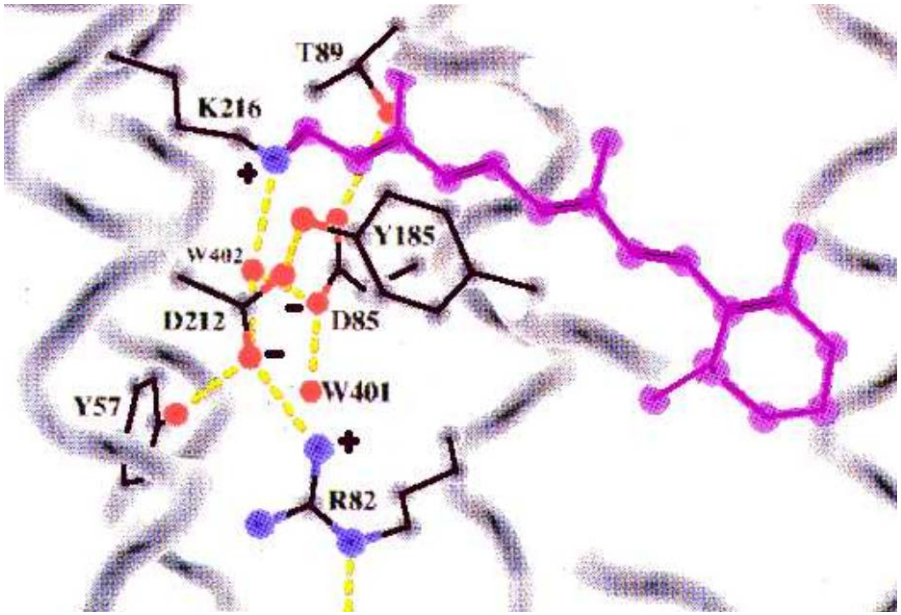

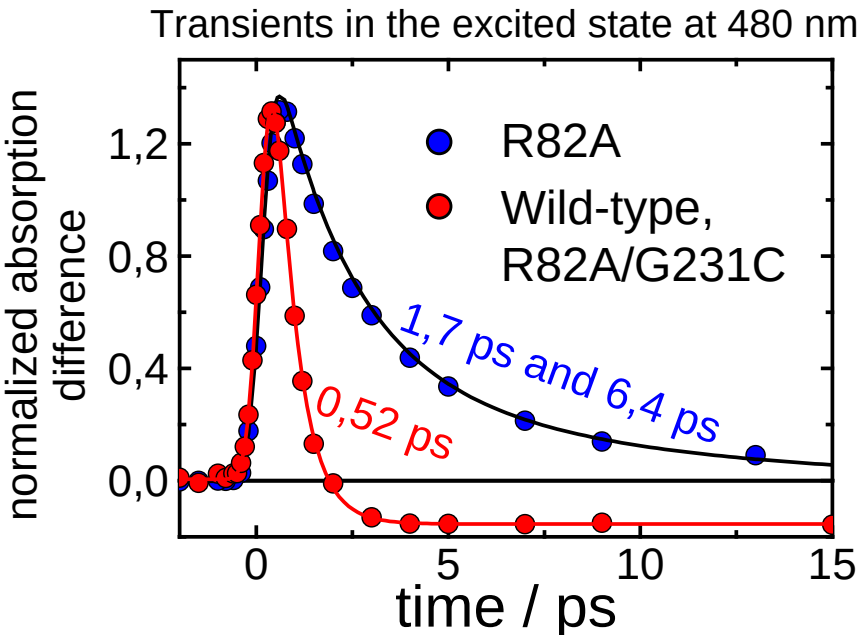

Counterion of the chromophore:

Asp85 $(D85)^-$,

Asp212 $(D212)^-$,

Arg82 $(R82)^+$

Changes of the geometry and charge of the counterion optimize / deoptimize the primary photoreaction

Heyne et al.,J. Phys. Chem. B ***104****, (*2000) 6053

Isomerization reaction dynamics

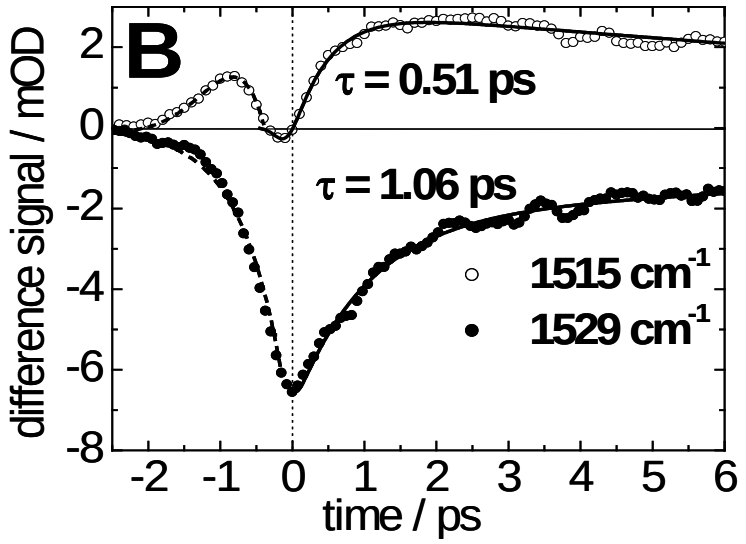

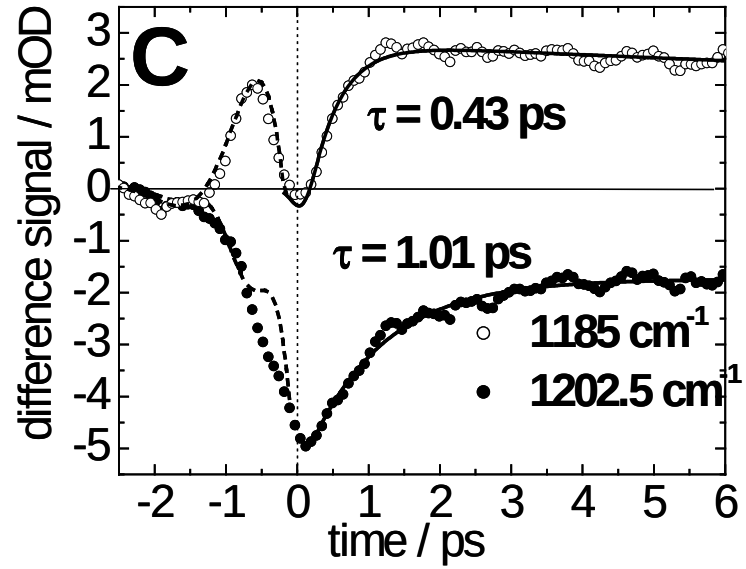

C-C stretching vibrational marker modes

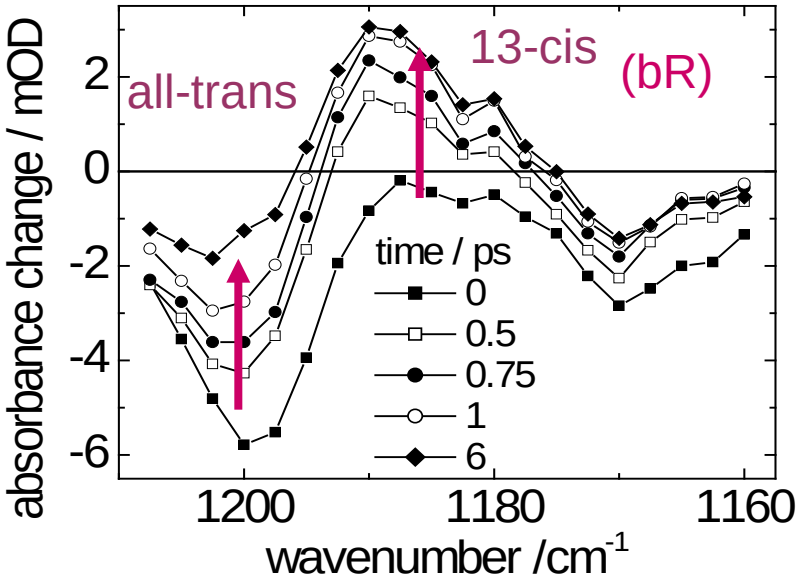

Reaction optimization in the protein

	product	yield	decay times
bR	13-cis	65%	500 fs
Retinal	11,13-cis	26%	2 ps, 7 ps

J. Herbst, K. Heyne, R. Diller, Science, **297**, (2002) 822.

Structural dynamics measured with time-resolved VIS-IR spectroscopy

Photoactive Yellow Protein (PYP)

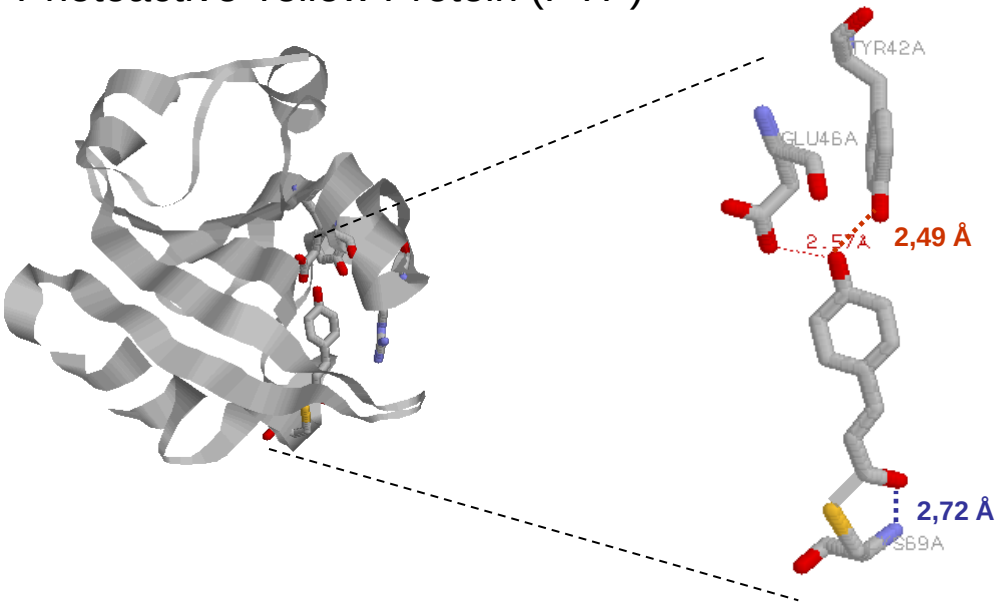

Electronic excited state

Photoreceptor Photoactive Yellow Protein

Negative phototaxis

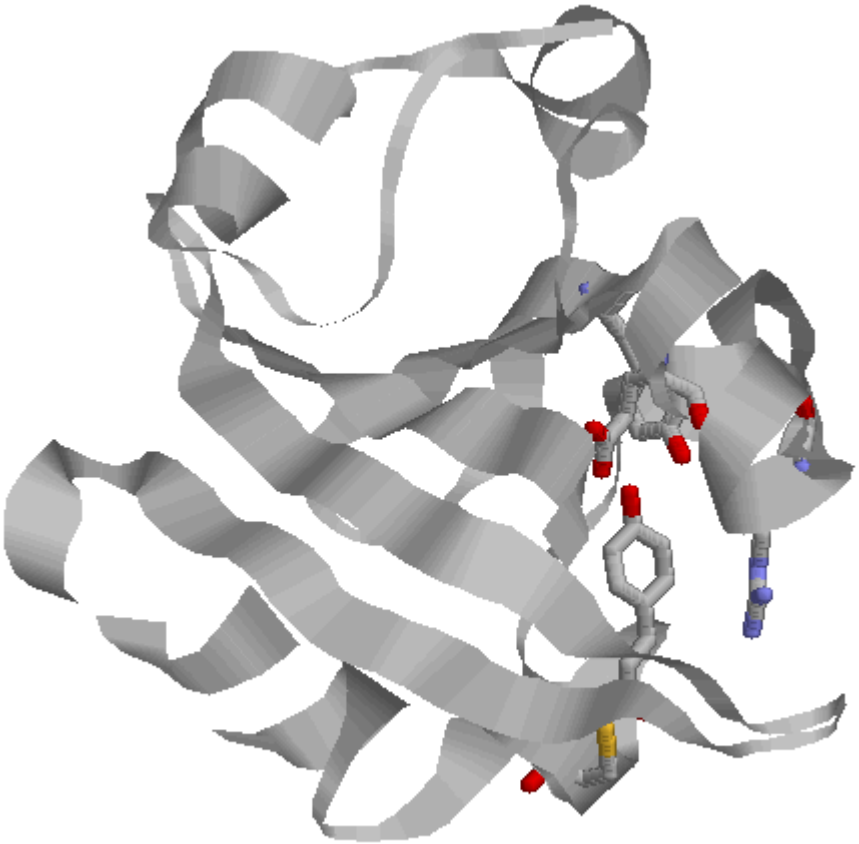

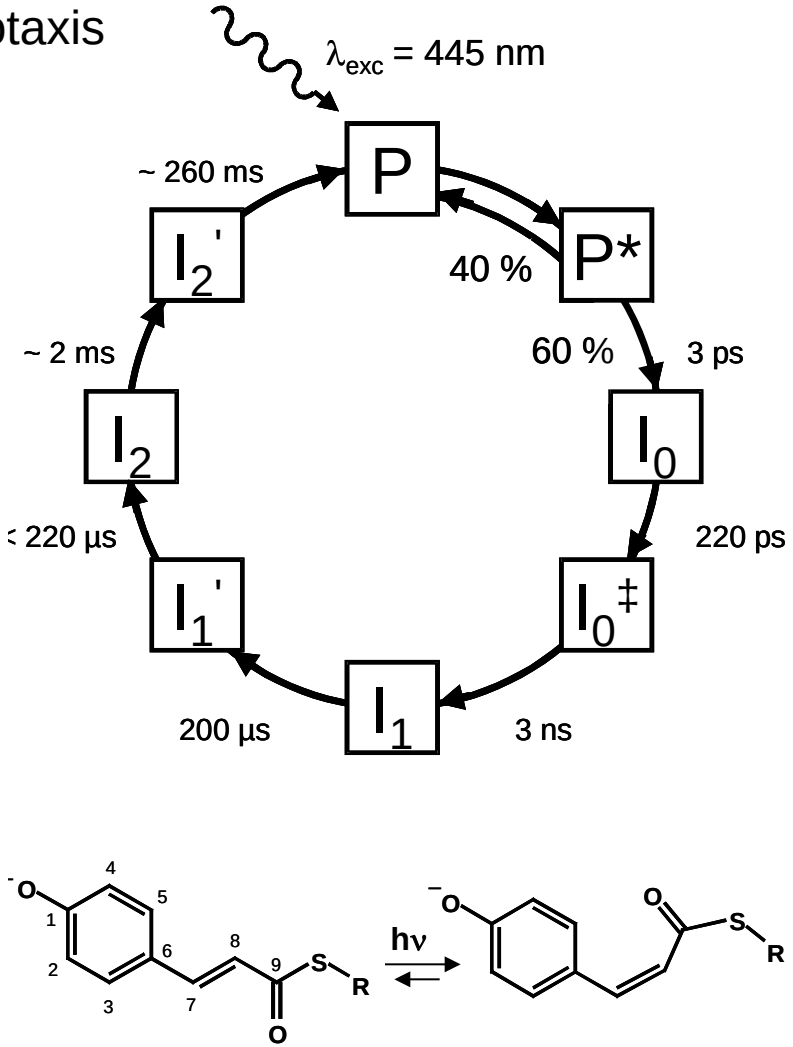

E. D. Getzoff et al., *Nat. Struct. Biol.* **10**, 663 (2003).

P state

I_0 state

Difference spectra

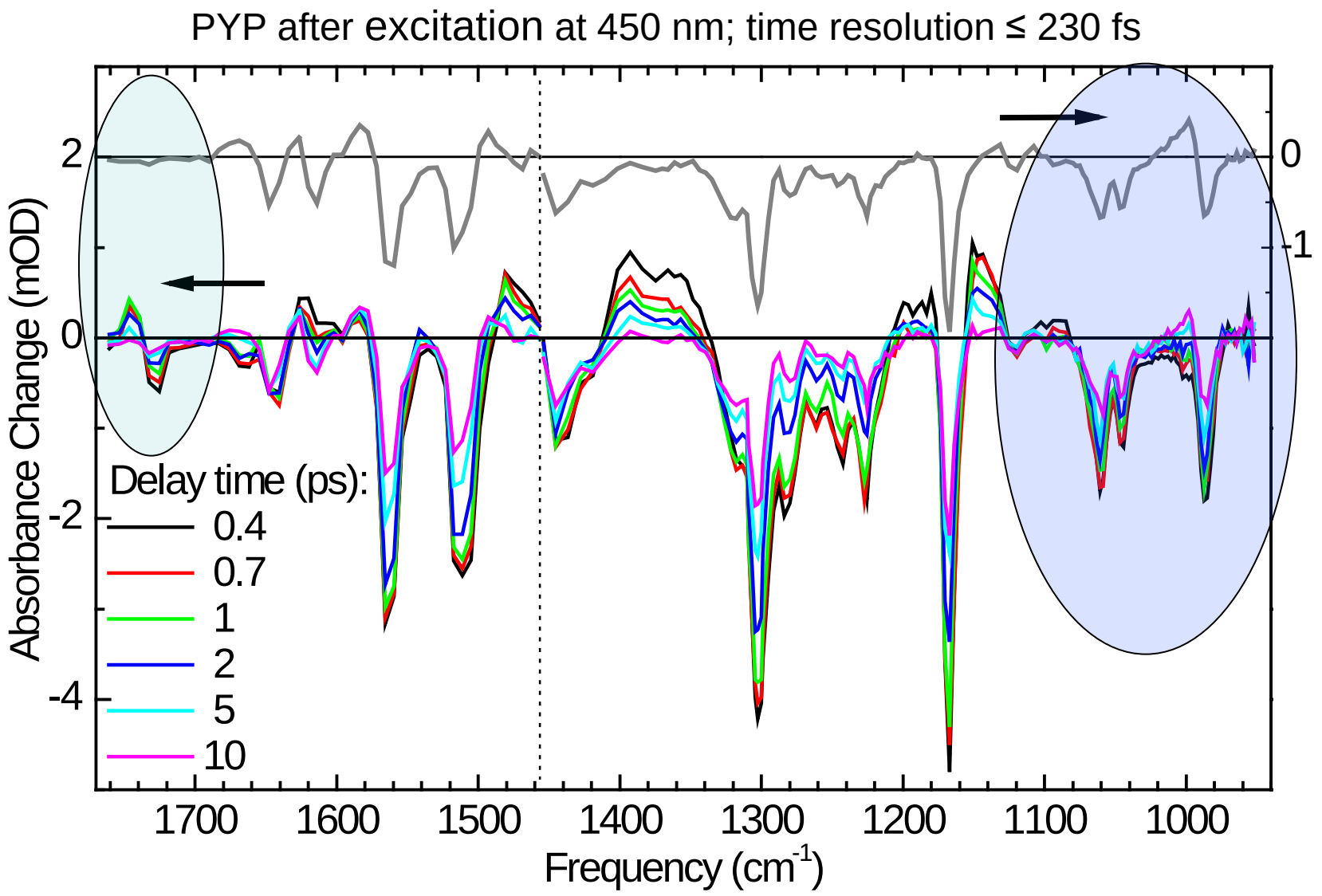

K. Heyne et al. J. Am. Chem. Soc. **127**, (2005), 18100-18106

Isomerization reaction

C_8-C_9 Vibrational marker modes of PYP

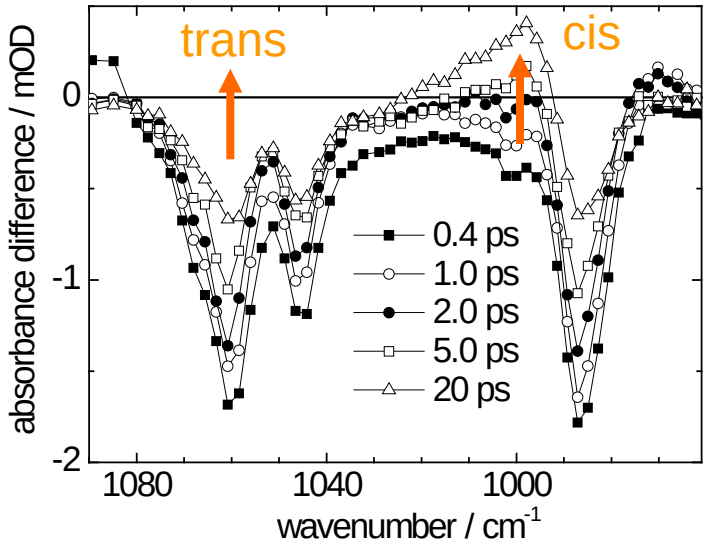

Protein optimizes the photoreaction

	product	yield	decay times
PYP	cis	40%	3 ps
PCT	cis	5%	10 ps

A. Usman et al. Chem. Phys. Lett., **401** (2005) 157

Polarization resolved fs IR-spectroscopy

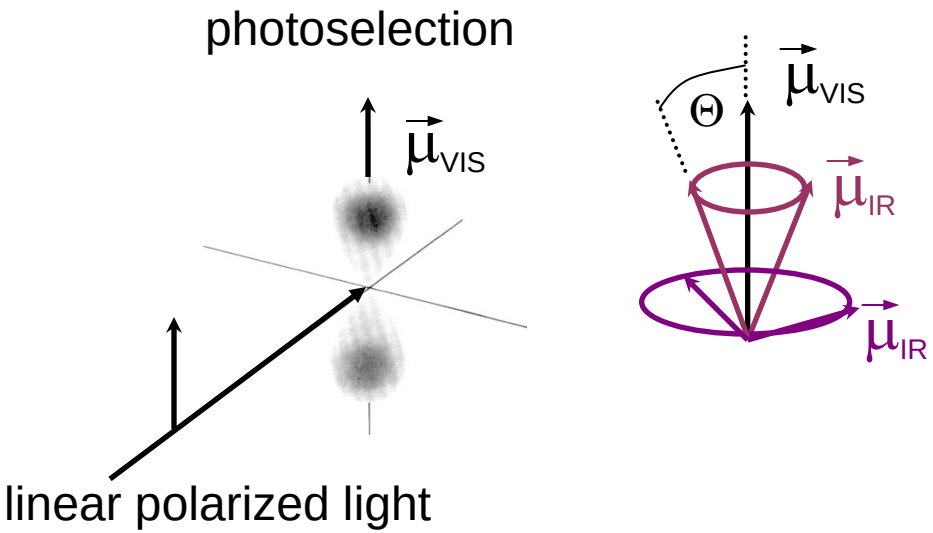

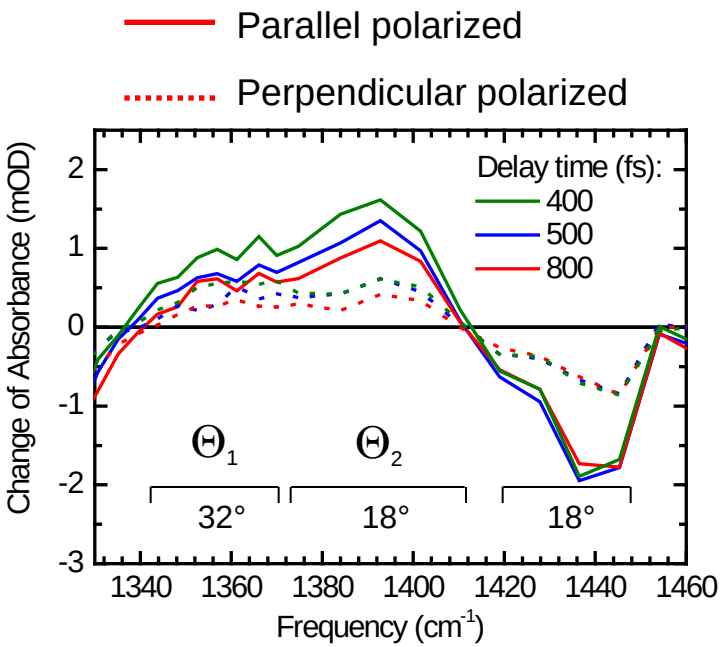

The relative angle allows to distinguish:

- Ground state bleachings
- Hot ground states
- Excited states
- Product states

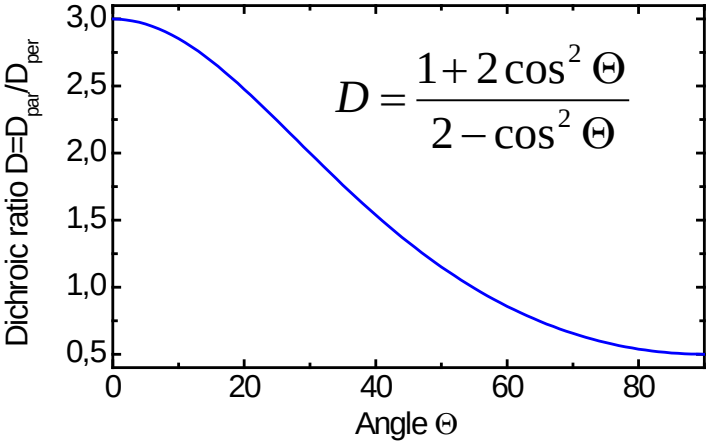

Polarization resolved transients

● parallel polarized probe pulse ; ○ perpendicular polarized probe pulse

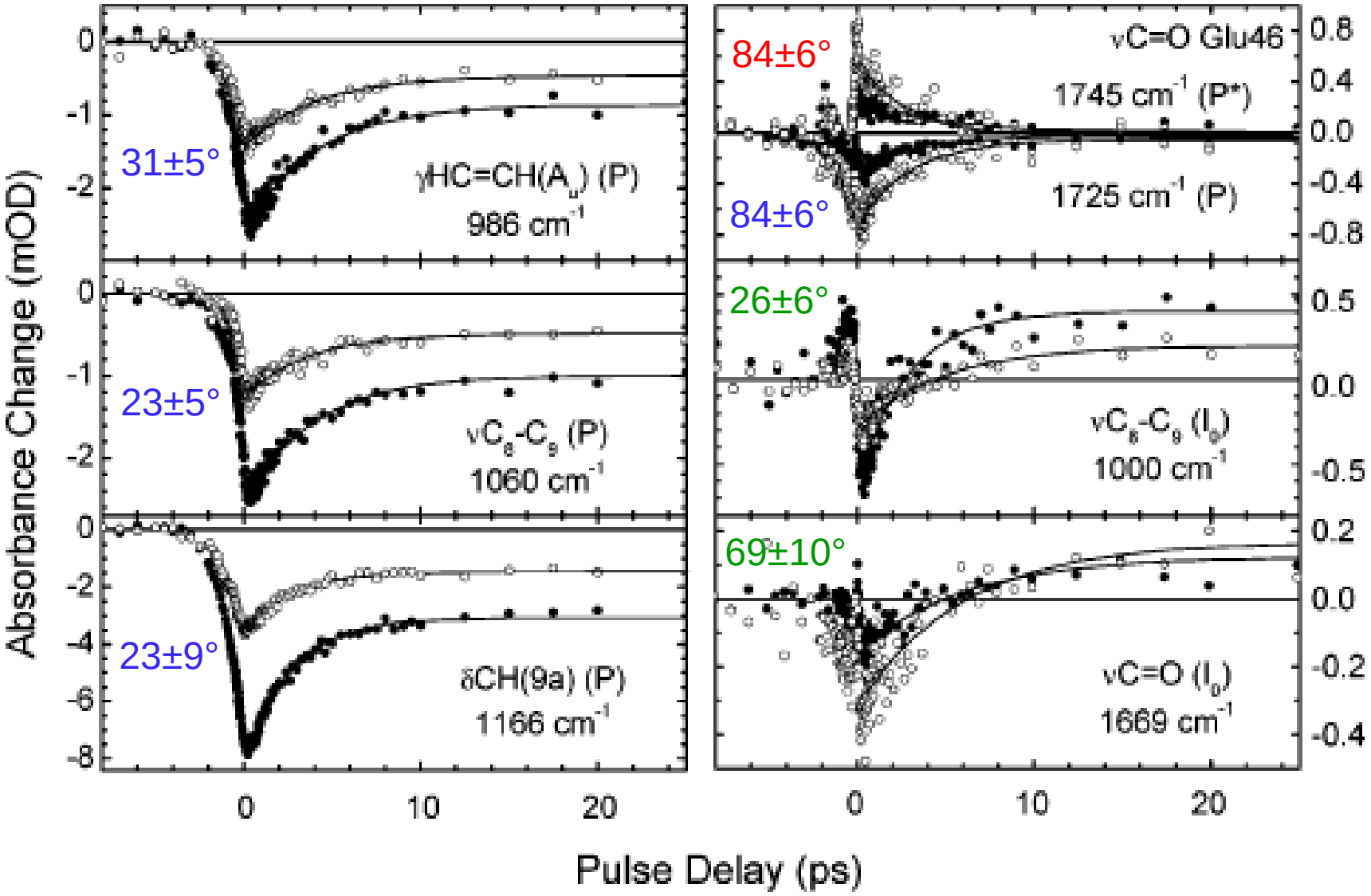

Structure changes in real time

Initial state P

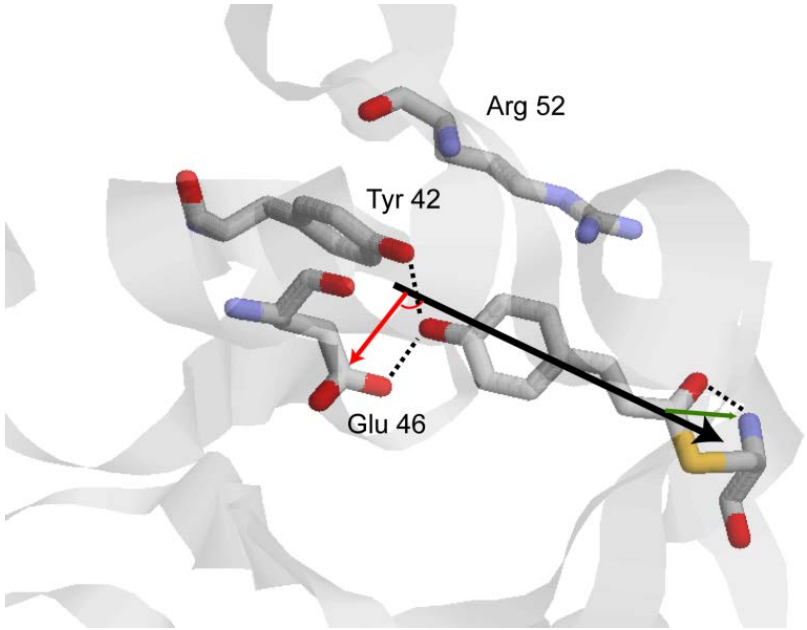

First product state I_0

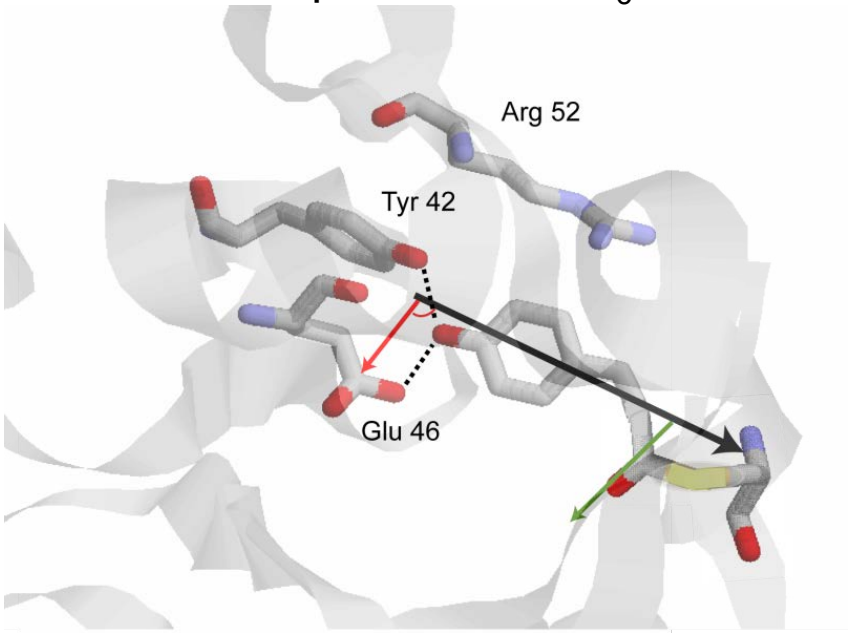

- Isomerization reaction within 3 ps (10 ps in solution)
- Quantum yield of 40 % (less than 5% in solution)
- Geometry of the first product state I_0 is planar
- Orientation of the v(C=O) vibration of Glu46 is conserved in the primary process

K. Heyne et al. JACS, **127** (2005) 18100

A. Usman et al. Chem. Phys. Lett., **401** (2005) 157

Structure changes in real time

Initial state Pr form

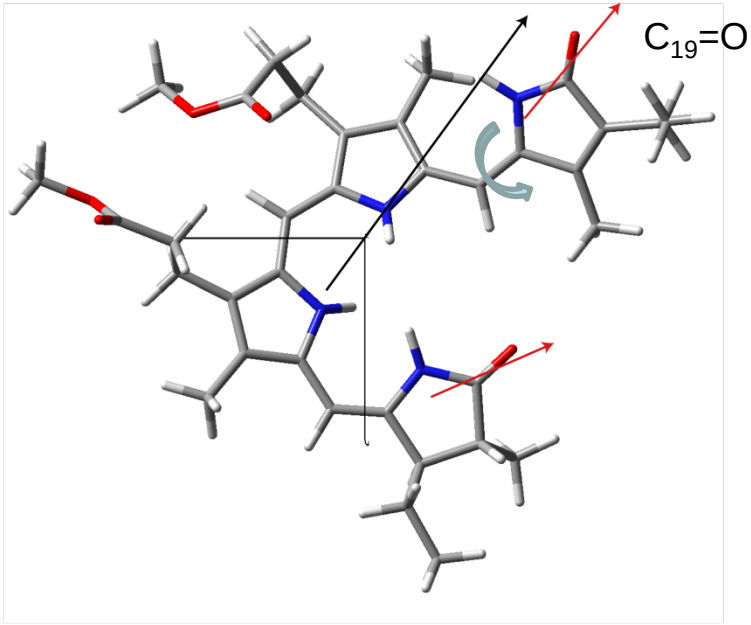

First photoproduct Lumi-R

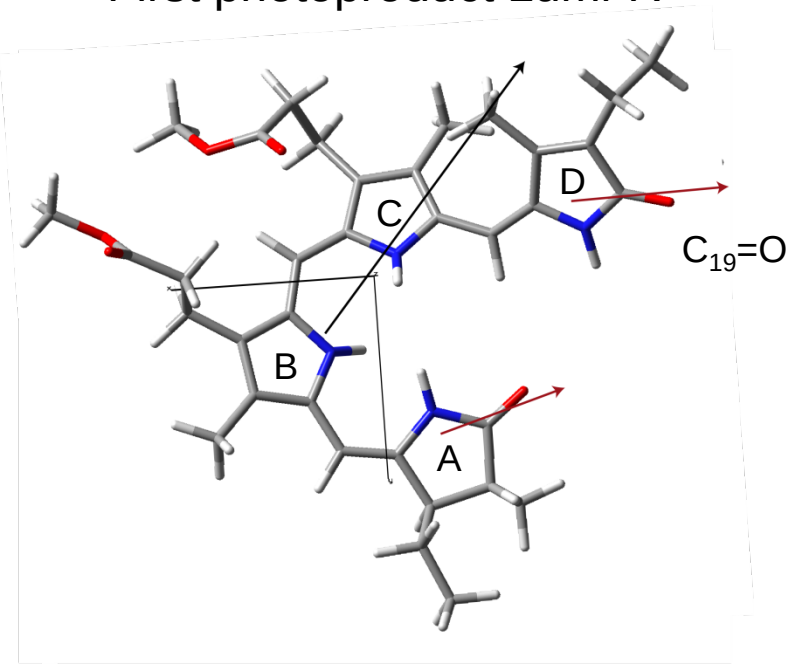

- Isomerization reaction within 30 ps
- Overall quantum yield of 12 % (depending on structural finetuning)
- Geometry of the first product state Lumi-R is ZZEsss
- Orientation of the v(C_{19}=O) vibration ring D changes in the electronic excited state

Chromophore of photosynthesis

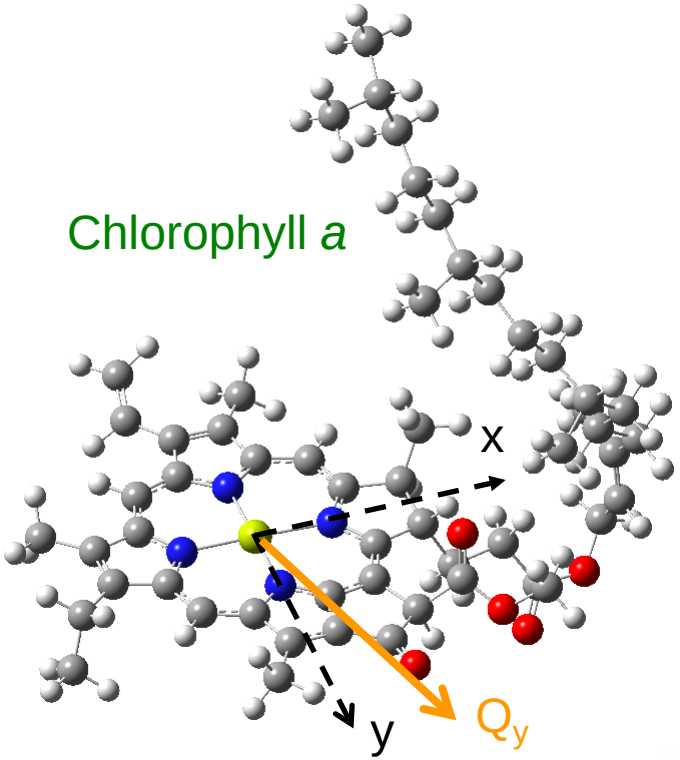

Photosystem I

Jordan, P., et al., Nature **411**, (2001), 909

Chlorophyll *a*

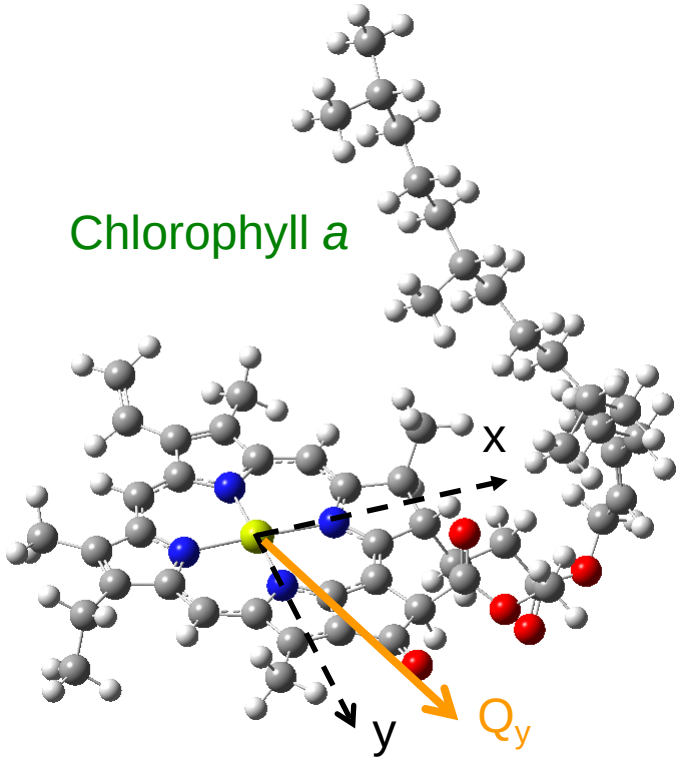

Chlorophyll *a* in toluene

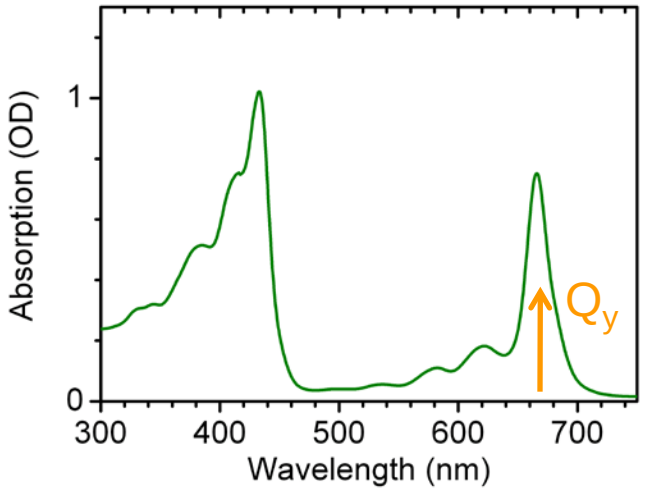

Experiments and calculations give an angle of ±20° to the y-axis

- No precise determination of the Q_y orientation

Pump-prope experiments on the Q_y transition

IR absorption of Chl *a*

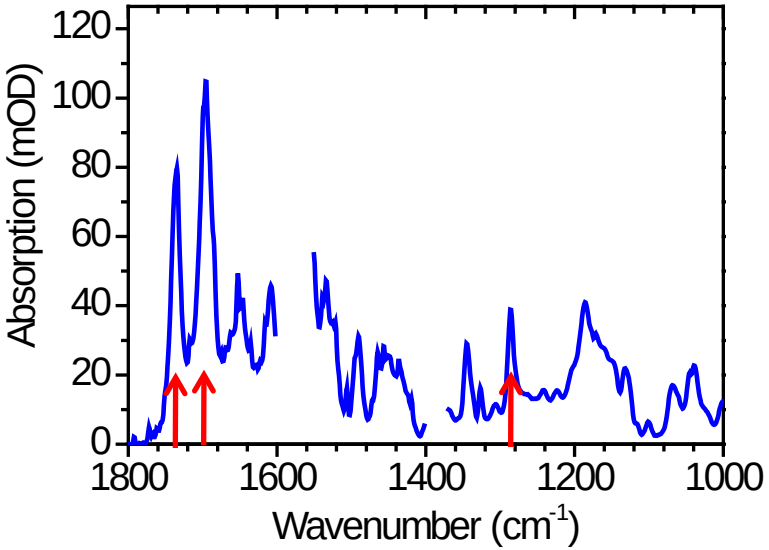

Chl *a* transients

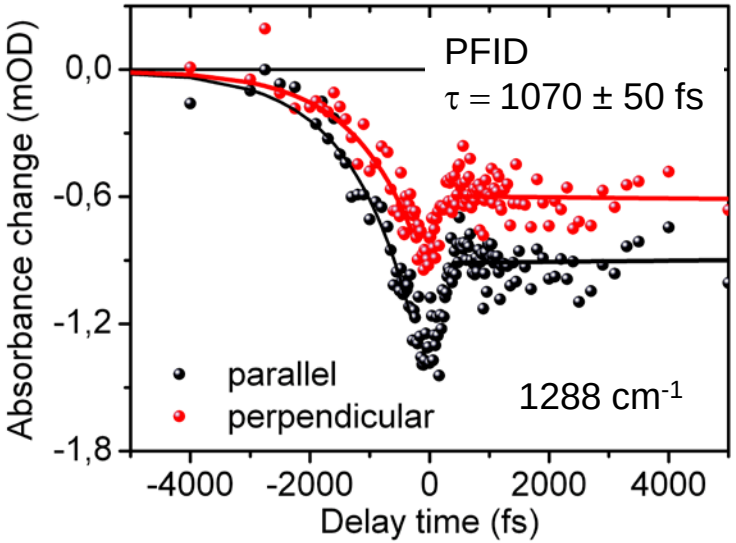

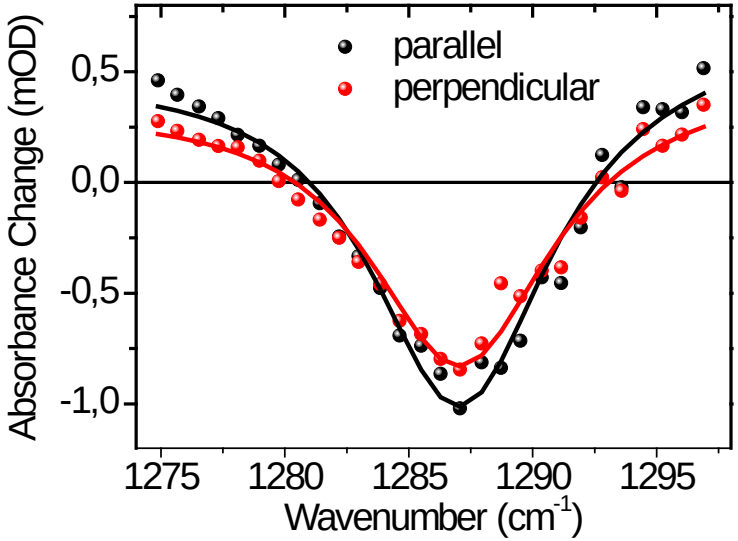

- PFID: Γ = 9.9 ± 0.5 cm^{-1}
- Linewidth of 9 ± 1 cm^{-1}
- Angle of the bleaching band: 47 ± 6°
- Exhaustive search analysis

  99 % range: 35.2°, …, 60.3°

Angles of the carbonyl vibrations

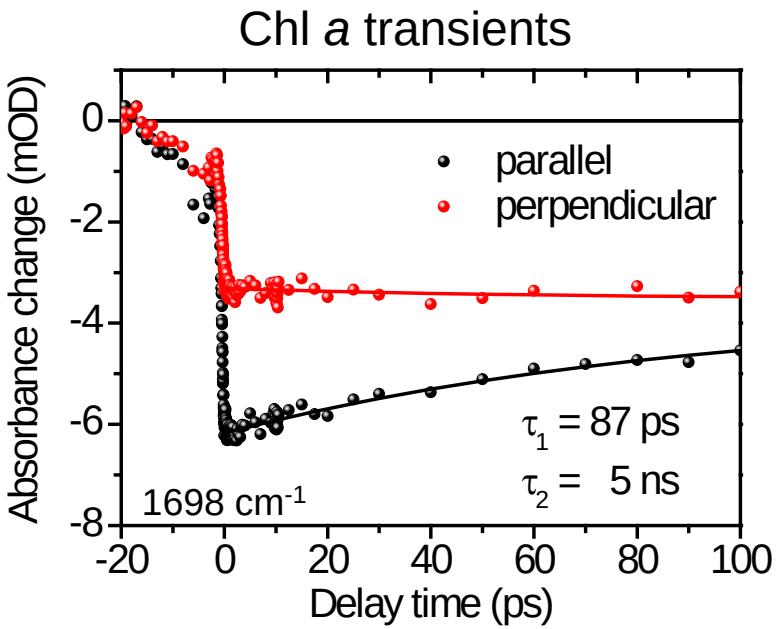

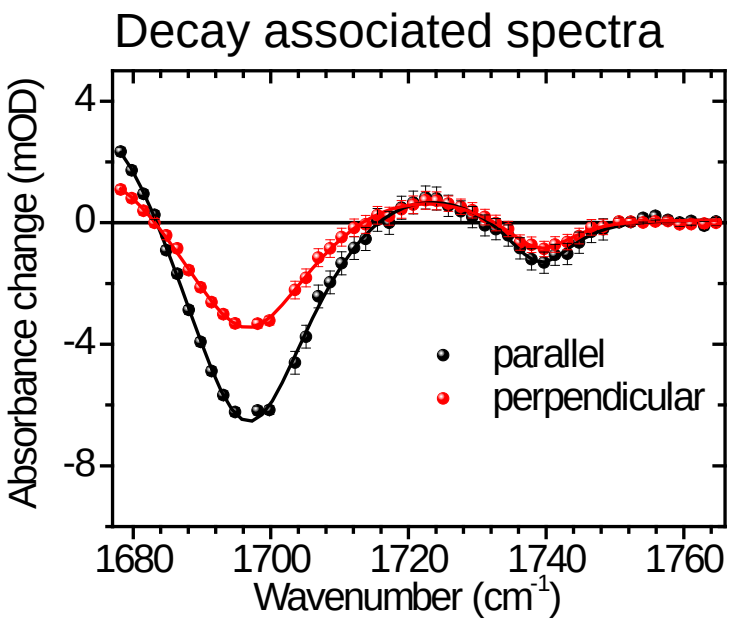

Angle of the bleaching bands, 99% range:

- 1698 cm^{-1}: 29.8°, …, 36.7°
- 1739 cm^{-1}: 26.3°, …, 65.8°

Calculation of the vibrational modes

Symmetric $\nu(C=O)_s$ stretch vibration

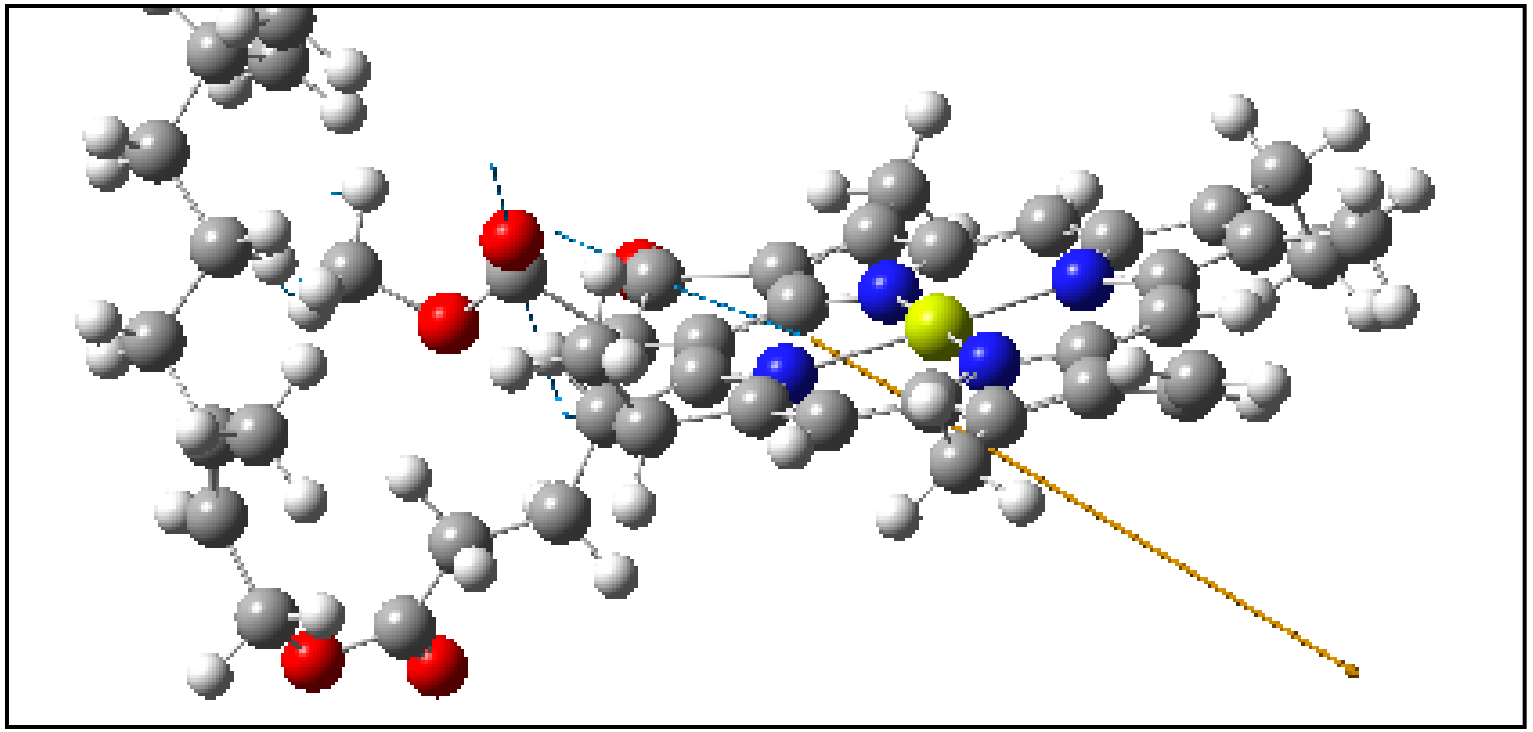

DFT calculation with Gaussian 03 (basis set: B3lyp/6-31G*)

Q_y transition dipole moment

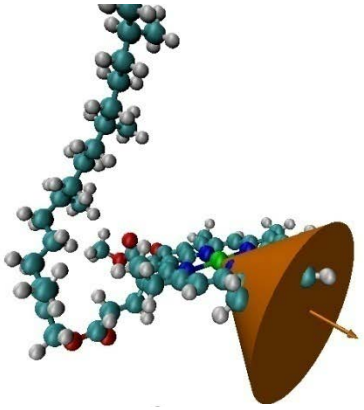

34°

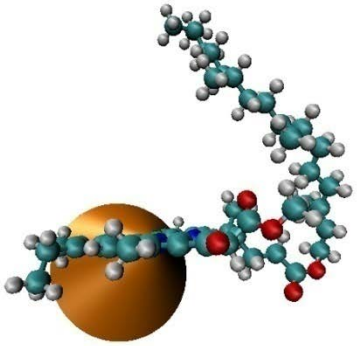

Symmetric $\nu(C=O)_s$: 26.3°…65.8°

Q_y transition dipole moment

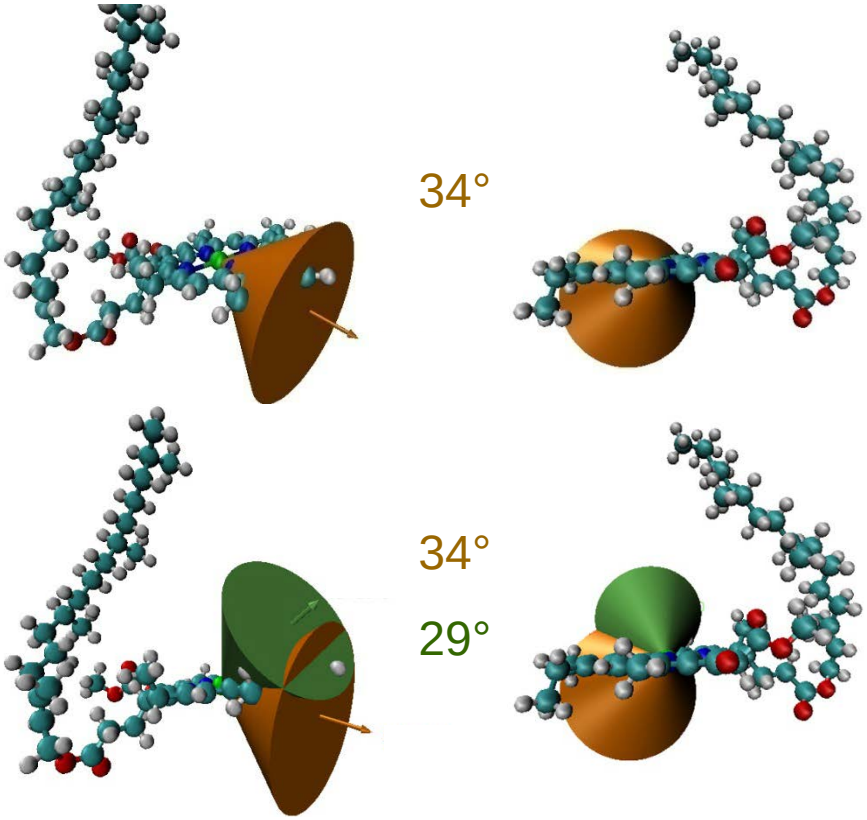

34°

34°

29°

Symmetric $\nu(C=O)_s$: 26.3°…65.8°

Symmetric $\nu(C=O)_s$ 26.3°…65.8°

Asymmetric $\nu(C=O)_{as}$ 29.8°…36.7°

Q_y transition dipole moment

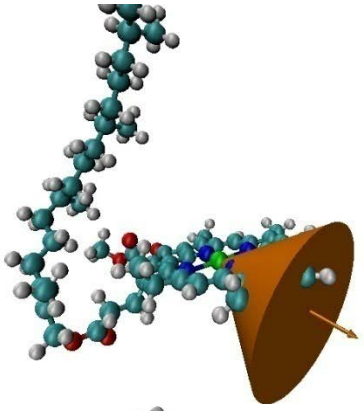

34°

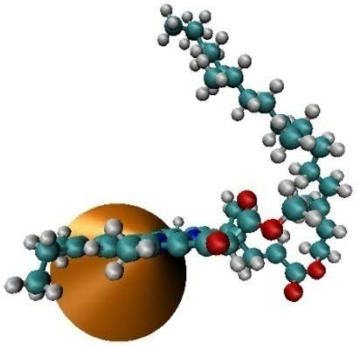

Symmetric $\nu(C=O)_s$: 26.3°…65.8°

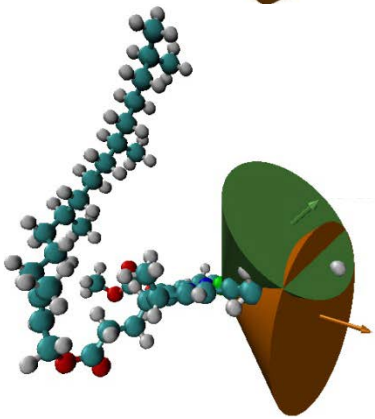

34°

32°

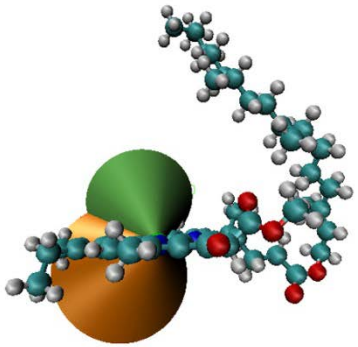

Symmetric $\nu(C=O)_s$ 26.3°…65.8°

Asymmetric $\nu(C=O)_{as}$ 29.8°…36.7°

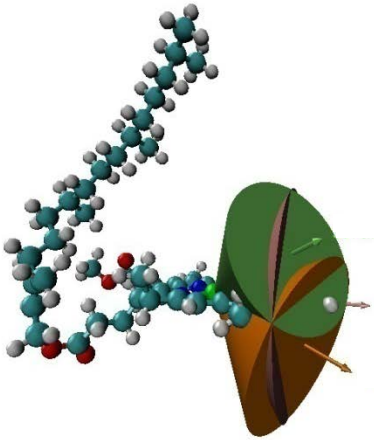

34°

32°

51°

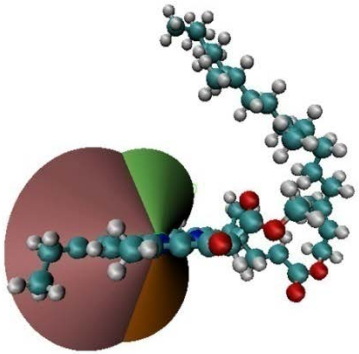

Symmetric $\nu(C=O)_s$ 26.3°…65.8°

Asymmetric $\nu(C=O)_{as}$ 29.8°…36.7°

Ring vibration $\nu(C=C)$ 35.2°…60.3°

- connected solution area

Orientation of the Q_y tdm

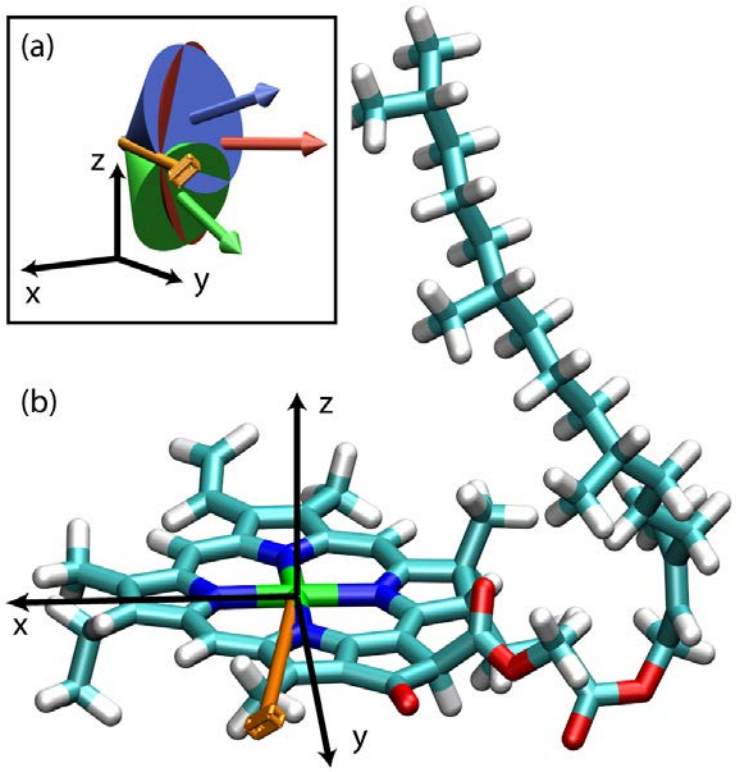

- Angle to the x-axis: 78° ± 3°
- Angle to the y-axis: 12° ± 3°
- Angle to the z-axis: 86° ± 2°
- New input for energy transfer calculations in photosystems
- Compare results with tdm calculations

Linke, M., et al., JACS, **130**, (2008), 14904-14905

Properties of Al-corroles

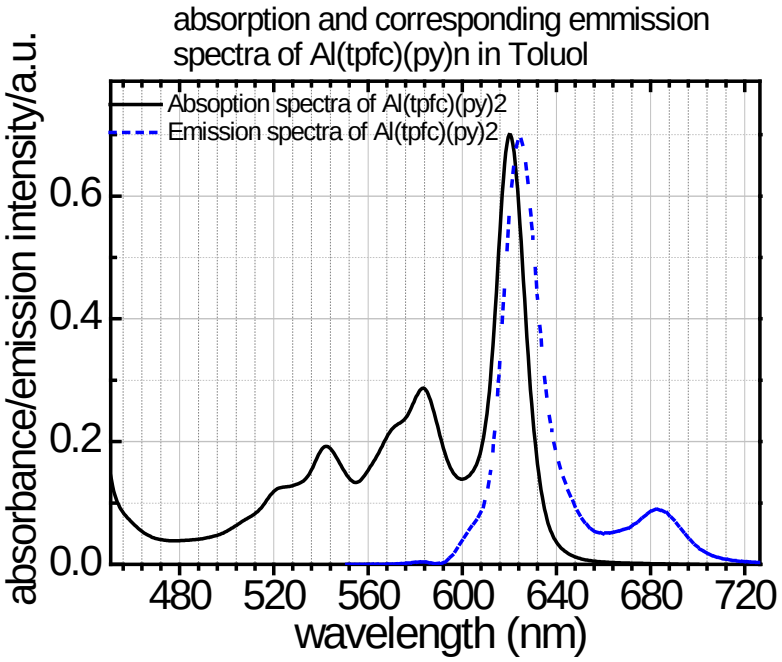

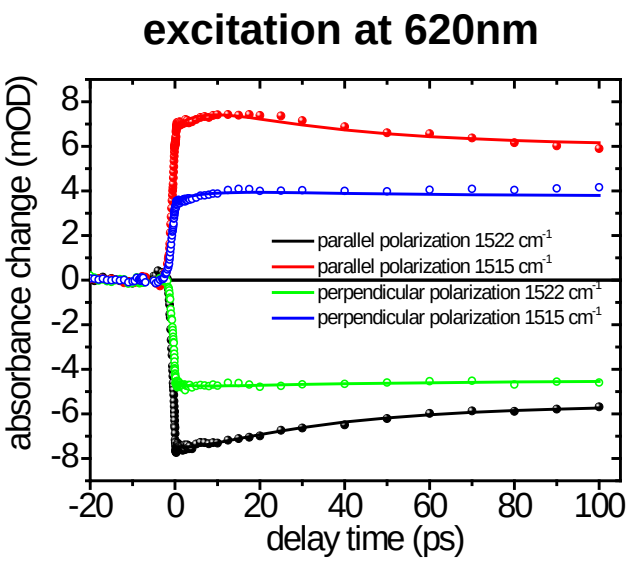

- Spectral shifts with 2nd pyrrole ligand
- C=C stretching band shows dichroism
- Relative between electronic and vibrational tdm: 35°

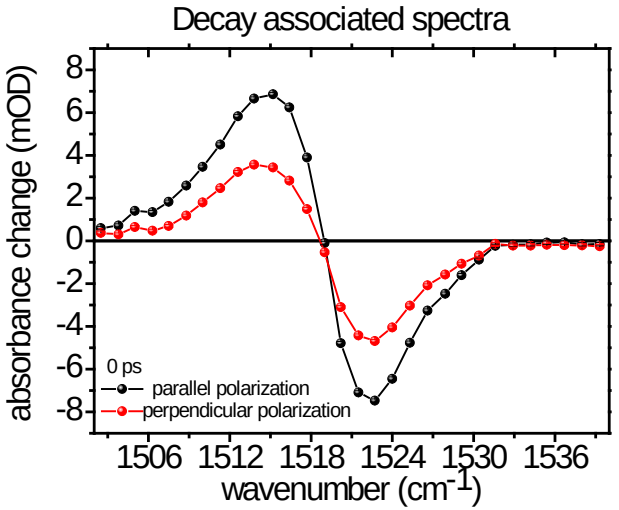

Absorption spectra of Al-corroles

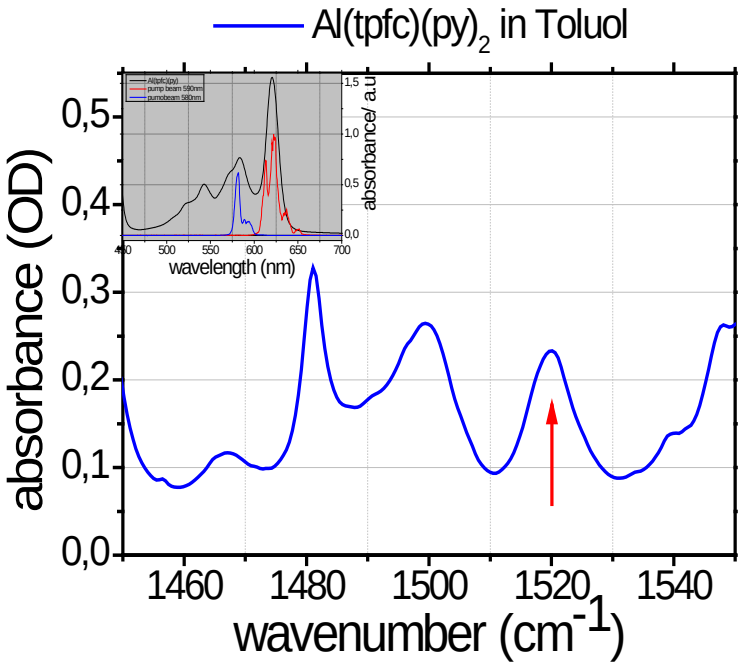

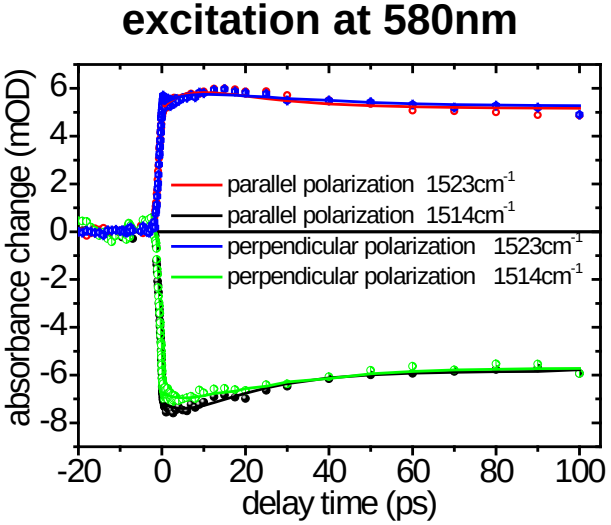

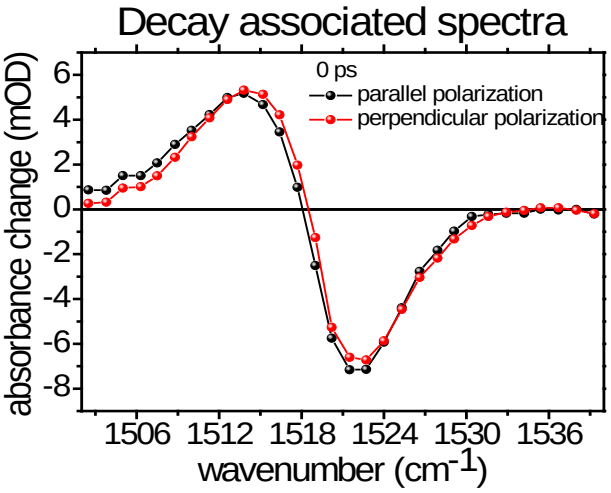

- C=C stretching band at 1520 cm^{-1}
- C=C stretching band shows no dichroism
- Relative between electronic and vibrational tdm: 54°

Orientation of the Q tdms

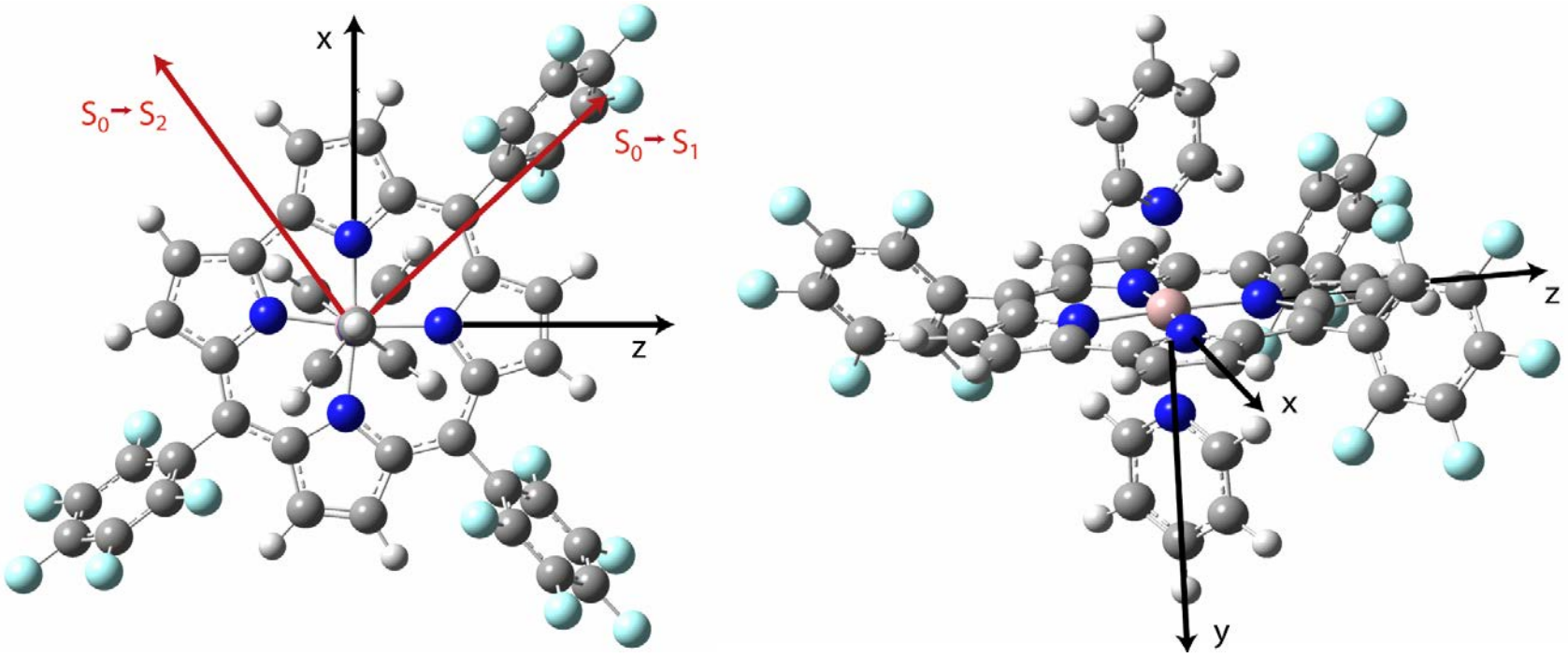

- Two different electronic states
- Angle of electronic transition dipole moments: ~ 90°
- Impact on energy relaxation processes